5-9-2014

Not All SecA Proteins Are Created Equal: A Study of the SecA1 and SecA2 Proteins of Mycobacterium tuberculosis.

Nadia G. D'Lima
University of Connecticut, nadia.d'lima@uconn.edu

Not All SecA Proteins Are Created Equal: A Study of the SecA1 and SecA2 Proteins of *Mycobacterium tuberculosis.*

Nadia Giselle D'Lima

University of Connecticut, 2014

In bacteria, most secreted proteins are exported through the SecYEG translocon by the SecA ATPase motor via the general Sec pathway. The identification of an additional SecA protein, particularly in Gram-positive pathogens, has raised important questions about the role of SecA2 both in protein export and establishment of virulence. In *Mycobacterium tuberculosis,* the causative agent of Tuberculosis (TB), the accessory SecA2 protein possesses ATPase activity that is required for bacterial survival in host macrophages, highlighting its importance in virulence. This study probes the biochemical differences between the two SecA proteins in order to gain insight into how they interact with the same translocon to exporting specific precursors. The study shows that SecA2 unlike SecA1 does not associate with the membrane under normal conditions. SecA2 also binds ADP with much higher affinity than SecA1 and releases the nucleotide more slowly. Nucleotide binding regulates movement of the precursor-binding domain in SecA2, unlike in SecA1 or conventional SecA proteins. This conformational change involving closure of the clamp in SecA2 may provide a mechanism for the cell to direct protein export through the conventional SecA1 pathway under normal growth conditions while preventing ordinary precursor proteins from interacting with the specialized SecA2 ATPase.

Not All SecA Proteins Are Created Equal: A Study of the SecA1 and SecA2 Proteins of *Mycobacterium tuberculosis.*

Nadia Giselle D'Lima

BSc, St. Xaviers College (2005)

A Dissertation

Submitted in Partial Fulfillment of the

Requirements for the Degree of

Doctor of Philosophy

at the

University of Connecticut

2014

APPROVAL PAGE

Doctor of Philosophy Dissertation

Not All SecA Proteins are Created Equal; A Study of the SecA1 and SecA2 Proteins of *Mycobacterium tuberculosis.*

Presented by

Nadia Giselle D'Lima, BSc.

Major Advisor_____

Carolyn M. Teschke

Associate Advisor_____

Arlene Albert

Associate Advisor_____

Nathan Alder

University of Connecticut

2014

ACKNOWLEDGEMENTS

I consider myself privileged to have been able to spend the past few years in graduate school at UConn. To my advisor Dr. Carolyn Teschke- thank you for accepting me into your lab, giving me the opportunity to do research and for believing in me. I am grateful to you for supporting and mentoring me these past years and teaching me the 'art of scientific investigation'.

To my committee members; Dr. Arlene Albert, Dr. Nathan Alder and examiners; Dr. Kenneth Campellone and Dr. Joerg Graf- thank you, not only for taking the time to attend my presentations and read my manuscripts but also for your guidance, suggestions and helpful feedback.

I have had the pleasure of working with some exceptional lab members over the years- Jie, Kristin, Maggie, Molly, Pauline, Juliana, Alex, Tina, Therese, Kevin, Jon and Aashay. The knowledge I have imbibed from you is invaluable. Jie Hou- I would especially like to thank you for being a patient teacher and showing me the ropes. Juliana Cortines- I am grateful to you for being a wonderful mentor and close friend. Alex Rizzo- you are my biggest critic and strongest supporter at the same time and I truly value our discussions- both scientific and otherwise.

I know I am incredibly blessed to have a family that has supported and encouraged me all along. To my parents- you are my inspiration. You taught me to always strive to do my best and nothing would be impossible. I couldn't have done this without you and words cannot express my gratitude to you.

TABLE OF CONTENTS

Page

Abstract i

Approval Page iv

Acknowledgements v

List of tables ix

List of figures x

Chapter One: Introduction

A. Sec dependent protein secretion- an overview 1

B. Accessory Sec systems in bacteria 7

C. The SecA motor 15

D. The Mycobacterial Sec system 22

E. Structure of *M. tuberculosis* SecA1 26

F. Domain organization of *M. tuberculosis* SecA2 29

G. Purpose of this study 32

Chapter Two: Methods

A. Molecular bilogy and cloning 33

B. Protein expression and purification 44

C. Agarose gel electrophoresis of proteins 49

D. Fluorescence spectroscopy 49

E. Circular dichroism spectroscopy 52

F. Proteolysis Experiments 52

G. Growth of *M. smegmatis* and preparation of membrane vesicles..... 53

H. Membrane floatation assay using OptiPrep..... 55

I. Western Blotting..... 56

J. Sedimentation Velocity Analytical Ultracentrifugation 57

Chapter Three: SecA2; A different kind of SecA protein

Introduction..... 59

Results

A. SecA2 shows a unique structural change upon binding to ADP..... 63

B. ADP bound SecA2 can be separated from nucleotide-free SecA2 using Blue-Sepharose chromatography..... 68

C. SecA2 binds ADP with high affinity and releases it significantly slowly compared to SecA1..... 70

D. The structural change in SecA2 is not due to changes in oligomeric state..... 75

E. The structural change in SecA2 is not due to changes in oligomeric state..... 77

F. SecA2 is significantly stabilized to heat when ADP bound..... 81

G. ADP binding confers protection to regions of the pre-protein binding domain in SecA2..... 83

H. ADP binding closes the clamp of SecA2 but not of SecA1 87

Discussion 98

Chapter Four: 'It takes two to tango'- or does it?

Introduction..... 102

Results and Discussion

A. Dimerization in *M. tuberculosis* SecA1 and SecA2 is salt-dependent 107

B. SecA1 does not exist as a salt resistant dimer 112

Chapter Five: Association of the *M. tb* SecA proteins with membranes

Introduction 116

Results and Discussion

A. Membrane vesicles containing HA-tagged *M. smegmatis* SecY are sealed and can establish a proton gradient 119

B. SecA1 interacts with the membrane while SecA2 does not 122

C. SecA2 K115R associates with membrane vesicles more than WT SecA2 125

Significance of this study 128

References 134

LIST OF TABLES

Page

Table 1-1: List of pre-proteins identified to date that require SecA2 for export in bacteria that have 'SecA2 only' secretion systems 13

Table1-2: List of pre-proteins identified to date that require SecA2 for export in bacteria that have 'SecA2/Y2' secretion systems..... 14

Table 1-3: Binding affinities of SecA for different ligands important in Sec- dependent protein translocation 21

Table 3-1: Kinetic constants for binding of MANT-ADP to *M. tb* SecA proteins determined by FRET..... 74

LIST OF FIGURES

Page

Fig 1-1: Graphical representation of co and post-translational translocation by the Sec pathway 5

Fig 1-2: Structure of the SecYEβ translocon of *M. jannaschii* 6

Fig 1-3: Genetic loci encoding *secA2* in bacteria containing SecA2 only as well as in bacteria containing SecA2/Y2 11

Fig 1-4: Structure of *E. coli* SecA 20

Fig 1-5: Structure of *M. tuberculosis* SecA1 28

Fig 1-6: Comparison of domain organization of SecA2 proteins 30

Fig 1-7: Alignment of amino acid sequences of *M. tb* SecA1 and SecA2 by PRALINE 31

Fig 3-1: Crystal structures of *Thermatoga maritima* SecA showing two conformational states 62

Fig 3-2: The unique mobility shift of SecA2 on an agarose gel is Mg^{2+}ADP dependent and is observed in SecA2 that is not His_6 –tagged 66

Fig 3-3: SecA2 reveals a unique structural rearrangement on binding ADP 67

Fig 3-4: ADP-bound and free forms of SecA2 can be separated by Blue-Sepharose chromatography 69

Fig 3-5: SecA2 binds ADP with high affinity 72

Fig 3-6: The ADP-induced rearrangement is not due to an oligomeric state change 76

Fig 3-7: Limited proteolysis experiments indicate the nucleotide-induced rearrangement is not due to a change in surface charge 79

Fig 3-8: The ADP-induced rearrangement is not due to a change in surface charge 80

Fig 3-9: Binding of ADP enhances thermal stability of SecA2 82

Fig 3-10: Limited proteolysis of SecA2 85

Fig 3-11: Probing the proximity of cysteines using pyrene excimer fluorescence 90

Fig 3-12: Probing clamp regulation in SecA2 using disulfide bond formation 92

Fig 3-13: Binding of ADP induces movement of the PPXD to close the clamp of SecA2 but not in SecA1 96

Fig 4-1: Dimer configurations of *M. tuberculosis* SecA1 106

Fig 4-2: Oligomeric state of *M. tb* SecA1 and SecA2 110

Fig 4-3: *M. tb* SecA1 does not form a salt-resistant dimer 115

Fig 5-1: Establishment of a proton gradient across *M. smegmatis* vesicles assessed by ACMA fluorescence quenching 121

Fig 5-2: *M. smegmatis* vesicles containing HA-tagged SecY are sealed and can maintain a proton gradient 124

Fig 5-3: *M. tb* SecA1 associates with the membrane while SecA2 does not 127

Fig 6-1: Model to explain Sec-dependent translocation in *M. tuberculosis* 133

Chapter 1

INTRODUCTION

A. Sec dependent protein secretion- an overview

In bacteria, about a third of the proteome is secreted. In order to export these proteins from the cytoplasm, bacteria have evolved several export pathways, of which the 'Sec' pathway is the only one that is essential for cell viability in bacteria, archaea and fungi (1). This pathway is comprised of a single essential SecA ATPase, the SecYEG translocon and several accessory proteins (2-4). A protein that is destined to be exported, is called a 'precursor-protein' or 'pre-protein' and is synthesized with an N-terminal signal sequence, which serves as an 'address tag' that directs its route to the SecYEG translocon (5). These 'tags' are around thirty amino acids in length and are surprisingly not conserved but highly variable. The signal sequence has a tripartite structure, comprised of a positively charged amino terminus, a hydrophobic core and a polar carboxyl end region that contains the sequence for recognition and cleavage by signal peptidase once exported (6). Pre-proteins are faced with several different export routes depending on whether their final destination is the integral membrane, periplasm, outer membrane or extra-cellular milieu. Based on certain features of the nascent chain, the SecYEG translocon facilitates the export of precursors in a co-translational or post-translational manner (7,8) (Figure 1-1).

Co-translational translocation

Precursors that are destined to be membrane proteins have extremely

hydrophobic signal sequences. A ribonucleoprotein complex called SRP (signal recognition particle) associates with the ribosome and is thought to 'screen' the nascent chain of a pre-protein as it emerges from the ribosome exit tunnel. SRP then binds to highly hydrophobic signal sequences with high affinity, forming the RNC (ribosome nascent chain)-SRP complex (9-11). In bacteria, this complex is recruited to the SRP receptor FtsY where it is stabilized by the GTPase domains of SRP and the receptor (12,13). FtsY possesses an acidic domain that interacts with the SecYEG translocon (14). The cargo RNC is then delivered by FtsY to the SecYEG translocon in a step involving GTP hydrolysis (13,15). Hydrolysis of GTP enables disassembly of the SRP-receptor complex facilitating the recycling of SRP (16).

Post-translational translocation

General pre-proteins once synthesized, must be maintained unfolded in order to be exported by the SecYEG translocon (17). This function is fulfilled by several chaperones such as Trigger factor, DnaK, GroEL and SecB (in case of Gram negative bacteria), which associate with the pre-protein after its emergence from the ribosome exit tunnel. SecB, however, is a unique chaperone because not only does it prevent folding of the pre-protein but also targets it to the SecA ATPase by directly binding to SecA itself (18). SecB is a tetramer, comprised of a dimer of dimers (19). A surface exposed groove is present which is hydrophobic and is thought to bind the signal peptide (18). The mechanism for recognition of pre-proteins by SecB is not well understood, however a 'kinetic partitioning' model for the same has been put forth, based on interaction of SecB

with maltose-binding protein (MBP) (20). Since SecB can interact with the precursor form of MBP or slow folding mutants of MBP, but cannot interact with mature MBP or other proteins with a fast folding rate, the model suggests that association of SecB with precursors is dependent on the rate of folding of the precursor. Since the signal peptide has been shown to slow down the folding rate of a precursor, association of precursors with SecB is favored (20,21). SecB delivers the unfolded pre-protein to the SecA ATPase by directly interacting with SecA. The extreme C-terminus of SecA is involved in SecB binding and is highly conserved (22). This site is positively charged and also comprises a zinc-binding site that is important for binding to both SecB and anionic phospholipids (23). SecA is a homodimeric protein that binds to to both the signal sequence and mature regions of pre-proteins (24) and targets them to the membrane. SecA also binds to the SecYEG translocon with high affinity (25) (Table 1-3) and drives the export of the unfolded precursor across the translocon using the energy of ATP hydrolysis and the proton-motive force (PMF) (26) (Figure 1-1). The translocon is a heterotrimeric protein complex that is made up of the main channel protein SecY that is comprised of ten transmembrane segments (TMSs), SecE and SecG. TMS 1-5 and 6-10 of SecY are arranged to resemble a clamshell (27) (Figure 1-2). The hinge between the two halves of the clamshell structure is provided by two helices of SecE that give the translocon its flexibility and stability. Opposite this hinge is a potential opening between TMS 2 and TMS 7 referred to as the ‘lateral gate’. This feature is thought to enable the translocon to open laterally into the membrane for insertion of membrane proteins. The

lateral gate has been shown to widen to different extents to translocate a range of pre-proteins that differ in amino acid composition (28). The SecG protein also interacts with SecY and forms part of the translocon but is not essential for translocation; however it enhances translocation efficiency (29). The overall structure of the translocon is that of an hourglass. At the constricted region, six hydrophobic residues are present that form a seal to provide a barrier for small molecules and ions. This is referred to as the 'pore ring' (30). Below the pore ring is a short helix called the 'plug'. Although the plug is not essential for cell viability or translocation, its role is to further seal the channel to water, small molecules and ions (30). The plug is thought to sense the hydrophobicity of the nascent polypeptide chain being translocated so that it can be displaced by hydrophilic polypeptide chains but would block hydrophobic polypeptides, potentially directing such segments into the membrane via lateral translocation (31). SecYEG has been shown to associate with other membrane protein complexes SecDFYajC and YidC for the export of some pre-proteins (32,33).

Once the pre-protein is translocated across the SecYEG pore, the signal sequence is cleaved by signal peptidase (SPaseI) if the final destination of the protein is the periplasm, and the mature protein folds with the assistance of periplasmic chaperones in case of Gram-negative bacteria (34). In case of outer membrane or lipoproteins, the pre-protein is further directed by chaperones to the BAM (β-barrel assembly machinery) (35) or LOL (lipoprotein outer membrane localization) complexes respectively (36). In some cases pre-proteins are exported across the outer membrane into the extracellular milieu.

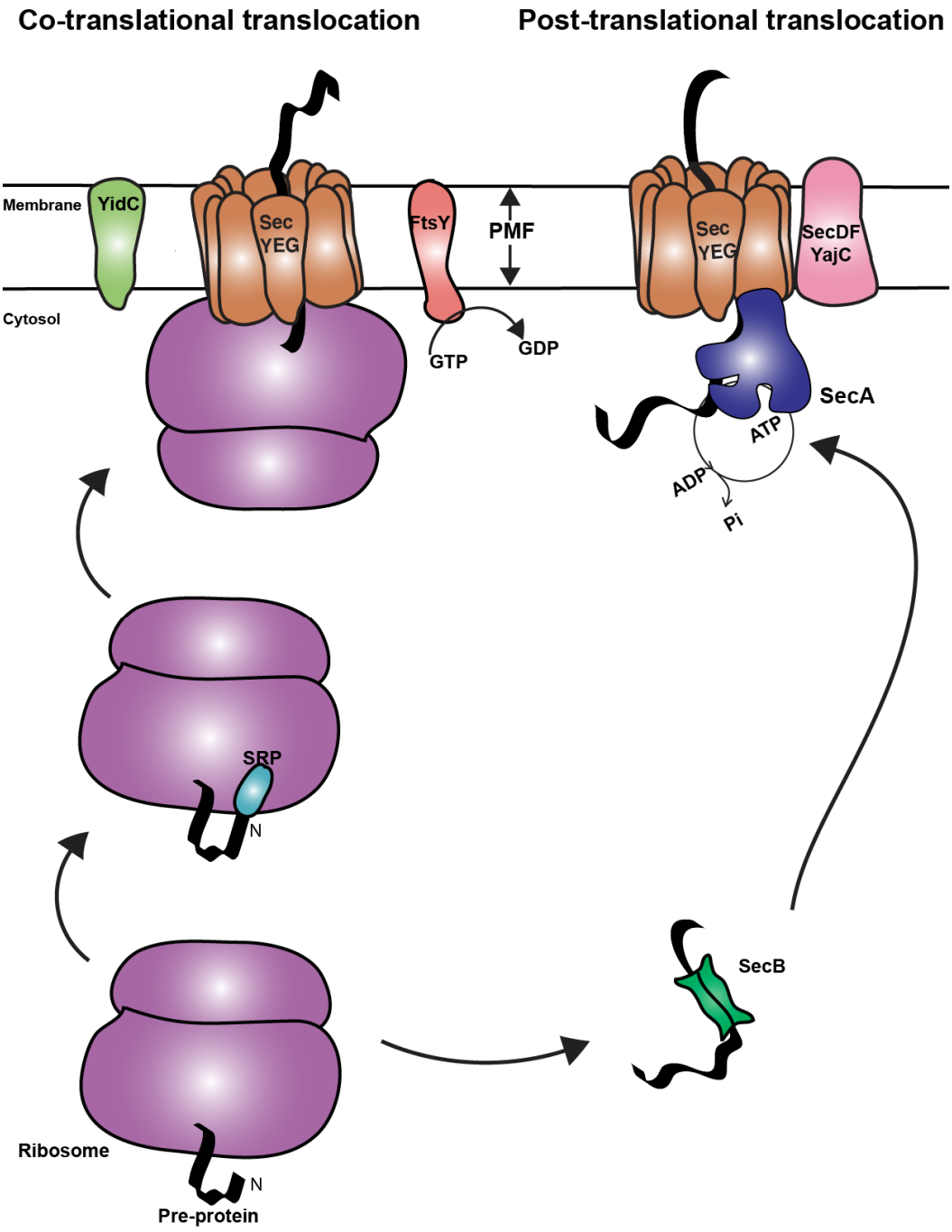

Figure 1-1: Graphical representation of co and post-translational translocation by the Sec pathway.

Detailed description can be found in the text.

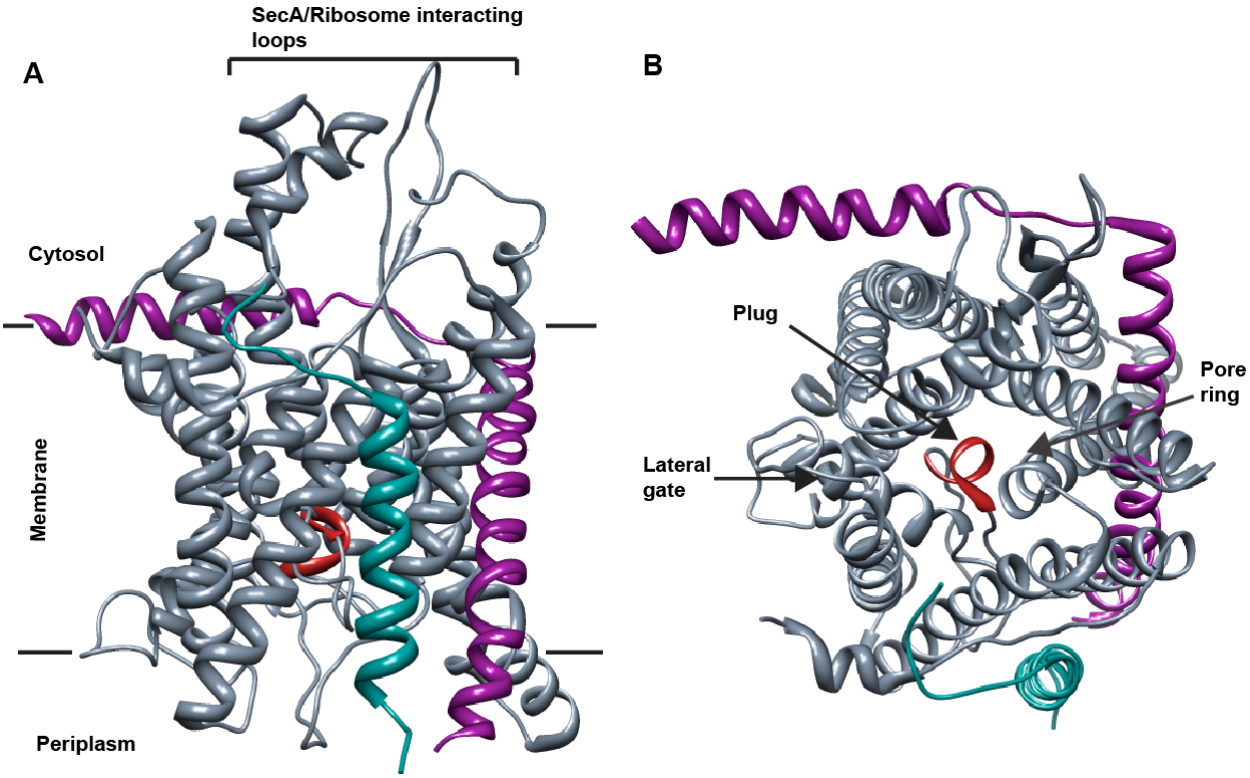

Figure 1-2: Structure of the SecYEβ translocon of *M. jannaschii* PDB ID 1RHZ (37).

The structure has been modified using Chimera (38) to show the side view (A) and top view from the cytosol (B). The SecY protein is show in dark gray, SecE in majenta and SecG (β) in deep cyan. The plug helix of SecY is shown in red.

B. Accessory Sec systems in bacteria

Even after decades of research on the Sec-dependent pathway, it was believed that bacteria had only a single essential SecA ATPase protein. In the past decade however, advances in proteomics and whole genome sequencing led to the identification of an additional *secA* gene in several Gram-positive bacteria. This additional SecA homolog called SecA2, is functionally distinct from SecA1 and has been shown to be a more specialized SecA protein, required for the export of only a subset of precursor proteins (39-42). Further research on the accessory SecA protein led to the broad classification of these systems into:

1) SecA2 only secretions systems

2) SecA2/Y2 secretion systems

SecA2 only secretion systems

These systems are found in bacteria like Mycobacteria, Corynebacteria and Listeria that have a SecA2 homolog but lack an additional SecY protein or other accessory secretion factors. In these systems the SecA2 protein is thought to function with the canonical SecYEG translocon either independently or in concert with SecA1. In Mycobacteria and Listeria, *secA2* is not essential but in pathogens like *Mycobacterium tuberculosis* (*Mtb*) and *Listeria monocytogenes* deletion of *secA2* attenuates virulence (39,43). However; in *Corynebacterium glutamicum* and *Clostridium difficile* SecA2 was found to be essential for viability (44,45). Precursor proteins that require SecA2 for export have been identified in Mycobacteria, Listeria and Clostridia (Table 1-1). Some of these pre-proteins

resemble a conventional Sec-dependent precursor and have a signal sequence while some of the pre-proteins do not (46).

SecA2/Y2 systems

Bacteria such as some Streptococci and Staphylococci that possess such systems, contain an additional SecY protein that is thought to function as a translocon in concert with the SecA2 protein. Unlike the loci in the 'SecA2 only' systems, the SecA2/Y2 genomic locus is highly conserved in bacteria possessing such systems (Figure 1-3). Additionally, such genomic loci also encode related genes such as genes encoding for SecA2-dependent substrates, enzymes involved in glycosylation of such substrates prior to export as well as accessory secretion proteins that associate with SecA2 or SecY2. Proteins that are exported by the SecA2/Y2 system are heavily glycosylated and cannot be exported by the conventional SecA1/YEG pathway (41). For each polypeptide backbone of GspB, a SecA2-dependent substrate, around 100 monosaccharide residues are added (47). These proteins are called serine-rich repeat (SRR) glycoproteins and have an unusually long N-terminal signal sequence (~ 90 amino acid residues) but possesses the characteristic tri-partite nature of the Sec signal sequence. This N-terminal region of the signal sequence has a KxYKxGKxW motif that is unique and predicted to be important for targeting the pre-protein to the membrane (48). The signal sequence is followed by an accessory Sec transport (AST) domain that is not conserved but required for SecA2/Y2 export (49), a short SRR region, a ligand binding region, a long SRR and a C-terminal LPXTG motif that is required for anchoring to the cell wall (50).

The mature region of the protein gets glycosylated at the SRR regions although the type of glycosylation and structure of the glycan is not yet known. Even though glycosylation is not required for SecA2/Y2 export, the addition of carbohydrate moieties distinguishes these pre-proteins from typical Sec-dependent precursors in stability, solubility, protease resistance and binding properties (50) and prevents them from being exported by the general SecA1/YEG pathway.

The SecY2 protein of the SecA2/Y2 system shares low sequence similarity to its SecY counterpart (20% identity, 60% similarity) but is expected to form a channel like SecY. The cytosolic loops in SecY that are important for SecA interaction are absent in SecY2, indicating that it probably does not interact with conventional SecA proteins. Pore ring residues of SecY2 consist of Leu and Met instead of Ile as in the case of SecYEG. There is no feature in SecY2 that would suggest any unique interaction with glycosylated substrates. In case of the conventional SecY protein, SecE is required for stabilizing the translocon. Two unique proteins Asp4 and Asp5 that have predicted transmembrane segments are thought to take the place of SecE and SecG in the SecA2/Y2 system (51). In addition to Asp4 and Asp5, bacteria that have SecA2/Y2 systems also have Asp or Gap (accessory secretion proteins or glycosylation associated protein) 1, 2 and 3 proteins. These proteins are thought to play an important role in SecA2/Y2 mediated export. Asp2 and 3 have been shown to bind to SecA2 as well as unfolded pre-proteins (52). In GspB, these proteins bind to the SRR regions (53).

The SecA2 proteins in such systems are smaller than their SecA homologs due

truncation of 45 C-terminal residues. They also have a proline residue at the C-terminus. They are around 70 % similar (~40 % identical) to their corresponding SecA homologs and most of the similarity lies in the motor domains. Nucleotide binding and hydrolysis is required for SecA2-dependent export (54). The SecA1 and SecA2 homologs are not interchangeable, suggesting a distinct role for SecA2 in pre-protein export. The SecA2 proteins in this system appear highly specialized for the export of their respective unique glycosylated pre-protein as *S. pneumoniae* SecA2 cannot export GspB in *S. gordonii* despite 79% sequence similarity (61% identity) between *S. pneumoniae* SecA2 and *S. gordonii* SecA2. Further, *S. sanguinis* SecA2 can only partially complement a *S. gordonii ΔsecA2* strain despite 91% similarity (81% identity) between *S. sanguinis* SecA2 and *S. gordonii* SecA2.

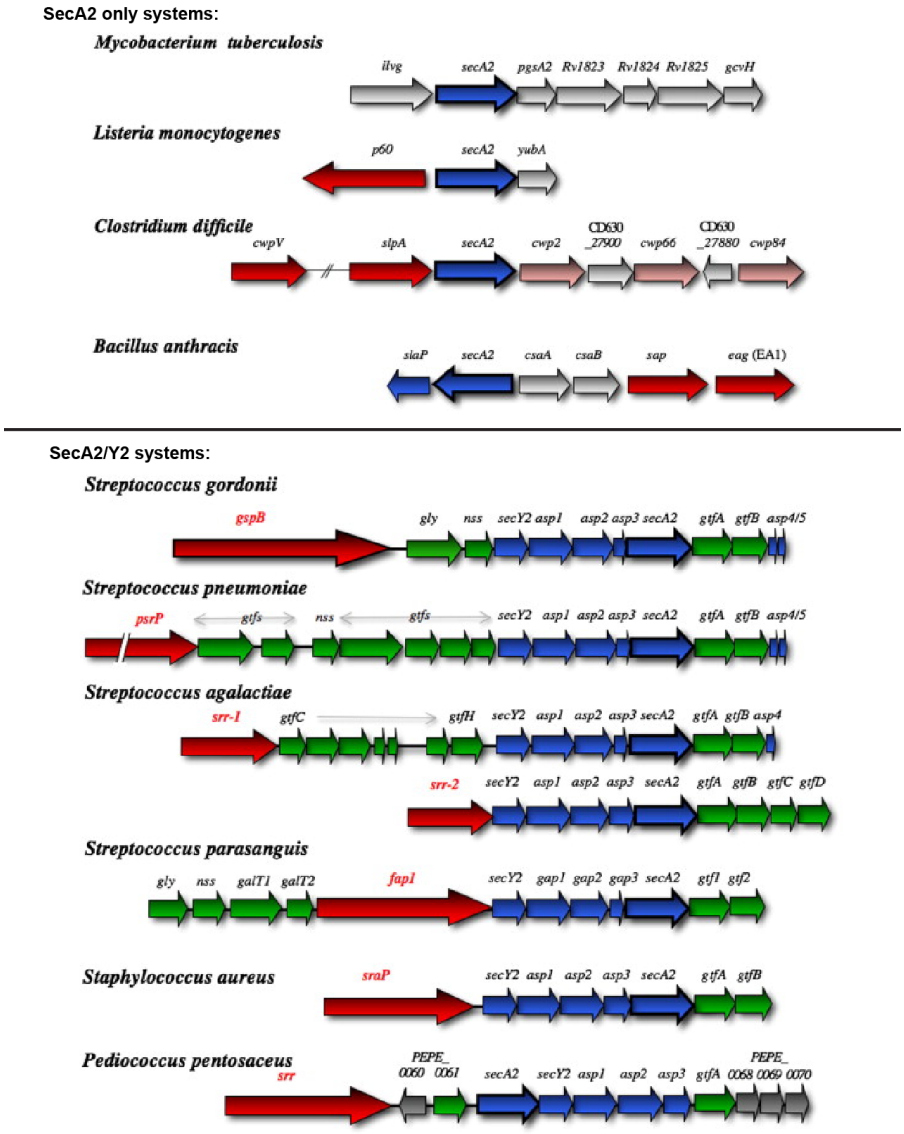

Figure 1-3: Genetic loci encoding *secA2* in bacteria containing SecA2 only as well as in bacteria containing SecA2/Y2.

The figure has been modified from Bensing et al. (50) to show gene organization in bacteria with SecA2 systems only, where the genomic locus is not conserved and contains genes encoding for SecA2-dependent pre-proteins in some cases as well as genes encoding proteins unrelated to the Sec system. On the other hand, in the SecA2/Y2 containing organisms, the genetic loci are highly conserved and contain genes directly involved in SecA2-dependent export such as genes encoding SecY2, pre-proteins and glycosylation enzymes.

Organism	Protein (s) exported	Signal	Function/Predicted Function	Refer-ence
Mycobacterium tuberculosis	Fe-superoxide dismutase (sodA)	No	Removal of reactive oxygen species, virulence factor	(39)
Mycobacterium smegmatis	Msmeg 1704 Msmeg 1712	Yes Yes	Sugar binding lipoproteins	(40)
Mycobacterium marinum	Protein kinase G (PknG)	No	Virulence factor	(55)
Listeria monocytogenes	p60 NamA Mn-superoxide dismutase (sodA) Lap (Listeria adhesion protein)	Yes Yes No No	Peptidoglycan hyrolysis Removal of reactive oxygen species Promotes paracellular translocation of Listeria	(56) (57) (58)
Clostridium difficle	S-layer protein A (SlpA) Cell wall protein (CwpV)	Yes Yes	Outer layer protein, adhesion Auto-aggregating factor	(45)
Bacillus anthracis*	S-layer proteins	Yes	Outer layer proteins, adhesion	(59)

*SecY2 present but not essential for SecA2-dependent export, also genetic locus is more similar to SecA2 only bacteria.

Table 1-1: List of pre-proteins identified to date that require SecA2 for export in bacteria that have 'SecA2 only' secretion systems.

Organism	Protein(s) exported	Signal	Function/ Predicted Function	Reference
Streptococcus gordonii	GspB (surface glycoprotein)	Yes	Platelet binding protein	(41)
Streptococcus parasanguinis	Fimbrial adhesion protein (Fap1) FimA*	Yes	Adhesion Surface protein	(60)
Streptococcus agalactiae	Serine-rich repeat glycoprotein (Srr1)	Yes	Binds human fibrinogen	(61)
Staphylococcus aureus	Serine-rich adhesin for platelets (SraP)	Yes	Platelet binding	(62)

*Not located within the SecA2 locus, and not a serine rich glycoprotein

Table 1-2: List of pre-proteins identified to date that require SecA2 for export in bacteria that have 'SecA2/Y2' secretion systems.

C. The SecA motor

The SecA protein is a member of the superfamily 2 DEAD (DExH/D) proteins that include DNA and RNA helicases (63). The nucleotide-binding domain (NBD) is made up of two RecA like folds that contain Walker A and Walker B motifs that are important for ATP binding and hydrolysis. In addition to the nucleotide binding domains, SecA contains a pre-protein binding domain (PBD or pre-protein cross-linking domain PPXD) (64,65) that has been shown to bind precursor proteins and a C-terminal region that is comprised of a helical wing domain (HWD), C-terminal linker (CTL) that contains a Zn ion (23) and is important for SecB and lipid binding (22,66) and a helical scaffold domain (HSD) (Figure 1-4).

SecA binds ATP with high affinity (Table 1-3), between nucleotide-binding fold 1 (NBF1 or NBD1) and nucleotide-binding fold 2 (NBF2, NBD2 or intra-molecular regulator of ATPase IRA2). ADP release from SecA is the rate-limiting step in catalysis (67-69). Association of SecA with SecY enhances ADP release, however ADP-release still remains rate-limiting (68,70). The ADP-release rate is greatly enhanced when SecA is bound to a pre-protein such that the population of SecA:ADP is shifted to a species rapidly inter-converting between SecA:ATP and SecA:ADP (68). In cytosolic SecA, the 'basal' ATPase activity is low in the absence of a bound pre-protein. This inhibition is due to a helix-loop-helix structure in the HSD also called the intra-molecular regulator of ATPase 1 (IRA1) that contacts both NBD2 and the PPXD (71). This IRA1 region is thought to stabilize the ADP bound form of the protein, thereby preventing futile ATP

hydrolysis. On binding pre-proteins, the ATPase activity of SecA is enhanced via a conserved salt bridge called ‘Gate 1’ that regulates the opening and closing of the nucleotide binding pocket (72).

Since SecA binds to several translocation ligands (Table 1-3), it undergoes different conformational changes (71,73,74). Most crystal structures of isolated SecA show the PPXD in close proximity to the HWD (73,75). The most dramatic conformational change in SecA is one revealed by the crystal structure of *Thermatoga maritima* SecA bound to the translocon. This structure shows the PPXD rotated all the way toward NBD2 (74). This groove formed between the PPXD and NBD2 is referred to as the ‘clamp’. The clamp contains conserved hydrophobic residues and is thought to hold the precursor protein in position (74) as it aligns the PPXD of SecA with the SecY translocon. SecA is thought to bind to precursors in the ‘open clamp’ conformation. Disulfide crosslinking experiments, as well as a structure of *B. subtilis* SecA with a hydrophilic peptide (PDB ID 3JV2), reveal that the pre-protein moves through the clamp of SecA (76). It is not yet known what regulates the movement of the PPXD that leads to opening or closing of the clamp in conventional SecA proteins. Two beta strands between the PPXD and NBD1 are thought to be important for interaction with the polypeptide backbone (76). Further insight into the SecA:precursor interaction comes from an NMR structure of SecA bound to a signal peptide from the LamB porin, KRR-LamB solved by transferred nuclear Overhauser effect spectroscopy (trNOESY) (77). The signal peptide was found to adopt an α-helical conformation and bind in the hydrophobic groove (clamp) of

SecA. Another interesting feature revealed by this structure was that the C-terminal region of SecA was found to obstruct the groove, consequently preventing signal peptide binding. This inhibition was overcome by SecB binding, resulting in an increased affinity of SecA for the signal peptide. Another important feature of SecA revealed in this structure is with respect to its helix-loop-helix (two-helix finger or arginine finger), earlier identified as IRA1. This two-helix finger dips into the SecY channel in a manner that the loop connecting the helices is positioned above the SecY pore suggesting a role for threading pre-proteins through the channel (74,78). Disulfide cross-linking experiments revealed that this region makes important contacts with the pre-protein and was hypothesized to move up and down dragging the pre-protein through the SecY pore (78). A later study showed that the arginine finger does not move during translocation, suggesting a different role for the finger such as opening the channel or simply just preventing back-sliding of the pre-protein during translocation (79).

The cytoplasmic concentration of SecA is around 8 µM (80) creating a large excess of SecA relative to SecYEG (13,000 copies of SecA compared to 500 copies of SecYEG) (63). With a dissociation constant of < 1 nM, significantly lower than the cytosolic concentration of SecA in *E. coli*, SecA is expected to be predominantly dimeric in the cytosol (81). SecA, however, has been shown to monomerize upon interaction with certain components of the translocation machinery (82,83), leading to a debate on the oligomeric state of the protein during translocation. Several SecA proteins from *E. coli* as well as other

organisms have been crystallized as dimers, but the positions of each monomer with respect to the other is different in each of the structures. Most form anti-parallel dimers in which the C-terminal domains face away from each other, in opposite directions (84).

Biochemical studies have shown that high protein concentrations, temperature and low ionic strength favor dimerization while increasing ionic strength favors monomerization (81,85,86). This suggests that the dimer interface is probably stabilized by electrostatic and hydrophobic interactions. Recent biochemical studies reveal two helices (called α0 and α1) at the extreme N-terminus of one SecA protomer form dimer contacts with C-terminal residues of the second protomer (87). The helix α0 forms hydrophobic contacts while α1 forms stronger electrostatic interactions. The study shows that these dimer contacts enable SecA to adopt several states with different orientations of the protomers.

Several models have been proposed to explain translocation of pre-proteins by SecA. Two of popular models are the ‘power-stroke model’ and the ‘Brownian rachet model’. The power-stroke model suggests that ATP binding and hydrolysis by SecA would induce conformational changes in SecA and cause it to exert a mechanical pushing force to direct precursors across SecY. The Brownian rachet model suggests that precursors pass through SecY by Brownian motion and back-sliding is prevented in an ATP-dependent manner by SecA (27).

Models have also been put forth by dissecting the translocation steps

further and suggest that dimeric SecA associates with SecYEG but only one protomer docks at the translocon. The association of 'peripheral' protomer with the docked protomer is salt-sensitive. Docking of the SecA dimer to SecY causes the dimer to become asymmetric and increases the affinity of the docked protomer for the pre-protein (Table 1-3). Once SecA binds a signal peptide, a conformational change is triggered in the SecA dimer causing it to become elongated. This conformation has been referred to as the 'triggered dimer'. These changes are relayed on to SecY, causing its pore to open. ADP is exchanged for ATP but hydrolysis is prevented due to the presence of the bound signal peptide. SecA could partially insert into the channel triggering ATP hydrolysis, which would cause SecA to monomerize and trap the mature region of precursor nascent chain in the translocase. Monomeric SecA would complete the translocation of the precursor across SecY (although the exact stage at which SecA monomerizes is debated in the field). Once the protein is translocated, SecA would loose affinity for SecY and re-dimerize in solution.

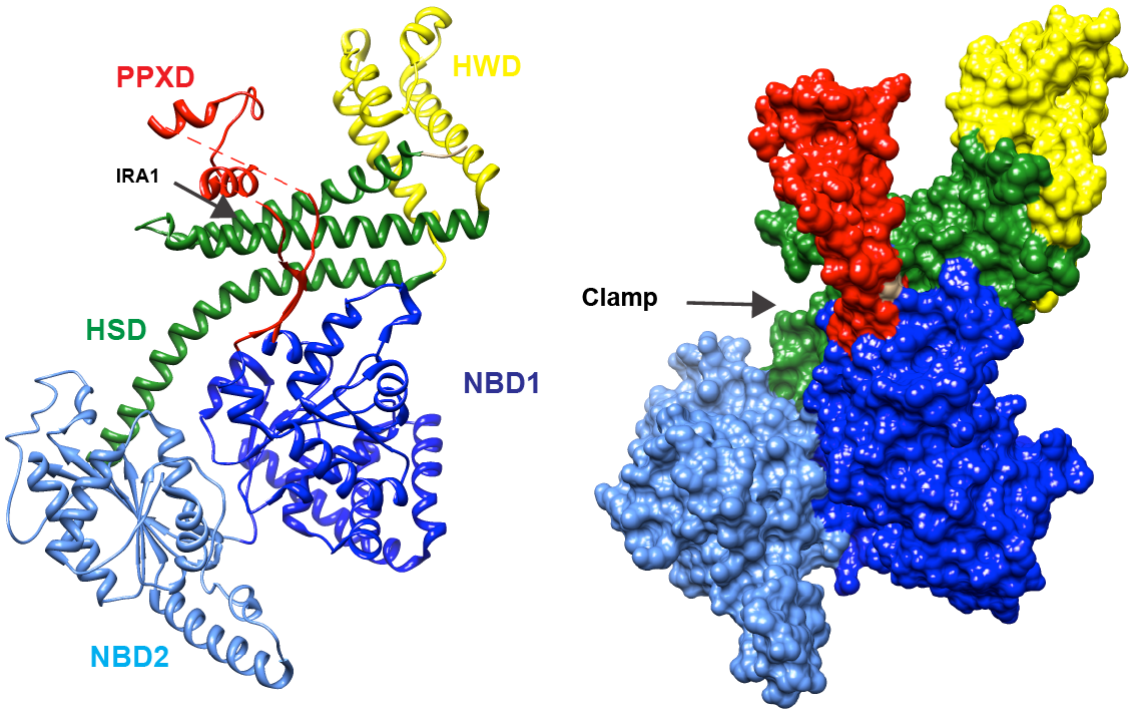

Figure 1-4: Structure of *E. coli* SecA

The *E. coli* SecA structure in its apo form is shown in ribbon representation (left) and surface representation (right). The structure was made using Chimera, based on the coordinates deposited in the Protein Data bank (2FSF) (88) and has been modified to show only one protomer. The nucleotide binding domains 1 (NBD1) (NBD2) are shown in dark and light blue respectively and the pre-protein binding domain (PPXD) is in red. The C-terminal domain is further divided into the helical scaffold domain (HSD) in green and the helical wing domain (HWD) in yellow. The intra-molecular regulator of ATPase region (IRA1) that is part of the scaffold domain is shown with an arrow. The groove formed between the PPXD and NBD2 called the 'clamp' is shown with an arrow in the surface representation.

Interaction	K_d	Reference
SecA:SecA	0.7 nM	(81)
SecA:SecB	1.6 µM	(89)
SecY-SecA:SecB	30 nM	(90)
SecY-SecA:SecB-preprotein	10 nM	(91)
SecA:preprotein (proPhoA)	3 µM	(24)
SecA:signal sequence (proPhoA)	32 µM	
SecA: mature protein (proPhoA)	7 µM	
SecY-SecA:preprotein (proPhoA)	0.23 µM	
SecY-SecA:mature protein (proPhoA)	0.6 µM	
SecA.Mg^{2+} : ATP	0.32 µM	(69)
SecA:SecY	~3-4 nM	(81)

Table 1-3: Binding affinities of SecA for different ligands important in Sec-dependent protein translocation.

D. The Mycobacterial Sec system

Sequencing of the *Mycobacterium tuberculosis* (*M. tb*) genome in 2000 led to the identification of the *secA2* gene, the first SecA2 homolog to be reported (92). In Mycobacteria, *secA1* was found to be essential for viability suggesting that it is the 'house-keeping' SecA and likely functions in a manner similar to *E. coli* SecA. Further studies revealed that *secA1* and *secA2* are not interchangeable (92); however *M. smegmatis secA2* can substitute for *M. tb* secA2 during growth of *M. tb* in macrophages. Further, *M. smegmatis* SecA2 can also restore the rough colony phenotype to a *M. tb ΔsecA2* strain, which shows a smooth colony phenotype unlike the rough colonies produced by a wild type *M. tb* strain. Full length *M. tb secA1* cannot compensate for a temperature-sensitive defect of an *E. coli* SecA *ts* strain but when the first 225 amino acid residues of *M. tb* SecA1 were fused to the remaining region of *E. coli* SecA (225-901), the chimeric protein was able to grow at non-permissive temperatures (93) suggesting that the C-terminal regions of SecA proteins responsible for interaction with SecY and lipids have evolved for interaction of the SecA protein with its own specific bacterial membrane making it unique.

Further analysis of the Sec system in Mycobacteria showed that when secA2 in *M. tb* is deleted, the bacteria are highly attenuated in virulence suggesting that SecA2 may be responsible for exporting virulence factors (39) This *M. tuberculosis ΔsecA2* strain shows enhanced priming of CD^+ T cells *in vivo*, is pro-apoptotic and combined with a defect for lysine auxotrophy (*M.*

tuberculosis ΔsecA2ΔlysA), the strain is a promising vaccine as it shows better protection and is safer than the traditional Bacillé Calmette- Guerin (BCG) vaccine (94,95). One strategy employed by *M. tb* to survive in host macrophages is the prevention of phagosome acidification by arresting the formation of phagolysosomes. After infection of macrophages with the *M. tuberculosis ΔsecA2* strain, phagosomes were more acidified suggesting that SecA2 is important for secretion of factors that play a role in phagosome maturation arrest and promotes the growth of *M. tb* in host macrophages (96).

M. tb SecA2 has been shown to be important for the export of Fe-dependent superoxide dismutase A (SodA), a protein that lacks a typical Sec signal sequence (39). The SodA enzyme functions to remove reactive oxygen intermediates (ROI) so it is believed that perhaps export of SodA by *M tb*. SecA2 is a strategy devised by the bacterium to counteract the oxidative burst by the host macrophages. Similar results are seen in *Listeria monocytogenes*, where Mn-SodA is secreted in a SecA2-dependent manner, however secreted SodA is differentiated from cytosolic SodA by phosphorylation (57). Secreted SodA is not phosphorylated while cytosolic SodA phosphorylated. In *Mycobacterium smegmatis*, two predicted sugar-binding lipoproteins (1704 and 1712) that have typical Sec signal sequences were shown to require SecA2 for export (40). In *L. monocytogenes*, four predicted lipoproteins were identified, one of them belonging to the same class as *M. smegmatis* 1704 and 1712 (56).

Biochemical studies have shown that both *M. tb* SecA1 and SecA2 are ATPases and are expressed at equal levels in the cell (43). Both proteins bind

ATP with high affinity and hydrolyze the nucleotide in a manner similar to *E. coli* SecA (43). Additionally, a Walker box variant of SecA2 that cannot bind ATP is unable to complement a *M. tb ΔsecA2* strain for growth in macrophages. The *M. tb ΔsecA2* strain could only be rescued when complemented with wild-type *secA2* on a plasmid confirming that the ATPase activity of SecA2 is required for the growth of *M. tb* in macrophages (43).

ATP binding is required for SecA2-dependent export even in *M. smegmatis* as a strain containing the corresponding Walker box mutation in SecA2, *M. smegmatis secA2 K129R* could not export 1704 and 1712 pre-proteins (97). A *M. smegmatis ΔsecA2* strain shows defective growth on rich agar and shows increased sensitivity to azide. Not only is the *M. smegmatis secA2 K129R* strain unable to complement the defects associated with *M. smegmatis ΔsecA2*, but also exacerbates the *M. smegmatis ΔsecA2* phenotype, characteristic of a dominant-negative phenotype (97). Based on quantitative immunoblot analysis of subcellular fractions, *M. smegmatis* SecA1 is equally distributed between the membrane and the cytosol, while SecA2 is only localized to the cytosol. The SecA2 K129R protein however, shifts localization to the membrane suggesting that the dominant negative phenotype may be due to the inactive SecA2 mutant trapped at the SecY translocon (97). Similar results were seen in *Clostridium difficile* when a Walker box mutant of SecA2 (SecA2 K106R) was generated.

M. smegmatis secA2 K129R phenotypes have been shown to be associated with decreased SecY levels. *S*uppressor analysis led to the

identification of two extragenic suppressors that mapped to the *secY* protomoter region (98). These suppressors were found to increase *secY* transcription and consequent expression levels. Further, these suppressors alleviated the *M. smegmatis secA2 K129R* phenotype. Other suppressors associated with increasing SecY expression levels were identified, but those suppressors did not map to regions within the *secY* gene. Together these results show that the defects associated with the *M. smegmatis secA2 K129R* phenotype are due to improper functioning of SecY either due to degradation of SecY or an inactive translocation complex, perhaps due to jamming of the translocon (98). Additionally, these results highlight the fact that Mycobacterial SecA2 likely functions with the conventional SecYEG translocon, as opposed to another channel like SecA2 in bacteria with SecA2/Y2 systems.

Since post-translational modifications seem important for directing export to the accessory Sec systems in SecA2/Y2 containing bacteria, it seemed likely that such modifications might play a role in SecA2 export in Mycobaceria, especially since SecA2-dependent precursors Msmeg1712 and Msmeg1704 have lipobox motifs. However; it was found that the signal sequence of precursors is not required for SecA2-directed export suggesting that SecA2 must recognize a feature of the mature chain of the pre-protein. Also since the signal sequence contains the lipobox motif, mutation of the lipobox still rendered the pre-proteins SecA2-dependent verifying that lipid modification is not a pre-requisite for SecA2 export (99). Using a SecA1 depletion strain of *M. smegmatis*, it was also shown that neither SecA1 nor SecA2 can solely export Msmeg 1712,

suggesting that SecA2 does require SecA1 for exporting pre-proteins (97).

E. Structure of *M. tuberculosis* SecA1

The *M. tb* SecA1 was crystallized in apo form (PDB ID 1NL3) with a resolution of 2.8 Å and the protein in complex with Mg^{2+}:ADP-β-S (PDB ID 1NKT) was crystalized at 2.6 Å (100). The protein crystallized as an antiparallel dimer, although cryo electron microscopy (EM) reconstructions done under conditions similar to those used in crystallization revealed a SecA1 tetramer. The overall domain organization of SecA1 seems similar to SecA proteins from other bacteria (Figure 1-5). The protein consists of two motor domains encompassing residues 2-221 and 360-589 (NBD1 and NBD2 respectively). Nucleotide is bound between these two domains. The protein also contains a probable pre-protein binding domain (PPXD or PBD) called the substrate specificity domain (SSD) and helical core domain (HCD) also called IRA1 in other SecA proteins. A long helix joins NBD2 to the HCD. The structure with bound nucleotide overlays well with the apo form of the structure, except for a few amino acid residues directly involved in nucleotide binding indicating no major conformational changes are caused by ADP binding to SecA1. The residues involved in forming dimer contacts in the crystal structure are highly conserved and hydrophobic in nature. Recently however, a bioinformatics program called EPPIC that identifies biologically relevant protein-protein contacts revealed a new dimer interface in *M. tb* SecA1 (PDB ID 1NL3) that is related to the *B. subtilis* SecA (PDB ID 1M6N) dimer interface. The new contacts would involve contacts between the extreme N-terminus of one protomer of SecA1 and C-terminal residues of the IRA1 region,

SD and HWD of the other protomer. These contacts at the interface involve both hydrophobic and electrostatic interactions.

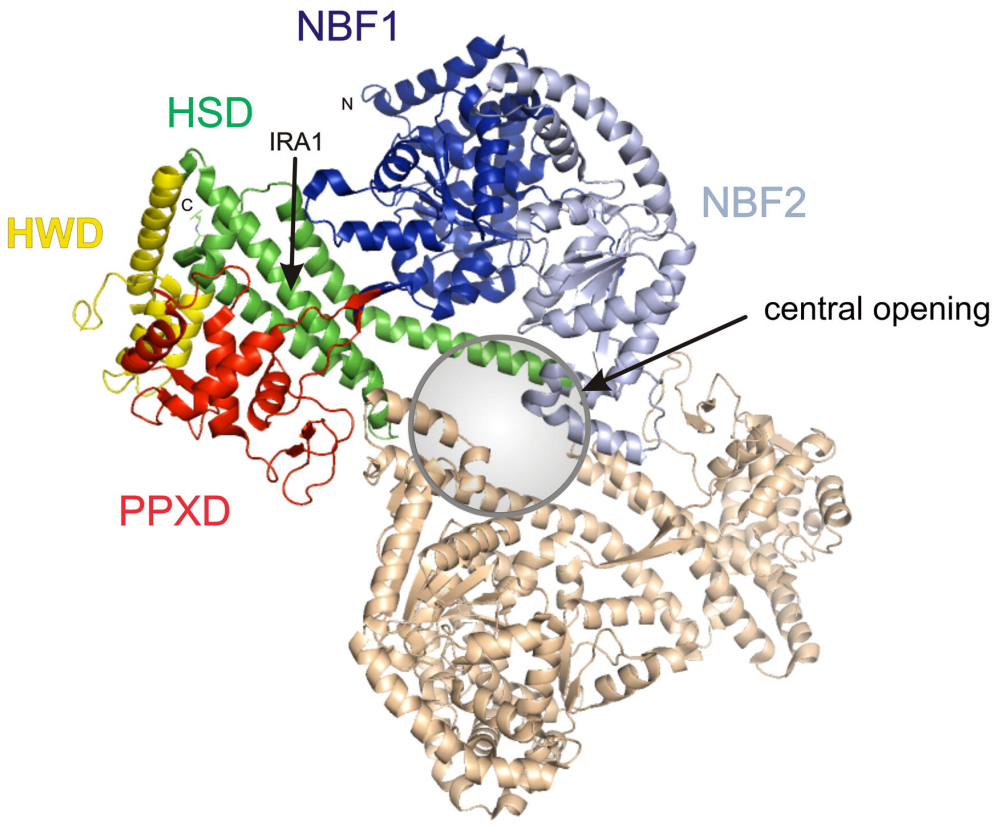

Figure 1-5: Structure of *M. tuberculosis* SecA1

The structure of the *M. tb* SecA1 dimer (1 NKT) (100), represented by du Plessis et al. in a review article (101) is shown. One protomer of SecA is colored to show the different domains; nucleotide binding domains 1 (NBD1) and 2 (NBD2) in dark and light blue respectively, pre-protein binding domain (PPXD) in red , helical scaffold domain (HSD) in green and the helical wing domain (HWD) in yellow while the second promoter arranged in anti parallel fashion is shown in beige. The positions of the extreme amino (N) and carboxyl (C) termini are shown. The intra-molecular regulator of ATPase region (IRA1) is shown with an arrow. The orientation of the two protomers in the structure gives rise to a central opening between the protomers. This opening is thought to be aligned with the opening of the channel SecY.

F. Domain organization of *M. tuberculosis* SecA2

M. tuberculosis SecA2 (86 kDa) is smaller compared to its SecA1 homolog (106 kDa) owing to a large truncation of its C-terminal domain (Figure 1-6). Even though this is a common feature among SecA2 proteins, *M. tb* SecA2 also has a deletion of around 35 amino acid residues between ATP binding motifs V and VI in NBD2 as well as deletions in the helical wing domain.

Based on amino acid sequence alignment, SecA2 only shares thirty-three percent sequence identity to SecA1 (Figure 1-7). The highest conservation lies in the nucleotide-binding domains, particularly among residues directly involved in nucleotide binding and hydrolysis. Like SecA1, SecA2 also contains Walker A and Walker B motifs that have been shown to be important for ATP binding. In fact, SecA2 has a higher affinity for ATP (K_d ~1.9 μM) than SecA1 (K_d ~21 μM) and the ATPase activity of SecA2 is essential for the survival of the bacteria in host macrophages (43). Substitution of the conserved lysine for arginine (K115R) or alanine (K115A) significantly reduces the ability of SecA2 to bind ATP *in vitro* (43).

The greatest variation between the two proteins lies in the C-terminal domain. To date, there is no structural information on any SecA2 protein. However, from analysis of the amino acid sequence, the *M. tb* SecA2 protein like SecA1 and conventional SecA proteins is a member of the superfamily 2 DEAD (DExH/D) proteins that include DNA and RNA helicases suggesting that the motor domains of SecA2 would be structurally similar to that of SecA1.

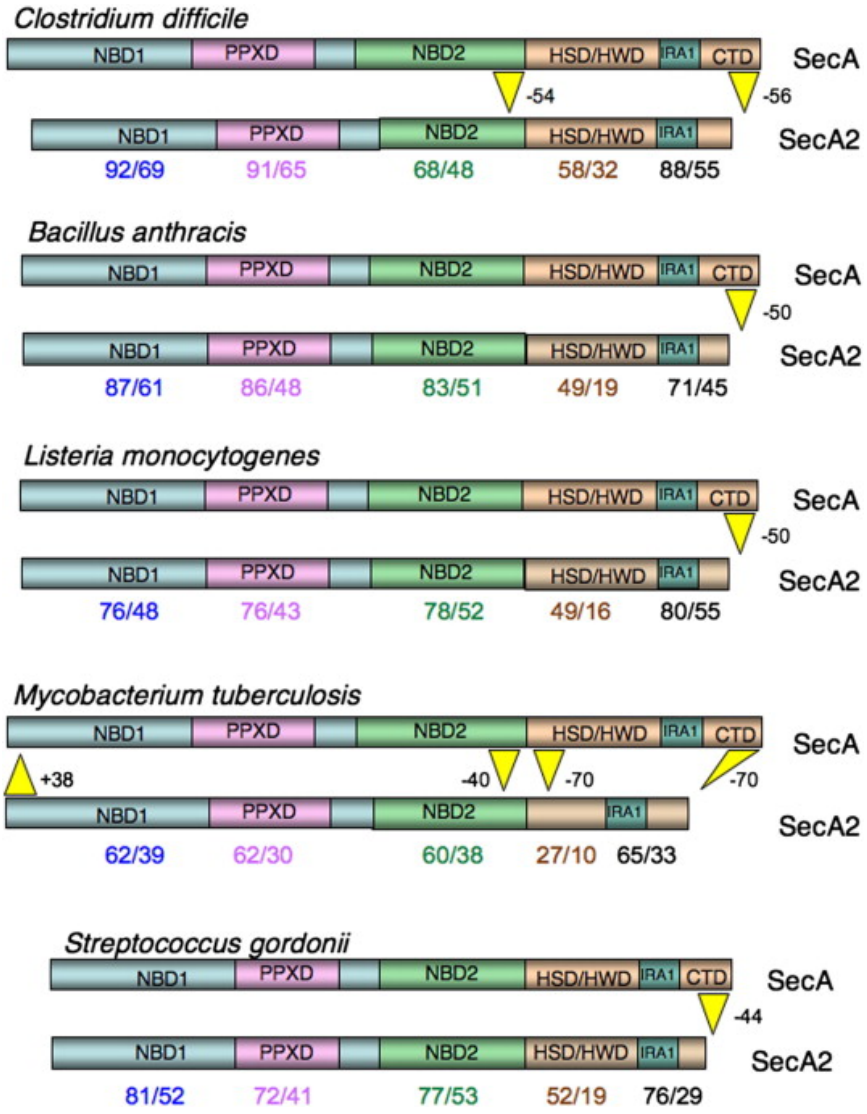

Figure 1-6: Comparison of domain organization of SecA2 proteins.

This figure taken from Bensing et al. (50) compares domain organization of SecA2 proteins and with their corresponding SecA1 homolog as well as with SecA proteins from other bacteria containing an accessory SecA protein. The numbers below represent percent similarity/identity to the corresponding SecA homolog.

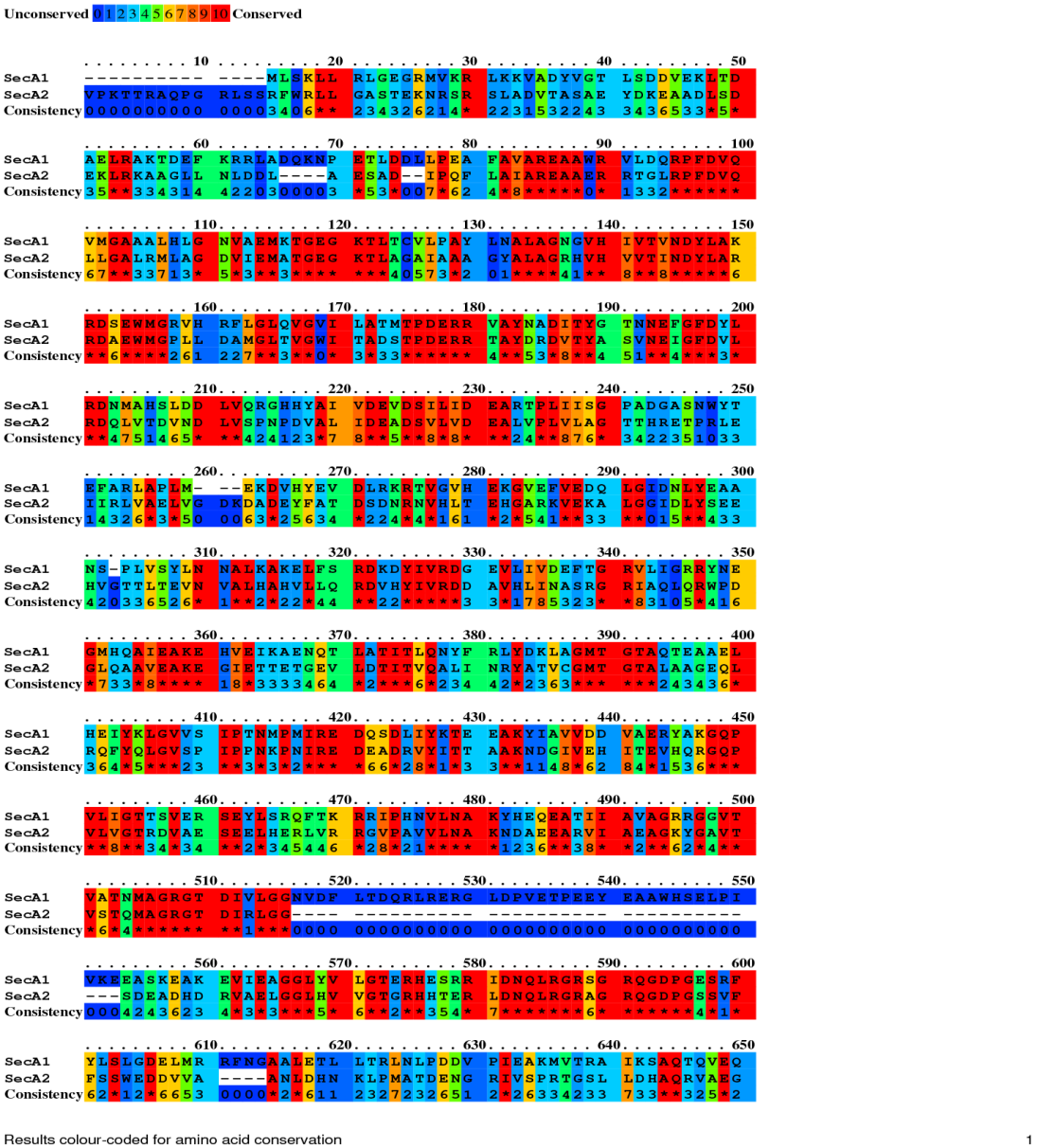

Figure 1-7: Alignment of amino acid sequences of *M. tb* SecA1 and SecA2 by PRALINE (102).

G. Purpose of this study

Since several Gram-positive bacteria, many of which are pathogens such as *M. tuberculosis* have two SecA proteins, several important questions are raised regarding the role and significance of the additional SecA protein. In *M. tuberculosis*, SecA2 is thought to play an important role in virulence by exporting virulence factors like superoxide dismutase (SodA) helping the bacterium to combat the oxidative burst in the host macrophage (39). SecA2 has also been implicated in arresting phagosome maturation, a critical survival strategy employed by *M. tuberculosis* in host macrophages (96). As deletion of the *secA2* gene highly attenuates *M. tuberculosis*, this strain has been further modified and is a promising vaccine candidate against TB (95). Since there is no mammalian SecA homolog, the SecA proteins are also attractive drug targets. However, the the main role of this protein and its mechanism of action is unknown. Despite high sequence similarity between the two SecA proteins, the components of the secretion machinery are able to distinguish them. Since SecA2 is required for exporting only a subset of proteins some of which have typical signal sequences and some of which do not (Table 1-1), certain features of the precursor nascent chain must dictate SecA2 dependence.

This biochemical study explores the atypical features of SecA2 with respect to nucleotide-binding kinetics and membrane association in an attempt to decipher why some bacteria may require an additional SecA proteins and how the secretion machinery may distinguish the two SecA proteins. The study helps to elucidate the role of SecA2 in secretion and its importance in virulence.

Chapter 2

METHODS

A. Molecular Biology and Cloning

All molecular biology work, restriction enzymes, polymerases, ligase and kinase enzymes were purchased from New England Biolabs (NEB) and pET vectors were purchased from Novagen unless specified otherwise. High fidelity versions of all restriction enzymes were used if available from NEB. Primers were synthesized by Integrated DNA technologies (IDT) and the sequence of constructs made was verified by Genewiz. Sterile distilled water was used in all reactions. Autoclaved PCR tubes were used for all reactions and micropipettors and bench surfaces were wiped with bleach to prevent DNA contamination and remove nucleases.

In order to make constructs for the expression of *M. tb* SecA1 and SecA2 proteins *secA1* and *secA2* genes were amplified from *M. tuberculosis* genomic DNA (a gift from Miriam Braunstein). The *secA1* gene was inserted between EcoRV and HindIII sites of a pET30b vector. In order to bring the gene closer to the ribosome binding site, the construct was further digested with Nde I and Nco I. Blunt ends were generated using the Klenow enzyme and ligated to put the *secA1* gene between NdeI and HindIII of pET30b resulting in pND1. The SecA1 protein is expressed with the sequence 'MAM' before the starting valine residue, coded for by a GTG start codon. Between the SecA1 protein and C-terminal His_6

tag, the vector-derived sequence KLAAALE is present. It is important to note that due to blunting of the ends, the NdeI site is disrupted in the final construct pND1. In case of the SecA2 expression vector (pND2), the *secA2* gene was directly inserted between NdeI and HindIII of pET30b. The stop codon before the His_6 tag was not removed when cloning, but was later modified by site directed mutagenesis to generate a construct pND2, in which SecA2 is expressed with a C-terminal His_6 tag. In case of *secA2* in the *M. tb* chromosome, the start site used is a GTG start site located at nucleotide position 91 from the annotated start site (NCBI accession number NP_216337) since this site represents the true start site (43). In pND2, An ATG start codon that codes for methionine was added before the GTG codon to ensure expression in *E. coli*. This construct also has the vector derived sequence KLAAALE between the protein and the C-terminal His_6 tag.

PCR Amplification of DNA

In order to generate the constructs pND1 and pND2, a 50 µl PCR reaction was used for amplification of *secA1* and *secA2* genes from genomic DNA. 1 µl of a 1:50 diluted stock of genomic DNA was used as template. Phusion master mix containing high GC buffer was used. Phusion is a high fidelity polymerase and binds to the template much more tightly than other polymerases available. Such a polymerase is required for amplification of genes from DNA that has a high GC content. Primers for amplification of the *secA1* and *secA2* genes were designed to incorporate the restriction enzyme sites flanking the gene. 6.25 µl of a 4µM stock of each primer was added to the reaction. DMSO at a final concentration of

5 % was added to facilitate separation of the DNA template strands. Sterile nuclease free water was added to a final volume of 50 µl.

For the PCR reaction, the initial denaturation was carried out for one cycle at 98 ºC for 30 seconds (step 1), followed by 30 cycles of denaturation at 98 ºC for 10 seconds, annealing for 30 seconds (annealing temperature was set using the online NEB Tm calculator that is specific for the DNA composition, concentration of primer, type of polymerase and buffer in the master mix) and extension at 72 ºC for 3 minutes (1 Kb of fragment/minute) (step 2). The final extension was carried out for one cycle at 72 ºC for 7 minutes (step 3) and the sample was held at 4ºC until further processed.

Restriction Digestion

The amplified product was verified by running 8 µl of the PCR product mixed with 2 µl of sample buffer on a 0.8 % agarose gel with SYBR safe (Invitrogen) incorporated into the gel, run at 100 V in 1X TAE buffer at pH 8.0 (40 mM Tris, 20 mM acetic acid and 1 mM EDTA). Once the presence of a broad band was detected, the PCR products were purified using the PCR purification kit (Qiagen). Later on, the NucleoSpin Gel and PCR Clean-up kit (Macherey-Nagel) was used routinely as it gave a much higher yield of product. DNA was eluted in 30 µls of water. Vector DNA was prepared by doing a plasmid prep from 4 mL of an overnight culture of *E. coli* DH5α cells using the StrataPrep plasmid mini prep kit (Agilent) and eluting the plasmid in 30 µl of water. Generally, this resulted in a yield of about 2-5 µg of insert and vector DNA. For cloning purposes, plasmid

vectors were always prepared fresh on the day of use, never from frozen stocks as freeze-thawing plasmids was found to make them unsuitable for restriction digestion resulting in smears on the gel instead of single bands. The insert and vector DNA were digested using 50 units of each restriction enzyme (2.5 µl of 20,000 U/mL). This also ensured that the final glycerol concentration did not exceed 5% in a final volume of 50 µl, thus preventing star activity. The appropriate NEB buffer and BSA (when required) were added to a final concentration of 1X and water was used to bring the final volume to 50 µl. When the two restriction enzymes were not compatible for double digestion, single digestions were performed sequentially; however this was very rare. The restriction digestion was performed at 37 ºC for 2 hours. DNA sample loading buffer (6µl) was added directly to the digestion products and they were separated on a 0.8 % agarose gel with SYBR safe, run at 100 V (described earlier) until the bands were well separated. Bands of the digested vector and insert corresponding to the correct molecular weight were cut out from the gel using a razor blade, transferred to a microfuge tube and weighed. DNA was extracted from the gel bands using the Qiaquick gel extraction kit (Qiagen). For a 0.8 % gel, 240 µl of buffer QG was added to 100 mg of gel followed by incubation at 50 ºC for 10 minutes (until the agarose was dissolved). One gel volume of isopropanol was added to the sample, mixed and transferred to a spin column that was centrifuged for 1 minute in a microfuge at maximum speed. This was followed by washes in 500 µl buffer QG and 750 µl buffer PE. After this the spin column was spun without any buffer at maximum speed for a minute to remove any residual

buffer. DNA was eluted in 30 µl of water. This process of gel extraction was found to be effective but resulted in a significant loss of DNA so this step was later modified to exclude gel extraction and PCR purification was performed instead to purify the digested products. In order to do this, verification of complete digestion (observed on a gel) is crucial. Once it was established that complete digestion was obtained, 30 µl of the digestion reaction was purified using the NucleoSpin Gel and PCR Clean-up kit (Macherey-Nagel). The products were eluted in 20 µl of NE buffer from the kit.

Treatement with Klenow

In cases where a region of the plasmid had to be cut, or if the restriction sites in the multiple cloning region of the vector could not be used to incorporate the insert, blunt ended cloning was performed using the large fragment of DNA polymerase I, commonly known as the Klenow fragment. This enzyme fills in 5' overhangs or removes 3' overhangs generating blunt ends. After digestion of the vector or insert or both, NEB buffer 2 was added to a final concentration of 1X, directly to 30 µl (or 20 µl) of the purified digestion products. To this mixture, 50 µM (final concentration) of dNTPs and 0.5 µl of Klenow were added and incubated at room temperature for 20 minutes. This was followed by the addition of 0.5 µl of 0.5 M EDTA and the reaction was heated at 75 ºC for 20 minutes to inactivate the enzyme.

Dephosphorylation of Vector

This step is required to prevent the vector from re-ligating without the

incorporation of the insert. It is mandatory when restriction digestion yields blunt ended products, but is recommended even for vectors with sticky ends, to prevent re-ligation of the vector population that was cut with only one restriction enzyme. The enzyme Antarctic phosphatase (AP) was used for dephosphorylation instead of shrimp alkaline phosphatase (SAP) or calf intestinal phosphatase (CIP) as unlike AP, the products of CIP and SAP reactions require PCR purification to remove the phosphatase before ligation. AP can be inactivated by heat and no further purification of the reaction is required before ligation. For the reaction, 1 µl AP was added to 20 (or 30 µl) of digested and purified vector DNA (or directly to the inactivated Klenow reaction). Antarctic phosphatase buffer was added to a final concentration of 1X. The reaction was incubated at 37 ºC for 15 minutes, followed by heat inactivation of the enzyme at 65 ºC for 5 minutes. The dephosphorylated vector was then directly used in the ligation reaction.

Ligation

Several vector:insert ratios were tested. Ultimately, after several experiences with cloning according to this protocol, 1-2 µl of vector mixed with 5-10 µl of insert in a final volume of 20 µl always resulted in successful ligation. Ligation buffer (final concentration 1X) and 1 µl of T4 ligase was added. Incubation was performed at room temperature for 1 hour. For this, the rapid ligation kit (Fermentas) or T4 ligase at 2,000,000 U/mL (NEB) should be used. Use of T4 ligase solutions at lower concentrations required significantly longer incubation times. Control reactions were always set up that did not contained

only the dephosphorylated vector (no insert) and ligase as well as dephosphorylated vector (no insert) without ligase.

Note that it was difficult to estimate the concentrations of vector (and calculate amount of vector) since the dephosphorylation buffer contains a high ATP, which absorbed significantly at 260 nm. However to calculate the vector:insert, the following formula can be used:

$$\text{Amount of Insert (ng)} = \frac{\text{50ng vector} * \text{size of insert (kbp)}}{\text{size of vector (kbp)}}$$

Use of a unique cutter

Once the ligation reaction was completed, the ligase enzyme was inactivated by heating the reactions at 65 ºC for 10 minutes and then cooled to room temperature. To this reaction, 1 µl of a restriction enzyme was added followed by incubation at 37 ºC for 30 minutes. A restriction site in the multiple cloning region of the vector was picked that would have actually been occupied by the insert. By targeting this site, only vectors that took up the insert would not be affected and remain intact. Care should be taken that the insert itself does not have restriction sites for this particular restriction enzyme and that this enzyme is a unique cutter in the vector.

Transformation

After digestion, the entire reaction was added to 50 µl of competent *E. coli*

DH5α cells on ice for 30 minutes. Heat shock treatment was carried out at 45 ºC for 45 seconds followed by recovery on ice for 3 minutes. 500 µl of SOC medium was directly added to the cells and incubated on a nutator at 37 ºC for 1 hour. The cells were spun down. The pellet was carefully resuspended in ~ 50 µl of SOC medium and the entire volume was plated on LB agar plates containing the appropriate antibiotic and incubated overnight at 37 ºC.

Screening of correct ligation products by colony PCR.

The colonies on plate were screened to check for ones that possessed the plasmids with the correct insert incorporated. The primers chosen for colony PCR were such that one primer would bind to the vector (such as T7 forward primer) and the other would bind to the insert (such as the reverse primer used to amplify the insert from template in the first step of the cloning procedure). This ensures that amplification only occurs when the insert is in the vector and decreases chances of false positive results due to amplification of insert that may be on the agar plate (due to the ligation mixture added to cells which get plated). For colony PCR, a micropipette tip was touched to a colony on the plate and then inserted into a tube containing the PCR reaction mixture (PCR reaction mixture described earlier, however to conserve the master mix, the reaction was reduced to a 25 µl volume reaction, instead of a 50 µl reaction). The same tip was then used to make a streak in one sector of an LB/antibiotic plate that was divided into several sectors. The streak from the colony was numbered according to the corresponding PCR tube it was inserted into. After this was repeated for several colonies, the plate was incubated at 37 ºC overnight. The tubes containing the

PCR reaction mixtures were subjected to PCR using the conditions described in the first part of this chapter. 10 µl of each PCR reaction were taken and added to 2 µl of sample loading buffer. 10 µl were loaded on a 0.8 % agarose gel and run as described earlier. Samples that showed amplification of the correct sized insert indicated successfully ligated products. Once the positive reactions were identified, the corresponding bacterial streak was used to inoculate 5 mL of LB/antibiotic. The cultures were grown overnight with aeration at 30 ºC. Plasmid was extracted from 4mL of the overnight culture using the StrataPrep kit (Agilent) and the presence of the insert was verified by sequencing (Genewiz).

Site Directed Mutagenesis

Site directed mutagenesis of amino acid residues was achieved using the staggered primer method (103). This method was used to decrease the chances of primer dimerization while increasing the chances of annealing the primer to the template. Following this method of primer design, 6-8 non-overlapping bases were added to the 3' end of each primer. The targeted mutation was introduced in both primers and both primers had a G or C base at each end. PCR was carried out in a total volume of 50 µl and the conditions for PCR were similar to those described earlier in this chapter, however instead of genomic DNA, 1 µl of 10 ng/µl plasmid DNA was used as template and DMSO was excluded from the reaction. Also Step 2 was reduced to 16 cycles instead of 30. After amplification, 5 µl of NEB buffer 4 and 2 µl of DpnI were directly added to the 50 µl reaction and incubated at 37 ºC for 2 hours. 10-20 µl was then transformed into *E. coli* DH5α cells by the heat shock method described earlier.

Example of primer design for a G➔A substitution:

The template strands are represented in italics while the primers are represented in bold letters. The base to be changed in shown in red. The arrows represent the direction in which the primers would advance.

Orginal sequence: 5′ tcctgaagtgcgaagcttgggccgcataatgcta 3′

5′ *tcctgaagtgcgaagcttgaggccgcataatgcta* 3′

3′<< **cacgcttcgaactccggcg** 5″

5′ **agcttgaggccgcataatg** >>

3′ *aggacttcacgcttcgaactccggcgtattacgat* 5′

Primer 1: 5′ agcttgaggccgcataatg 3′

Primer 2: 3′ gcggcctcaagcttcgcac 5′

Insertion or deletion of residues by PCR

Insertion or deletion of several bases was done by designing primers that either had the bases to be incorporated (in case of insertion) or excluded a region of the template (in case of deletion). In case the insertion was fairly large, the inserted segment was split between the forward and reverse primer. Examples of such primers are shown below. The template strands are represented in italics while the primers are represented in bold letters. The bases to be inserted or deleted are shown in blue. The arrows represent the direction in which the primers would advance.

Example1: Insertion of FLAG tag (in blue) at N-termimus of SecY in pBAD24.

5′
atggatatcgattacaaggatgacgacgataaggtgctgtctgcctttattag 3′

3′ <<<**gctgctattccacgacagac** 5′

5′ **atggatatcgattacaaggatga**>>> 3′

3′
tacctatagctaatgttcctactgctgctattccacgacagacggaaataatc 5′

Forward primer: 5′ atggatatcgattacaaggatga 3′

Reverse primer: 5′ cagacagcaccttatcgtcg 3′

Example 2: Deletion of DEAD box 3 in SecA2.

5′
cgacatcaggctcggcgggtccgacgaagctgaccacgacagggtcgcggaat 3′

<<<tgtagtccgagccgcccagg 5′

5′

cacgacagggtcgcggaat>>>

3′
gctgtagtccgagccgcccaggctgcttcgactggtgctgtcccagcgcctta 5′

Forward primer: 5′ cacgacagggtcgcggaat 3′

Reverse primer: 5′ ggacccgccgagcctgatgt 3′

The PCR conditions used for amplification were the same as those described earlier in this chapter, except 1 µl of 10 ng/µl plasmid DNA was used as template. 10 µl of the PCR reaction was then mixed with 2 µl of DNA gel loading buffer and 10 µl was subjected to agarose gel electrophoresis in a

manner described earlier. Once it was verified that the product had been amplified, the product was phosphorylated as follows: 4 µl of the PCR product was added to 5 µl of 10X Ligation buffer. 1 µl of T4 polynucleotide kinase was added and the volume was brought up to 50 µl with sterile distilled water. The phosphorylation reaction was incubated at 37 ºC for 30 minutes. The kinase was then inactivated by heating at 65 ºC for 5 minutes and cooled to room temperature. To 4 µl of the phosphorylated product, 2 µl of 10X ligation buffer and 1 µl T4 ligase (2,000,000 U/ mL) was added and the reaction volume was brought up to 20 µl with sterile distilled water. The ligation reaction was incubated at room temperature for 1 hour followed by transformation of the entire reaction into into *E. coli* DH5α cells by the heat shock method described earlier. 200 µl of the transformed cells were plated on LB/antibiotic plates and incubated at 37 ºC overnight till colonies developed.

B. Protein Expression and Purification

The respective plasmids were transformed into *E. coli* Rosetta2(DE3)pLysS competent cells (Novagen) for expression. Expression tests were carried out by inoculating 5 mL LB/antibiotic with a colony, incubated overnight at 37 ºC with aeration. In a similar way, several colonies were inoculated separately in LB broth. A 1:100 dilution of the overnight culture was done in fresh LB/antibiotic and grown to $O.D_{600}$ ~ 0.5. Day cultures were induced with 0.5 mM isopropyl-β-D-thiogalactopyranoside (IPTG) and grown further for 4 hours. Before induction and 4 hours after induction, 0.2 O.D*mL were taken and spun down at maximum speed in a microfuge. The pellets were resuspended in

3X SDS sample buffer and 10 µl was loaded on a 10 % SDS gel, run at 200 V and stained with Coomassie blue. The culture that showed the best induction was chosen for growth on a large scale. The large scale culture (3L) was grown in a similar manner as the ones tested for induction and harvested 4 hours after induction by centrifuging at 4000 rpm (35000 x g) in an SLC 6000 rotor (Sorvall). All purification steps were carried out at 4 ºC. Cell pellets were suspended in Wash 1 buffer (10 mM imidazole pH 8.0, 20 mM Na_2HPO_4, 300 mM NaCl) containing 1X protease inhibitor cocktail (Sigma) or 1X Complete mini EDTA-free cocktail (Roche) and frozen at -80 ºC. Cells were thawed on ice followed by the addition of 1X protease inhibitor cocktail, 450 µg/mL each of DNase and RNase and 10 mM $MgCl_2$ (final concentrations). When the cell density was high and total volume of resuspended cells was ~25 mL, cells were lysed with a French pressure cell (SLM-Aminco) at 20,000 lb/in^2. If the cell density was low, cells were lysed by sonication on ice, using a regular probe on the sonicator (Misonix). The amplitude was set to 35. The pulse was set to remain on for 15 seconds and off for 30 seconds, for a total of 2 minutes of 'on' time. The lysates were centrifuged at 15,000 rpm (32,000 x g) in an F18S-12X50 fixed angle rotor (Sorvall) for 15 minutes to sediment broken cells, followed by ultracentrifugation at 40,000 rpm (162,000 x g) in a T-865 rotor (Sorvall) for 1 hour to spin out the membranes.

Metal affinity chromatography

The clarified lysate (supernatant from the ultracentrifugation spin) was applied to a 10 mL column with Talon Superflow metal affinity resin (Clontech) at

1 mL/min. Unbound protein was eluted with six column volumes of Wash 1 buffer. The His_6 tagged proteins were eluted with six column volumes of 250 mM imidazole pH 8.0, 20 mM Na_2HPO_4, 300 mM NaCl. The flow rate was maintained at 1 mL/min throughout the run and 1.5 mL fractions were collected during the elution step.

SDS PAGE of column fractions

To analyze the fractions by SDS-PAGE, 20 µl of a fraction was added to 10 µl of SDS sample buffer and 10 µl was loaded onto a 10% SDS gel. The gel was run at 200 V and stained with Coomassie blue to visualize the bands.

Concentration of protein by ammonium sulfate precipitation or concentration device

When the volume of protein to be concentrated was large, fractions containing pure protein were pooled and concentrated by ammonium sulfate precipitation at 60 % saturation. To do this, 36.1 g of solid ammonium sulfate was added per 100 mL of protein solution, stirring slowly at 4 ºC for approximately one hour. The solution was centrifuged at 15,000 rpm (32,000 x g) in an F18S-12X50 fixed angle rotor for 20 minutes. The pellet was resuspended in 0.5-1 mL of dialysis buffer and then dialyzed against one liter of 10 mM 4-(2-hydroxyethyl)-1-piperazineethanesulfonic acid (HEPES), pH 7.6 in a dialysis bag with a molecular weight cut-off of 10,000 kDa, overnight at 4 ºC. After this, the buffer was changed twice while dialysis was allowed to proceed for three hours in 1 L of buffer each time.

In case the total volume of pooled protein was around or below 30 mL, an Amicon centrifugal filter device (Millipore) with the appropriate molecular weight cut-off filter was used for concentration. The filter device was rinsed with water to remove glycerol from the membranes before use. The device containing pooled protein was then centrifuged at 4,000 x g in a swinging bucket rotor at 10 minute intervals. The protein concentration was checked each time and when the desired concentration was achieved the protein was dialyzed as described earlier. Once buffer exchange was achieved, aliquots of pure protein were made, frozen at -80ºC and were never refrozen once thawed.

Removal of bound nucleotide by Blue Sepharose chromatography

Blue Sepharose (GE Healthcare) chromatography was used to separate the nucleotide-bound form of SecA2 from the nucleotide-free form. After purification using the Talon column, SecA2-$(His)_6$ was dialyzed into 25 mM Tris pH 7.6 buffer instead of HEPES buffer. The dialyzed protein was loaded onto a 10 mL Blue Sepharose column, washed with 25 mM Tris pH 7.6 for 2.5 column volumes. Nucleotide-free SecA2 was then eluted over 6 column volumes with 2 M NaCl. Fractions of 1.5 mL were collected throughout the run, and also during the wash steps. The flow rate was maintained at 1 mL/min during the entire run. The protein content of the fractions was analyzed by SDS PAGE as described earlier. Fractions containing nucleotide-free SecA2 were pooled, dialyzed against 10 mM HEPES pH 7.6, 25 mM KCl and stored as aliquots at -80 ºC.

Size Exclusion Chromatography

Purified SecA proteins were characterized by size exclusion chromatography using a BioLogic Duo-Flow system (Bio-Rad). Protein (250 µl) was applied at ~ 20 mg/mL to a Superdex 200 10/300 GL column (GE Healthcare), and eluted at 0.25 mL/min in either low salt buffer (10 mM HEPES, pH 7.6, 25 mM KCl, 1 mM $MgCl_2$, 0.1 mM Tris (2-carboxyethyl)phosphine (TCEP-HCl) (Pierce)) or high salt buffer (10 mM HEPES, pH 7.6, 300 mM KCl, 1 mM $MgCl_2$, 0.1 mM TCEP-HCl). Ultrapure ATP or ADP (Sigma) was added to the buffer at a final concentration of 1 mM for chromatography with nucleotide. The UV absorbance was recorded at 280 nm. The molecular weight was estimated based on high molecular weight calibration standards ferritin, catalase, aldolase (GE Healthcare) and creatine phosphokinase that were run on the column under similar conditions to the SecA proteins.

Ion (Anion) Exchange Chromatography

Nucleotide-free or nucleotide-bound SecA2 was loaded onto a 1 mL Hi-Trap Q column (GE Healthcare) in 25 mM Tris pH 7.6 using a BioLogic Duo-Flow system (Bio-Rad). The column was washed with 5 mL of 25 mM Tris pH 7.6. A linear gradient from no salt to 1.5 M NaCl in 25 mM Tris pH 7.6 was run over 25 mL followed by 5 mL of 1.5 M NaCl. Fractions of 1.5 mL were collected throughout the run. Where required, nucleotide-free SecA2 was incubated with a ten-fold molar excess of ADP on ice for 30 minutes before being loaded onto the Hi-Trap Q column.

C. Agarose Gel Electrophoresis of proteins

Protein agarose gel electrophoresis was carried out using 1% SeaKem HGT agarose (Lonza) in 40 mM Tris, 20 mM acetic acid pH 8.0 using a horizontal gel apparatus (BioRad). Samples were prepared at room temperature in low salt buffer with the final protein concentration at 6 µM monomer. Wherever necessary, nucleotides or nucleotide analogs were added to a final concentration of 0.5 mM. The samples were incubated for ~ 30 minutes at room temperature before the addition of native gel sample buffer. The gel was run at 100 V, followed by staining with Coomassie blue to visualize the bands.

D. Fluorescence spectroscopy

Nucleotide Binding Kinetics by fluorescence

Kinetics of nucleotide binding and release were studied by fluorescence resonance energy transfer (FRET) between the tryptophans of SecA and N'–methylanthraniloyl (MANT) nucleotides (Molecular Probes) in an Aminco Bowman Series 2 luminescence spectrometer. The excitation and emission monochromators were set to 295 nm and 450 nm, respectively, with 4 nm bandpasses. The sample chamber was maintained at 20 ºC. Varying concentrations of SecA from 0.05 µM to 0.5 µM were assessed, keeping the MANT nucleotide concentration in excess at 1.2 µM. Since there was no change in the kinetic constants for this SecA concentration range tested, further kinetic experiments were performed using 0.5 µM SecA to improve the fluorescence signal. The SecA protein was incubated in buffer (10 mM HEPES pH 7.6, 25 mM

KCl, 1mM $MgCl_2$) in a 1 cm cuvette with stirring. After the addition of MANT nucleotide, the increase in MANT fluorescence was monitored with time. Once saturation was reached, 1 mM unlabeled nucleotide was used to compete the MANT nucleotide from the SecA proteins. The curves were fit to a first order rate equation to give the apparent rate constants for the association reaction (k_{obs}) and reverse reaction (k_{off}). The rate constant k_{on} was calculated using the equation:

$$k_{obs} = k_{on}\,[\text{MANT nucleotide}] + k_{off}$$

The dissociation constant (K_d) was calculated by dividing the k_{off} by the k_{on} (104,105).To verify pseudo-first order kinetics, the k_{obs} was determined at varying MANT-ADP concentrations with the SecA proteins held at 0.5 µM. From the plots of k_{obs} vs. MANT-ADP, the kinetics parameters k_{on} and k_{off} were obtained from the slope and y-intercept, respectively, when fitted by linear regression.

Pyrene fluorescence studies

In order to label the SecA proteins with N-(1-pyrene) iodoacetamide (Life Technologies) via cysteine residues, 0.5 µl of 0.1 M *tris* (2-carboxyethyl) phosphine TCEP-HCl pH 7.0 was added to 100 µl protein (~45 µM) for thirty minutes at room temperature, followed by the addition of 5 µl of 10 mM N-(1-pyrene) iodoacetamide. The samples were incubated on a nutator at 4 ºC overnight. Unbound label was removed by the loading the samples on micro Bio-Spin 6 column (BioRad), pre-washed with 10 mM HEPES buffer pH 7.6, 25 mM

KCl. The samples were eluted by centrifuging the column at 1000 x g for 1 min. The absorbance at 280 nm and 338 nm was read to determine the extent of labeling of the proteins.

Pyrene emission scans of 0.5 µM labeled protein in 10 mM HEPES buffer pH 7.6, 300 mM KCl in a total volume of 300 µl, were taken using an Aminco Bowman Series 2 luminescence spectrometer. The excitation and emission monochromators were set to 338 nm and 375 nm, respectively; with 4 nm bandpasses at 25 ºC. Emission scans were performed from 350 to 600 nm.

ACMA fluorescence assay to check membrane vesicle integrity

2 µl of membrane vesicles (MVs) (preparation described later) were added to 1 mL of buffer (10 mM HEPES pH 7.6, 100 mM KCl, 5 mM MgCl2), stirring in a cuvette at 20 ºC. The excitation and emission wavelengths were set to 410 and 480 nm respectively with 4 nm bandpasses. ACMA (9-amino-6-chloro-2-methoxyacridine) (Molecular Probes) and CCCP (carbonyl cyanide *m*-chlorophenyl hydrazine) (Sigma) were prepared in dimethyl sulfoxide (DMSO). ACMA was added to the MV solution in the cuvette at a final concentration of 2 µM and the baseline was monitored for approximately 5 minutes. Substrate was added at a final concentration of 1 mM and the fluorescence signal was monitored with time. After no more quenching of ACMA fluorescence was observed, the uncoupler CCCP was added at a final concentration of 1 µM and the consequent increase in the ACMA signal was monitored.

E. Circular dichroism (CD) spectroscopy of proteins

Thermal melts by CD spectroscopy

Thermal melts were carried out in a 2 mm path length cuvette with an Applied Photophysics Pi-Star 180 circular dichroism (CD) spectropolarimeter. The protein concentration used was 0.1 mg/mL in 10 mM HEPES pH 7.6, 25 mM KCl buffer. Wherever necessary, nucleotide was added to the buffer at a final concentration of 0.5 mM. The temperature was increased using a circulating water bath and the CD signal at 222 nm was recorded with slits set to 2 nm. The step size was 0.5 ºC and the tolerance was set to 0.2 ºC. The data were averaged for 300,000 points and were normalized to show the fraction unfolded with temperature.

CD spectra of proteins

CD spectra were obtained using 100-200 µg/mL protein in 20 mM sodium phosphate buffer at pH 7.6 in a 1 or 2 mM path length cuvette at 20 ºC. Slits were set to 2 nm and scans were performed from 200 to 250 nm with a 1 nm step size with a settling time of 12.5 seconds at each wavelength.

F. Proteolysis Experiments

Thrombin proteolysis of SecA2

SecA2 (0.8 mg/mL) was digested with 0.08 U of biotinylated thrombin (Novagen) in the presence or absence of 2 mM ADP in 20 mM sodium phosphate buffer pH 7.6 supplemented with 1 mM $MgCl_2$ at room temperature.

Aliquots in duplicate were taken at various times and added to SDS sample buffer. The digested products were separated by SDS PAGE. One set of samples on the gel was stained with Coomassie to visualize the bands while the second set was transferred to a PVDF membrane and stained with Coomassie blue. The membrane was destained with 100% methanol briefly to remove excessive background stain. Four proteolytic fragments were cut from the membrane and the sequence of the amino terminus of each fragment was determined using 4 cycles of automated Edman degradation (Tufts University Core facility).

Limited proteolysis of SecA2 by Trypsin and V8

For digestion, 9 µM SecA2 either with or without 1 mM ATP (or ADP) was incubated with 45 µM protease (Trypsin or V8) in 20 mM sodium phosphate buffer at pH 7.6 containing 1 mM $MgCl_2$ at room temperature in a final volume of 100 µl. Aliquots of 10 µl were taken at varying time points and added to 1µl of 1 mg/mL bovine pancreatic trypsin inhibitor (BPTI) on ice for 15 min. After incubation, 10 µl of SDS sample buffer was added to each aliquot and 10 µl of the sample was separated on a 10 % SDS gel

G. Growth of *M. smegmatis* and preparation of *M. smegmatis* membrane vesicles

The *M. smegmatis* strain (LL099) used for the preparation of membrane vesicles (MVs) was a gift from Miriam Braunstein. This strain contains two *secY* genes. The first copy is that of native *secY* on the chromosome and the second

is that of *secY* expressed with a hemagglutinin (HA) tag on a plasmid that integrates into the tweety site. The plasmid that encodes for SecY confers resistance to hygromycin. The strain was streaked on a Mueller Hinton agar plate that contained 10 µg/mL cyclohexamide (CHX) (Sigma), 50 µg/mL ampicillin, 0.05 % Tween 80 and 50 µg/mL hygromycin B (HYG) (Gold biotechnology). CHX was used to prevent the growth of mold and was prepared in ethanol. Ampicillin was used to prevent the growth of other bacteria, as Mycobacteria are naturally resistant to ampicillin due to the production of beta lactamases. Tween 80 was used to prevent clumping of Mycobacteria as a result of their mycolic acid-rich cell wall. The plate was incubated at 37 ºC until colonies appeared (3-4 days). A single colony from the plate was used to inoculate a 10 mL Erlenmeyer flask of sterile Mueller Hinton broth (Difco) containing the above components present in the plate at the same final concentration. Additionally, ~ 5 sterile glass beads were added to the culture to prevent clumping of mycobacteria while the culture was rotated on a shaker at 150 rpm at 37 ºC overnight. This culture was then used to inoculate a 2 L flask containing 500 mL of sterile Mueller Hinton medium (with all the additional components and sterile glass beads) to achieve an $O.D_{600}$ ~ 0.02. This culture was grown at 37 ºC rotating at ~150 rpm to an $O.D_{600}$ ~ 0.8-1.0 and spun down in 150 mL volumes/bottle in a swinging bucket rotor (Sorvall) at 4000 rpm for 15 minutes. The pellets were frozen until further required.

MVs were always prepared just before use and tested for configuration and seal using the ACMA fluorescence-quenching assay before use. For preparation of MVs, one tablet of complete protease inhibitor cocktail (Roche)

was resupended in 0.5 mL distilled water and added to the frozen pellet. The pellet was thawed and resuspended in a minimum volume of 50 mM, MOPS-KOH (pH 7.5) 2mM MgCl2. 1500 units of DNAse and 15 mM MgCl2 were added to the cells. The cells (~2mL in volume) were lysed using a sonicator (Misonix) fitted with a micro tip. The cells were kept on ice during sonication. The amplitude was set to 35 and the pulse was set to remain on for 15 seconds, off for 30 seconds, for a total of 2 minutes of 'on' time. The broken cells were pelleted in a microfuge at maximum speed for 5 minutes. The supernatant was subjected to centrifugation at 60,000 rpm (163,000 X g) in 1 mL tubes using a S120AT2 rotor at maximum acceleration and deceleration. The brown pellet containing MVs was resuspended in 50 mM MOPS-KOH (pH 7.5), 2mM MgCl2.

When endogenous SecA had to be stripped from the membranes, the brown pellet was resuspended in 1 mL of 6 M urea made in MOPS buffer (above) and allowed to stand for 30 minutes at room temperature. This was followed by centrifugation at 75,000 rpm as done above. The pellet was resuspended in 1 mL of MOPS buffer and centrifuged again to remove any residual urea. The pellet from this spin was then resuspended in ~ 100 µl of MOPS buffer and used for experiments.

H. Membrane floatation assay using OptiPrep gradients

A working solution (WS) of 50 % iodixanol (OptiPrep) was prepared by mixing 5 mL of 60 % (w/v) OptiPrep (Sigma) having density 1.32 g/mL with 1 mL of diluent (120 mM HEPES-KOH, pH 7.6, 30 mM MgCl2). A 35 % overlay was

further prepared by diluting the WS with diluent. Samples were prepared directly in centrifuge tubes in a final volume of 50 µl using 1 X buffer (10 mM HEPES-KOH, pH 7.6, 10 mM KCl, 2 mM $MgCl_2$). The final amount of SecA protein used in the gradient was 20 µg. The volume of MVs used was 25 µl. Wherever required nucleotide was added at a final concentration of 1 mM. The samples were allowed to incubate at room temperature for 30 mins before being mixed with 200 µl of the WS to make a 40 % solution. The solution was overlayed with 750 µl of the 35 % solution. The 1 mL gradients were spun at at 4ºC at 100,000 rpm for 1hr in the S120AT2 fixed angle rotor. The acceleration and deceleration were set to 5 and 1 respectively. Since the concentration of MVs could not be assessed and a fixed volume was used each time, only samples from the same run or vesicle preparation were compared with each other.

For analysis of the gradients, 200 µl fractions were taken from the top using a positive displacement pipette. 20 µl of each of the fractions was further taken and mixed with 10 µl of 3X SDS sample buffer and 10 µl was used to run SDS PAGE followed by Western Blotting.

I. Western Blotting

The SDS gel was transferred to an Immobilon P^{SQ} PVDF membrane (Millipore) that was pre-incubated for a few minutes in methanol before transfer. The transfer was carried out using a mini Trans-Blot cell (BioRad) in 25 mM Tris, 192 mM glycine pH 8.3, stirring at 30 V overnight or 100 V for 1 hour. A cooling pack was used to prevent over-heating of the buffer. The blot was blocked with

10 % powdered milk in 1X TBS (50 mM Tris, pH 7.6, 150 mM NaCl) for 30 minutes on a shaking platform. The milk solution was filtered using a Whatmann filter paper to remove particulate casein prior to blocking. 4 µl of primary antibody; rabbit polyclonal biotinylated anti-His antibody (Genscript) was added to the blot in 10 mL of 1X TBS, 10 % milk. Incubation was carried out for 2 hours on a shaking platform. The blot was washed with distilled water, allowed to incubate for 5 minutes in 50 mL 1X TBS containing ~ 0.05 % Tween 20 and washed. The washing step was repeated 5 times followed by the addition of 5 µl of secondary antibody (Alexa-532 goat anti-rabbit antibody) or reagent (Streptavidin-Phycoerythrin conjugate) (Molecular Probes) in 10 mL of 1X TBS, 10 % milk. Incubation was carried out as done before for 1 hour and 30 minutes followed by washing of the blot five times as done before. The blot was then visualized using a Typhoon scanner (GE Healthcare life sciences) using excitation and emission filters for Alexa-532 at 450 V or Personal Molecular Imager (BioRad).

J. Sedimentation Velocity Analytical Ultracentrifugation

The peak of the pure SecA2 eluted in high salt buffer from the Superdex column was concentrated using an Amicon centrifugal filter device (Millipore) and used for sedimentation velocity analytical ultracentrifugation in a Beckman Coulter Optima XL-I centrifuge (University of Connecticut Analytical Ultracentrifugation Facility). Samples consisted of increasing concentrations of SecA1 and SecA2. The solvent compartment was loaded with the high salt buffer used to run the Superdex column. Samples were centrifuged with a Beckman

XL-I AU at 40,000 rpm at 20 °C and data were collected with interference optics. Data from sedimentation velocity runs were first analyzed with DCDT+ (106).The program Sedinterp was used to estimate the solvent density and partial specific volume of the protein (107).

Chapter 3*

SECA2: A DIFFERENT KIND OF SECA PROTEIN

***Parts of this chapter have been published.**

(D'Lima NG, Teschke CM, J Biol Chem. 2014;289(4):2307-17)

Introduction

According to the World Health Organization, approximately one third of the world's population is infected with *Mycobacterium tuberculosis*, the causative agent of the disease Tuberculosis (TB). TB is the leading cause of death by a bacterial pathogen. In 2011 alone, it claimed the lives of 1.4 million people. Additionally, the emergence of multi-drug resistant (MDR) strains has caused worldwide concern. In 2011, of the 310,000 cases of MDR TB, nine percent had extensively drug resistant (XDR) TB. (World Health Organization fact sheet on "Tuberculosis" located online at: www.who.int/mediacentre/factsheets/fs104/en). Despite substantial efforts to forge effective countermeasures, the development of antibacterial drugs and vaccines has been hampered because the survival strategies employed by *M. tuberculosis* and its mechanisms of pathogenesis are not well understood.

Protein export pathways are promising therapeutic targets that have yet to be fully exploited in this bacterium (108). The *M. tuberculosis* SecA2 protein is one such target. In fact, a *ΔsecA2* strain of *M. tuberculosis* promotes apoptosis of infected macrophages and shows enhanced priming of CD8+ T cells in mice (94).

The combination of lysine auxotrophy and *secA2* deletion to produce a *ΔsecA2 ΔlysA* strain of *M. tuberculosis* was shown to be a strong vaccine candidate and was safer and more effective than the traditional BCG (Bacille Calmette-Guérin) vaccine for Tuberculosis (95). However, because the role of SecA2 in the Mycobacteria, and its implications for virulence are not well understood, the development of this vaccine is hindered by stringent pharmacological guidelines. This study reports extensive biochemical characterization of SecA2 that sets the stage for elucidation of SecA2's role in Mycobacterial protein secretion. In a previous study we showed that SecA2, like SecA1, is an ATPase. It binds ATP with high affinity and the ATPase activity of SecA2 is essential for bacterial survival in macrophages (43). The factors by which the translocation machinery and precursor proteins distinguish the two SecA homologs are not known. SecA proteins undergo large conformational changes, particularly involving movement of their precursor-binding domain (PPXD) (26,63,76,77). For example, the crystal structure of *Thermatoga maritima* SecA in the ADP bound form shows the PPXD rotated towards the helical wing domain (HWD) leaving a large groove open between the PPXD and nucleotide-binding domain 2 (NBDII) (76) (Figure 3-1). This grove, referred to as the 'clamp', is thought to facilitate the binding of the precursor protein by SecA (76). *Thermatoga maritima* SecA bound to the SecYEG channel shows a large movement (~ 80º) of the PPXD towards NBDII, resulting in the closing of a grove between these two domains (74).

Here we show that *M. tuberculosis* SecA2 has a significantly higher affinity for ADP, and releases the nucleotide extremely slowly, compared to SecA1. In

addition, we find that SecA2 undergoes a large conformational change upon ADP binding that is easily observable with standard biochemical techniques. Our data suggest that this structural rearrangement is due to closure of the 'clamp' in SecA2, which may be unique to the accessory SecA class of proteins, as nucleotide-binding does not induce this structural change in *M. tuberculosis* SecA1 or *E. coli* SecA. This may serve as a mechanism for distinction between the two SecA proteins by the Mycobacterial translocation machinery.

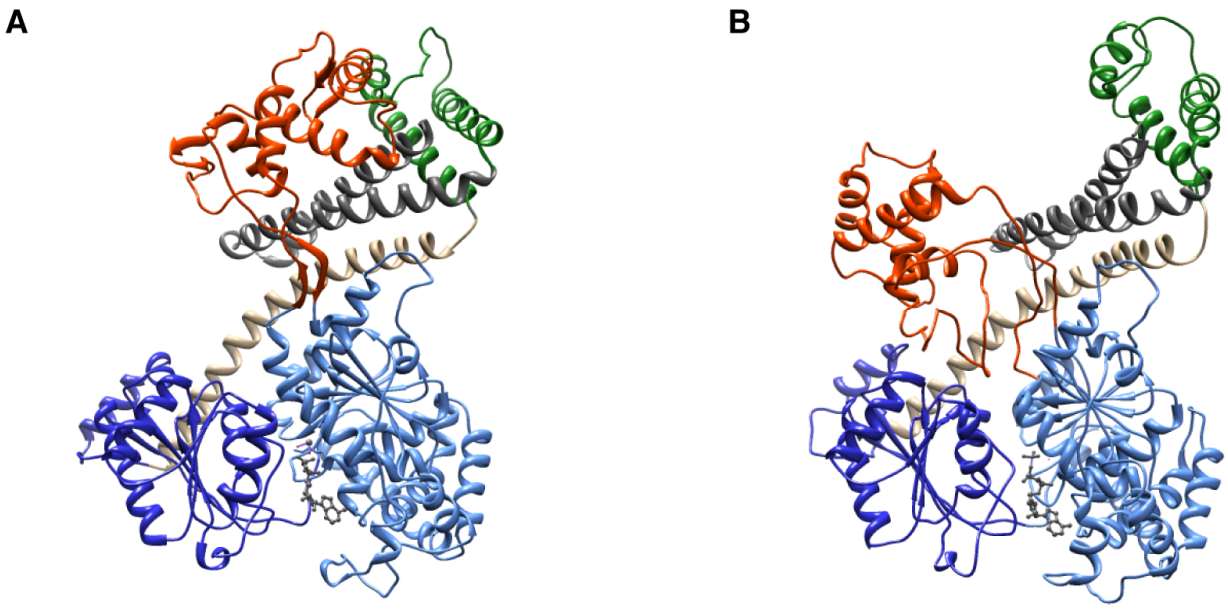

Figure 3-1: Crystal structures of *Thermatoga maritima* SecA showing two conformational states.

(A) Structure of *T. maritima* SecA in the ADP-bound form exposing the clamp (PDB ID 3JUX) (76). The nucleotide binding domains (NBD) I and II are shown in light and dark blue respectively. The pre-protein crosslinking domain (PPXD) is shown in orange. The helical scaffold domain (HSD) is shown in tan and the two-helix finger that is part of the HSD is shown in dark gray. The helical wing domain (HWD) is shown in green. (B) Structure of *T. maritima* SecA bound to the channel (PDB ID 3DIN) in presence of ADP- BeF_3 (74). In this structure, the PPXD has rotated toward NBD II sequestering the clamp. The structure (B) has been modified to show only SecA. The program *Chimera* was used to generate these structures based on PDB files (38).

Results

A. SecA2 shows a unique structural change upon binding to ADP.

Conventional SecA proteins have been shown to undergo conformational changes upon nucleotide binding and hydrolysis. These changes are closely coupled with precursor binding and release, as well as association of SecA with the translocon (26,76). The presence of two SecAs in Mycobacteria raises questions about how these homologs are regulated in the cell. Since both proteins are ATPases with significant sequence homology, could unique conformational changes upon binding nucleotides dictate specific interactions with other translocation components? In order to investigate potential structural changes, the SecA proteins (without His_6 tags) were incubated with increasing concentrations of ATP in buffer containing 1 mM $MgCl_2$. Since the effect of nucleotides on the conformation of *E. coli* SecA has been studied extensively, *E. coli* SecA was used as a control. Interestingly, SecA2 showed a dramatic mobility shift in the presence of ATP (Figure 3-2). In fact, SecA2 exists as two species in equilibrium. In the absence of nucleotides, the slow migrating species predominates. The addition of nucleotides shifts the equilibrium to the faster migrating form. No shift in mobility was seen with *E. coli* SecA or SecA1 even at high ATP concentrations (Figure 3-2). A Walker A Box variant of SecA2 (K115R), which we have previously shown does not bind ATP (43) also did not show a mobility shift on the agarose gel. Next, the SecA proteins were incubated with varying concentrations of $MgCl_2$ while the ATP concentration was held constant.

At very low concentrations of Mg^{2+} (below 100 µM), no mobility shift was observed, but as the Mg^{2+} concentration was increased, the mobility shift of SecA2 became apparent however; SecA1, E. coli SecA and SecA2 K115R did not show a mobility shift even at high concentrations of Mg^{2+} (Figure 3-2). Further, the mobility shift shown by SecA2 was not observed when Mg^{2+} was substituted with divalent cations or when EDTA was included in the buffer (data not shown). These data show that the mobility shift of SecA2 is unique and is solely Mg^{+2} • nucleotide-dependent.

The SecA proteins were further incubated with hydrolyzable nucleotides (ADP or ATP) or fluorescently labeled hydrolyzable analogs such as N'–methylanthraniloyl (MANT) ADP or MANT-ATP in buffer containing Mg^{2+} before being subjected to native agarose gel electrophoresis. Note that His_6 versions of SecA1, SecA2 and SecA2 K115R were used in this experiment. Once again, SecA2 showed a mobility shift in the presence of ADP and hydrolysable ATP analogs but no mobility shift was observed with the non-hydrolysable ATP analog (AMP-PNP). No shift in the mobility of the protein bands for either *E. coli* SecA or SecA1 in response to binding of any nucleotide was observed (Figure 3-3 A). Additionally, the observation of two discrete bands of SecA2 (especially in the His_6 version of the protein) on the agarose gel suggests the exchange between the species is slow relative to the rate of electrophoresis.

SecA2, being an ATPase, would hydrolyze ATP to ADP. If ADP release were rate limiting, as is the case with *E. coli* SecA (67,68) then the change in SecA2 mobility observed on the agarose gel might be induced by ADP rather

than ATP. In the presence of AMP-PNP, only a small fraction of SecA2 shows a mobility shift compared to SecA2 bound to hydrolyzable nucleotides or ADP. This observation suggests the mobility shift is not due to binding of ATP, but must occur further along SecA2's enzymatic cycle. In order to verify that SecA2 did in fact bind AMP-PNP, we used fluorescently labeled MANT AMP-PNP. The MANT AMP-PNP binding kinetics were followed by fluorescence resonance energy transfer (FRET) between the intrinsic tryptophan residues of SecA2 and the MANT nucleotide analog. From the fluorescence traces, it is evident that SecA2 bound MANT AMP-PNP, and release it when excess unlabeled ATP was added (Figure 3-3B). Nevertheless, a mobility shift as seen with hydrolyzable nucleotides was not observed when MANT AMP-PNP was incubated with SecA2 and subjected to agarose gel electrophoresis, consistent with results for unlabeled AMP-PNP (Figure 3-3A).

These data indicate that SecA2 can exist in two structural forms that are in equilibrium with each other. Binding of ADP, but not ATP, causes structural rearrangements in SecA2 and shifts the equilibrium such that one conformation is favored over the other. Furthermore, this change is unique to SecA2, as SecA1 and *E. coli* SecA do not show it, despite their ability to bind nucleotides with high affinity. Even though *E. coli* SecA has been shown to undergo conformational changes upon nucleotide binding (73,74) these changes do not cause a gel mobility shift in our experiments.

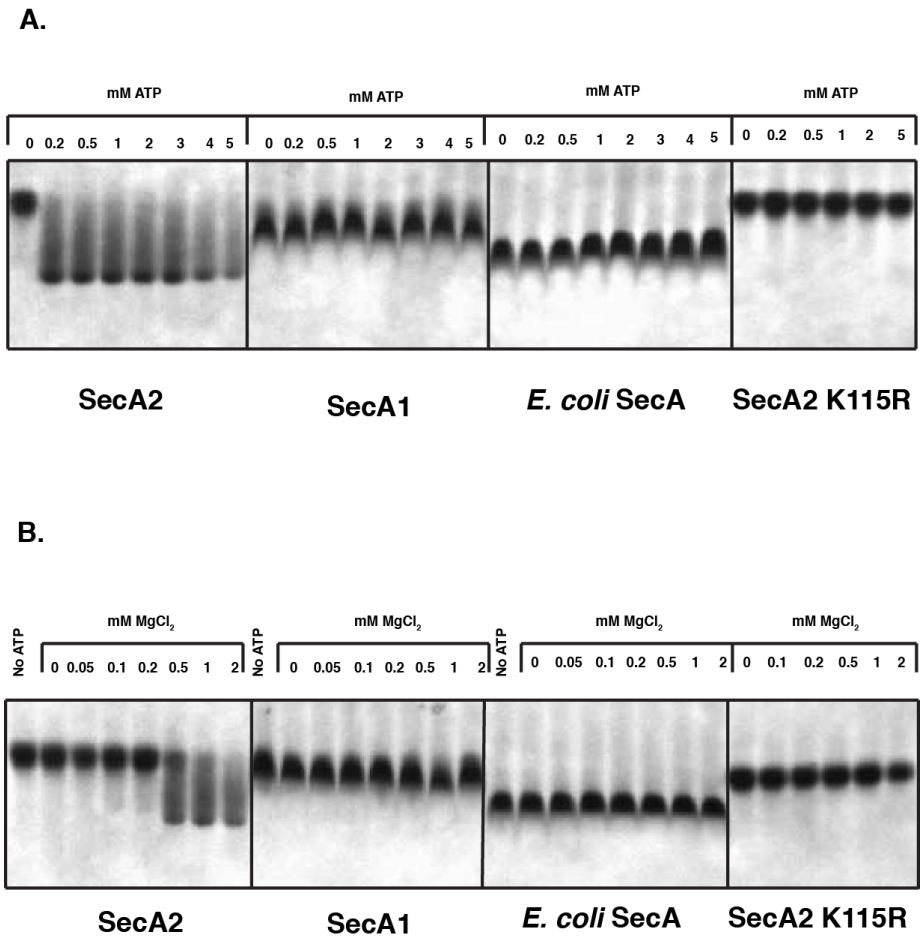

Figure 3-2: The unique mobility shift of SecA2 on an agarose gel is Mg^{2+}. ADP dependent and is observed in SecA2 that is not His_6–tagged.

A. SecA proteins (~ 6 µM) were incubated with increasing concentrations of ATP in buffer containing 1 mM $MgCl_2$ and subjected to native gel electrophoresis on a 1% agarose gel. The band of SecA2 shows an increase in mobility in the presence of ATP that is not observed with *E. coli* SecA, *M. tuberculosis* SecA1 or a Walker box mutant of SecA2. B. SecA proteins were incubated with increasing concentrations of $MgCl_2$ in buffer containing 1 mM ATP and subjected to agarose gel electrophoresis.

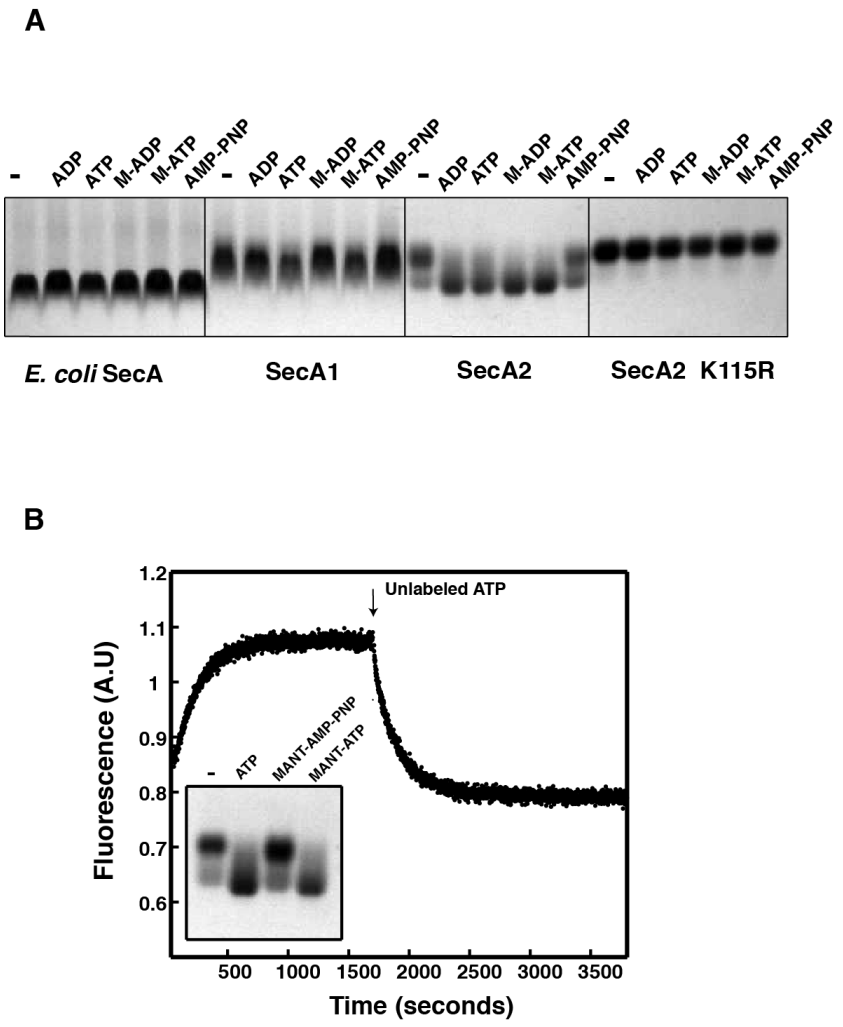

Figure 3-3: SecA2 reveals a unique structural rearrangement on binding ADP.

(A) SecA proteins (~ 6 µM) were incubated with nucleotides or nucleotide analogs (0.5 mM) and subjected to native gel electrophoresis on a 1% agarose gel. The band of SecA2 shows an increase in mobility in the presence of hydrolyzable nucleotides that is not observed with *E. coli* SecA, *M. tuberculosis* SecA1 or a Walker box mutant of SecA2. (B) Fluorescence traces showing increase in MANT-AMP-PNP (1.2 µM) fluorescence upon binding to SecA2 (0.5 µM) and release upon the addition of unlabeled ADP (1 mM).

B. ADP bound SecA2 can be separated from nucleotide-free SecA2 using Blue-Sepharose chromatography.

The mobility shift of SecA2 upon nucleotide binding on an agarose gel, a distinctly non-equilibrium condition, suggested that the affinity of SecA2 for ADP must be quite high. This observation likewise indicated that a fraction of SecA2 might remain ADP-bound even after purification on the metal affinity column. To separate the ADP-bound fraction from the nucleotide-free protein, Cibacron Blue F3G-A-Sepharose column (Blue-Sepharose) was used. This dye associates with the nucleotide fold found in ATP-binding proteins (109). The column fractions were run on a 10% Bis-Tris gel, and SecA2 was observed to elute in two peaks. A portion of SecA2 eluted immediately in the flow-through, corresponding to SecA2 that did not bind to the blue column. A larger portion of SecA2 bound to the column tightly and eluted in 2 M NaCl (Figure 3-4A). An aliquot from each of the two peaks was run on a native agarose gel. Based on the mobility of the SecA2 band, it is evident that the first peak of SecA2 did not bind to the Blue-Sepharose column because it was ADP-bound and showed the distinct faster mobility on the agarose gel, while the fraction of SecA2 that bound tightly to the column was ADP-free and showed slower mobility (Figure 3-4B).

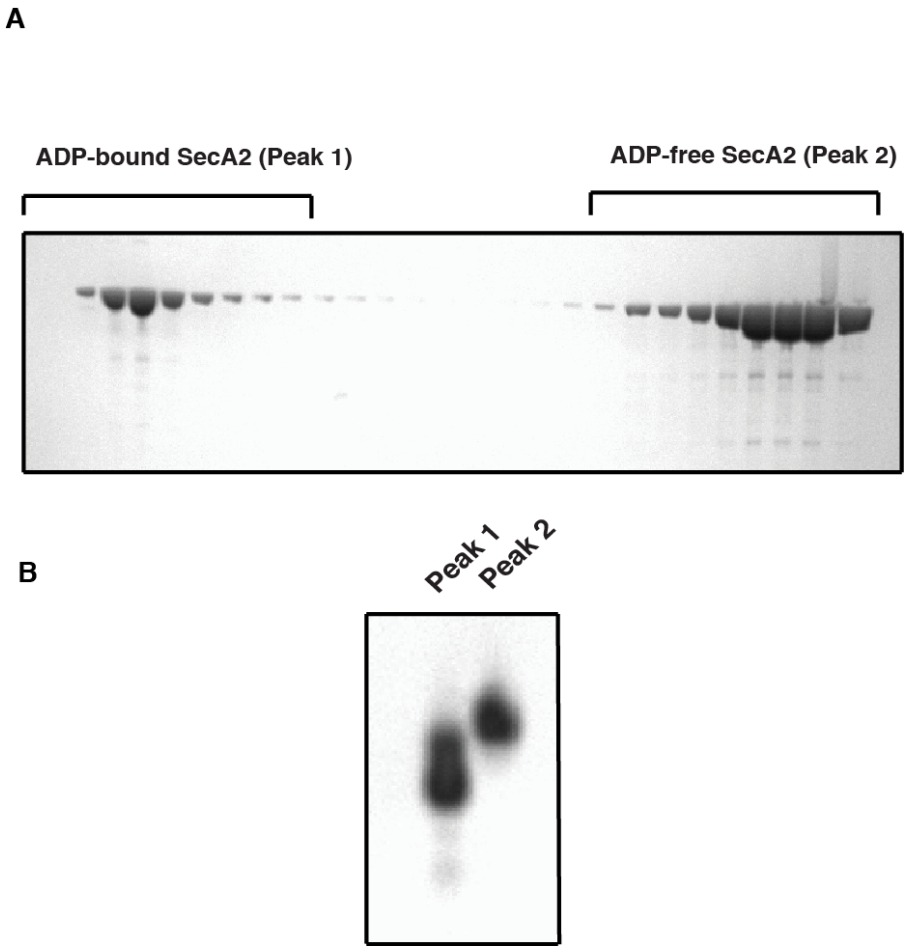

Figure 3-4: ADP-bound and free forms of SecA2 can be separated by Blue-Sepharose chromatography.

A 10 % Bis-Tris gel of column fractions of SecA2 purified on a Blue-Sepharose column. The first peak corresponds to ADP-bound SecA2 that does not bind to the column and elutes in buffer without salt. The second peak corresponds to ADP-free SecA2 that binds tightly to the column and elutes in 2 M NaCl. (B) The two peak fractions from the Blue Sepharose column were subjected to native gel electrophoresis on a 1% agarose gel. The fraction of SecA2 that did not stick to the column shows the distinct mobility shift verifying that it is ADP-bound.

C. SecA2 binds ADP with high affinity and releases it significantly slowly compared to SecA1.

To characterize the interaction between SecA2 and ADP, the kinetics of nucleotide binding were assessed using FRET between the intrinsic tryptophans of SecA2 (donor) and MANT nucleotides (acceptor). Since MANT nucleotides were able to induce a structural rearrangement in SecA2 in a manner similar to unlabeled nucleotides (Figure 3-3A), the binding of MANT nucleotides to SecA1 and SecA2 likely mimics the association of the unlabeled nucleotides with these proteins. Additionally, MANT-ATP has been shown to support translocation of precursors by the *E. coli* SecA ATPase in an *in vitro* translocation assay, highlighting that substitution of ATP with MANT nucleotides allows for physiologically relevant activity (70).

The tryptophans of *M. tuberculosis* SecA proteins were excited, and upon binding of MANT nucleotides, the increase in MANT fluorescence due to energy transfer was monitored with time (Figure 3-5). The data were fit to a single exponential function to obtain the apparent rate constant for association (k_{obs}). After binding was saturated, excess unlabeled nucleotide was added to compete the MANT nucleotide from the protein. The decrease in MANT fluorescence was followed with time. These data were fit with the equation for a first order decay to determine the dissociation rate constant (k_{off}). These constants were further used to calculate the association rate constant (k_{on}) and the dissociation constant (K_d) as described in the Materials and Methods. In order to verify pseudo-first order kinetics, k_{obs} was determined at varying MANT-ADP concentrations while the

concentrations of SecA1 or SecA2 were held constant. The plot of k_{obs} vs. [MANT-ADP] was linear for both SecA1 and SecA2 (Figure 3-5C), indicating that binding of MANT-ADP to the SecA proteins follows pseudo-first order kinetics.

From analysis of the rate constants obtained from single exponential fits (Table 3-1), SecA2 showed very slow release of bound ADP (k_{off} $1x10^{-4}$ s^{-1}) compared to SecA1 (k_{off} $1x10^{-3}$ s^{-1}) Also, the affinity of SecA2 for MANT-ADP (K_d ~ 0.05 µM) was about 120 fold tighter than that of SecA1 (K_d ~ 6 µM). The kinetic constants were similar to those obtained from linear regression when k_{obs} was plotted as a function of MANT-ADP concentration (Table 3-1) consistent with pseudo-first order kinetics. These data suggest the slow release of ADP from SecA2 may regulate its function *in vivo*.

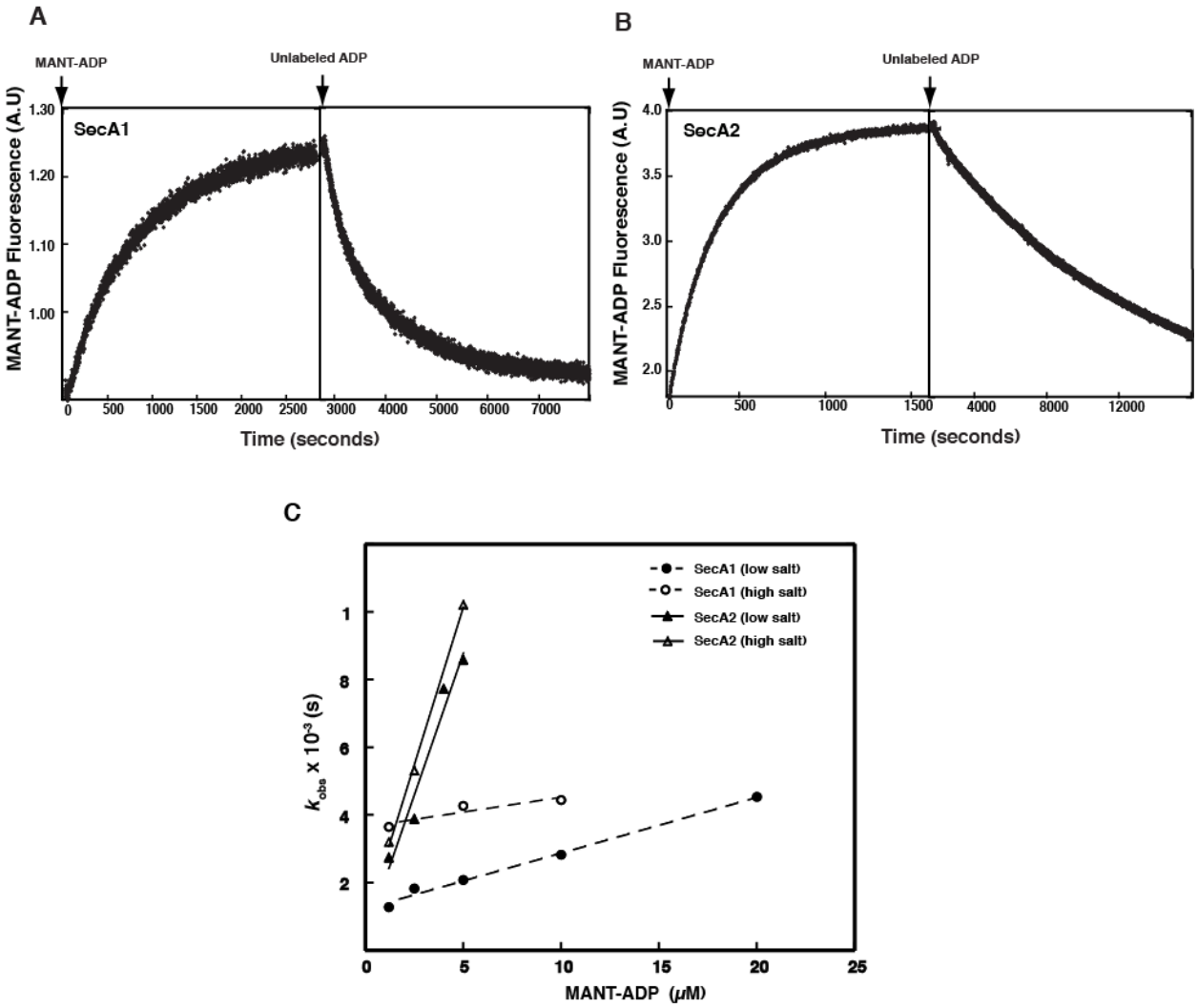

Figure 3-5: SecA2 binds ADP with high affinity.

Kinetics of MANT-ADP binding to SecA1 (A) and SecA2 (B) were assessed by FRET between the intrinsic tryptophans in SecA (donor) and MANT-ADP (acceptor). The increase in MANT-ADP was monitored with time when 1.2 μM MANT-ADP was added to SecA (0.5 μM) in HEPES buffer. MANT-ADP dissociation was observed by the addition of 0.5 mM unlabeled ADP. These data

were fit to kinetic models as described in the Materials and Methods. (C) Kinetics of MANT-ADP binding to SecA1 and SecA2 was observed at varying MANT-ADP concentration and the apparent rate constant (k_{obs}) was calculated from single exponential fits of the data. Data are plotted to show the variation in k_{obs} with MANT-ADP concentration.

Protein (Low salt conditions)	Kinetic constants determined from direct fits to rate equations				Kinetic constants determined from plots of k_{obs} vs. concentration of MANT-ADP		
	k_{obs} x 10^{-3} (s^{-1})	k_{off} x 10^{-3} (s^{-1})	k_{on} ($M^{-1}s^{-1}$)	K_d (μM)	k_{off} x 10^{-3} (s^{-1})	k_{on} ($M^{-1}s^{-1}$)	K_d (μM)
SecA1 (Dimer)	1.3	1	232	**6**	1	165	**6**
SecA2 (Dimer)	2.7	0.1	2 x 10^3	**0.05**	0.4	1.6 x 10^3	**0.25**

Protein (High salt conditions)	Kinetic constants determined from direct fits to rate equations				Kinetic constants determined from plots of k_{obs} vs. concentration of MANT-ADP		
	k_{obs} x 10^{-3} (s^{-1})	k_{off} x 10^{-3} (s^{-1})	k_{on} ($M^{-1}s^{-1}$)	K_d (μM)	k_{off} x 10^{-3} (s^{-1})	k_{on} ($M^{-1}s^{-1}$)	K_d (μM)
SecA1 (Monomer)	3.6	3.5	84	**42**	1	87	41
SecA2 (Monomer)	3.2	0.12	2.6 x 10^3	**0.05**	0.8	1.8 x 10^3	0.4

Table 3-1. Kinetic constants for binding of MANT-ADP to *M. tuberculosis* SecA proteins determined by FRET.

D. The structural change in SecA2 is not due to changes in oligomeric state

Change in oligomeric state could reasonably cause a shift in the mobility of SecA on an agarose gel. SecA proteins are well documented to undergo association reactions (84,85). To investigate the possibility the observed structural rearrangements in SecA2 were due to a change in the oligomeric state caused by the presence of nucleotides, SecA2 was subjected to size exclusion chromatography. This was done in the presence of buffer supplemented with 25 mM or 300 mM KCl since presence of high salt has been shown to dissociate the *E. coli* SecA dimer (85,86). The elution profiles for SecA2 in the presence of high salt or low salt buffers were consistent with the proteins being predominantly monomeric in high salt and dimeric in low salt based on calibration standards run over the column (Figure 3-6). When the low salt buffer was supplemented with ADP or ATP there was no shift in the elution peak of dimeric SecA2 Similarly, no change in the elution of the SecA2 monomer peak was observed when the high salt buffer was supplemented with nucleotides. Monomeric SecA2, in high salt buffer, is able to bind nucleotides with similar affinities to SecA2 in low salt buffer (Table 3-1). These data show that nucleotides do not change the oligomeric state of SecA2.

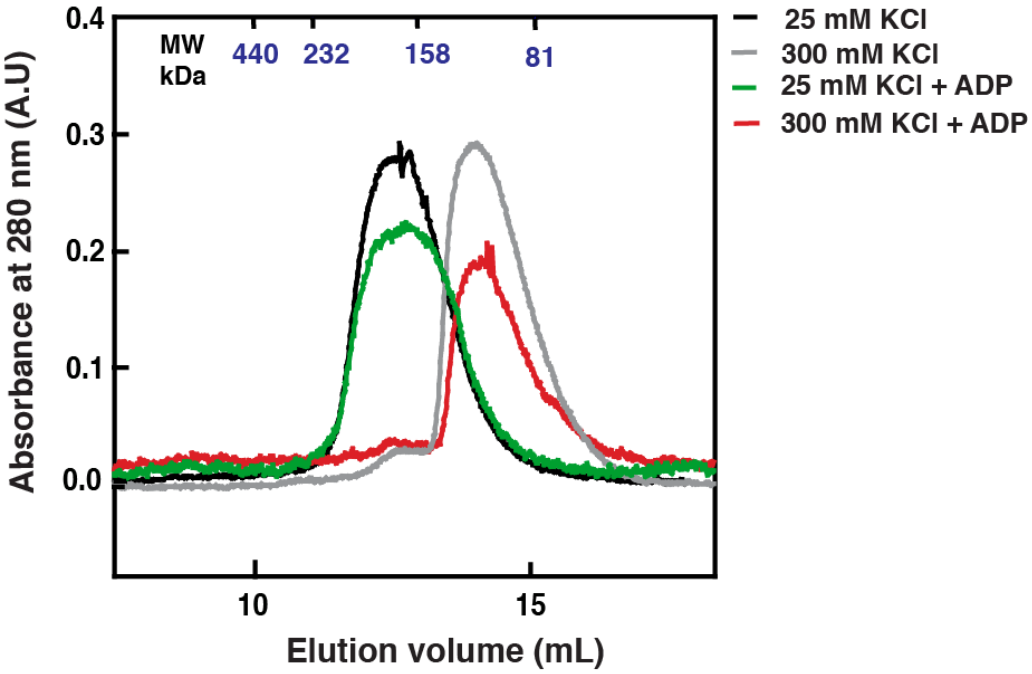

Figure 3-6: The ADP-induced rearrangement is not due to an oligomeric state change.

Superdex 200 size exclusion column profiles of SecA2 in the presence of low or high salt buffer either with or without added ADP. The elution volumes of the peaks of the calibration standards are marked along the top X axis along with their corresponding molecular weight. The addition of ADP does not cause a shift in the dimer or monomer peak verifying that ADP does not induce a change in oligomeric state in SecA2.

E. The structural change in SecA2 is not due to changes in surface charge.

Another determinant of migration on a native agarose gel is surface charge of a protein. Since ADP-SecA2 migrates further on the agarose gel compared to apo-SecA2, we speculated the conformational change induced by ADP could lead to exposure of negative charges or sequestering of positive charges on SecA2. In order to test this possibility, limited proteolysis experiments were performed in the presence and absence of ADP using V8 protease in phosphate buffer at pH 7.6 to allow for specificity for both aspartic and glutamic acid residues. Limited proteolysis experiments were also performed using trypsin to allow for specificity for lysine and arginine residues. However, no change in the protease digestion pattern of SecA2 was observed upon binding of ADP in the presence of V8 protease or trypsin. Only increased protection of full length SecA2 to V8 digestion was seen showing that nucleotides stabilize the protein (Figure 3-7).

Another approach was taken to further verify the possibility of changes in surface charge of SecA2 upon ADP binding. Ion exchange chromatography of SecA2 at pH 7.6 using a Hi-Trap Q anion exchange column was performed. Altered binding to the Q-column in the presence of ADP, would be indicative of a significant change in surface charge. The elution profiles showed no shift in the ADP-bound SecA2 peak (Figure 3-8). However; when fractions from each of the peaks were run on an agarose gel, samples corresponding to the ADP-bound SecA2 showed the distinct mobility shift, confirming that ADP remained bound through the column. Even though binding of proteins to an ion exchange column

is dependent on average surface charge and a shift in elution peak on such a column would only occur in case of a drastic overall surface charge change, the gel mobility shift observed in response to nucleotides in SecA2 seems like it might require such a dramatic charge or conformational change. However, these data indicate that the ADP-induced conformational change in SecA2 is likely due to a structural rearrangement resulting in a change in the overall shape of the protein, rather than a change in oligomeric state or surface charge.

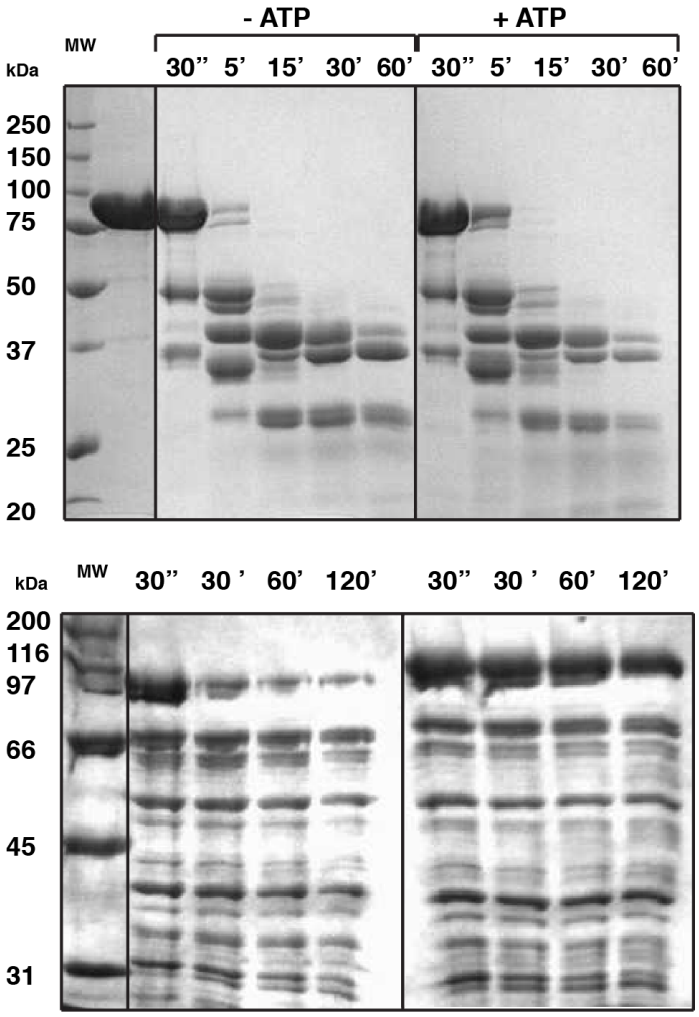

Figure 3-7: Limited proteolysis experiments indicate the nucleotide-induced rearrangement is not due to a change in surface charge.

Separation of proteolytic fragments of SecA2 alone or in the presence of ATP by SDS PAGE using the proteases Trypsin (Top gel) or V8 protease (bottom gel) show that there is no change in cleavage pattern of SecA2 in the presence of nucleotide. Only increased protection of full length SecA2 to V8 protease in the presence of ATP can be seen. The same results are obtained even when ATP is substituted by ADP.

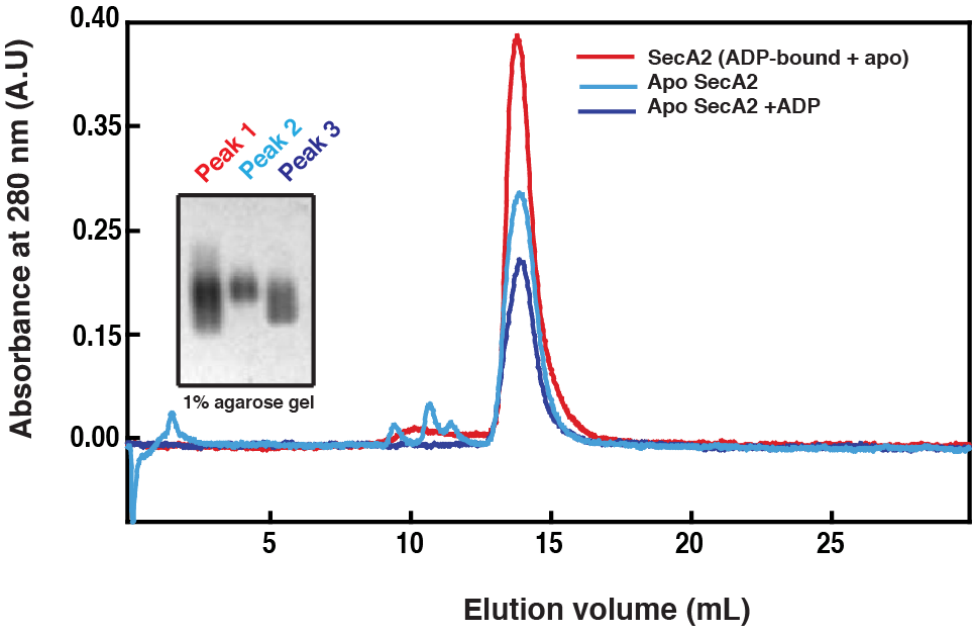

Figure 3-8: The ADP-induced rearrangement is not due to a change in surface charge.

Hi-Trap Q-column elution profiles for SecA2 in the presence or absence of ADP. SecA2 was loaded onto the column under three conditions: 1) A mixture of ADP- and apo-SecA2; 2) apo-SecA2; 3) ADP-free SecA2 pre-incubated with ADP for 30 minutes before being loaded onto the Q column. The column was eluted with a linear salt gradient. An aliquot from each SecA2 peak was run on an agarose gel (Inset). No shift in the elution peak was observed when SecA2 was nucleotide bound indicating that nucleotides do not cause a dramatic change in surface charge of SecA2.

F. SecA2 is significantly stabilized to heat when ADP bound.

To further investigate the role of ADP in conformational changes in SecA2, circular dichroism spectroscopy was used. The thermal stability of SecA2 was assessed in the presence and absence of nucleotide. The CD signal of the highly helical SecA2 protein was monitored at 222 nm as a function of temperature and the data were plotted to show the fraction unfolded with temperature (Figure 3-9). The melting temperature (T_m) was estimated from the mid-point of the transition. In the absence of nucleotide, SecA2 showed a T_m of ~ 34 ºC. However, the addition of ADP significantly stabilized the protein and caused a shift in the T_m of ~ 10 ºC. The T_m of SecA2 K115R was 34 ºC and did not change with the addition of nucleotide, confirming that nucleotide binding of ADP to wild type SecA2 confers stability of the protein to heat.

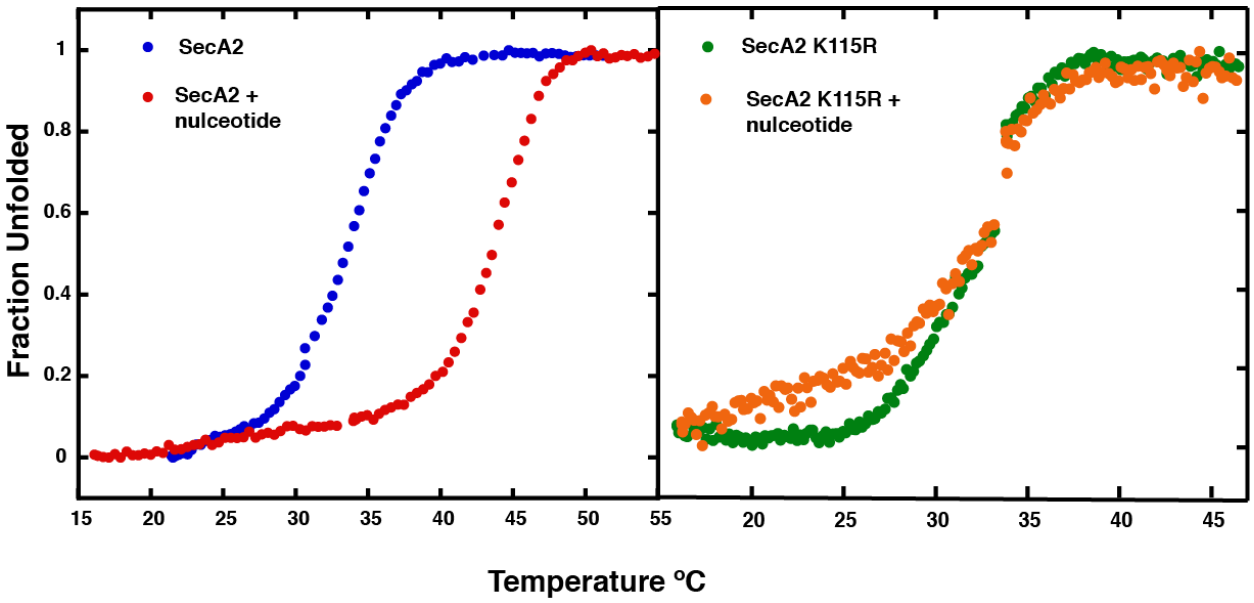

Figure 3-9: Binding of ADP enhances thermal stability of SecA2.

Thermal stability of SecA2 was assessed in the absence and presence of 0.5 mM ADP by monitoring the circular dichroism at 222 nm with increasing temperature. Data are plotted to show the fraction unfolded with temperature. ADP binding increases the T_m of SecA2 but does not cause any change in the T_m in SecA2 K115R, the Walker box variant of SecA2 that does not bind nucleotide.

G. ADP binding confers protection to regions of the pre-protein binding domain in SecA2

To investigate the ADP-dependent conformational change, SecA2 was subjected to limited proteolysis by thrombin in the presence or absence of ADP. The proteolytic fragments were analyzed by SDS PAGE (Figure 3-10A). When ADP-bound, SecA2 showed significant protection to cleavage by thrombin compared to the unbound form. In the presence of ADP, there was a new proteolytic fragment indicating exposure of a new thrombin cleavage site in SecA2, which is consistent with a conformational change in the protein. The predominant thrombin cleavage sites on SecA2 (indicated by the arrows in Figure 3-10A) were identified by N-terminal sequencing of the fragments by Edman degradation.

Three (blue arrows in Figure 3-10A) out of the four fragments had the sequence IAQL at the N-terminus, indicating that the predominant cleavage site on SecA2 was the bond between R335 and I336, while the fourth fragment (black arrow) had the sequence TTRA, the first threonine being the fourth residue from the N-terminus of the protein. The mass of the fragment starting at TTRA is consistent with C-terminus cut site at R335. The highest MW band starting with IAQL (top blue arrow) is consistent with the entire C-terminus after the cleavage. There is another predicted thrombin cleavage site in SecA2 located between R502 and G503, which would explain the lowest MW fragment. The fragment with MW ~ 40 kDa must be caused by a non-canonical cut site. Regardless, the R335 site is protected in SecA2 bound to ADP but exposed in apo-SecA2. When

mapped onto a structural model of SecA2 generated using 3D Jigsaw (110) the site (blue ball representation) generating IAQL fragments is located in the probable pre-protein binding domain (PPXD) of SecA2 (Figure 3-10B). The model of SecA2 is overlaid with the structure of *T. maritime* SecA in the open clamp form (76) as well as in the closed clamp conformation of *T. maritima* SecA when bound to the translocon channel (74). From a sequence alignment of *T. maritima* SecA with *M. tuberculosis* SecA2, the corresponding thrombin cleavage site on *T. maritima* SecA was identified and mapped onto the structures (purple ball representation). From comparison of the two overlays, it is evident that this region undergoes a dramatic conformational change. We postulate that in the ADP-bound conformation of SecA2, this site could be protected if it comes in close proximity to the nucleotide-binding domain (NBD2) in a manner similar to *T. maritima* SecA (Figure 3-10B). A hypothesis can be made based on these data, that for SecA2, binding of ADP might induce the movement of the PPXD such that SecA2 exists in the 'closed clamp' state when ADP bound.

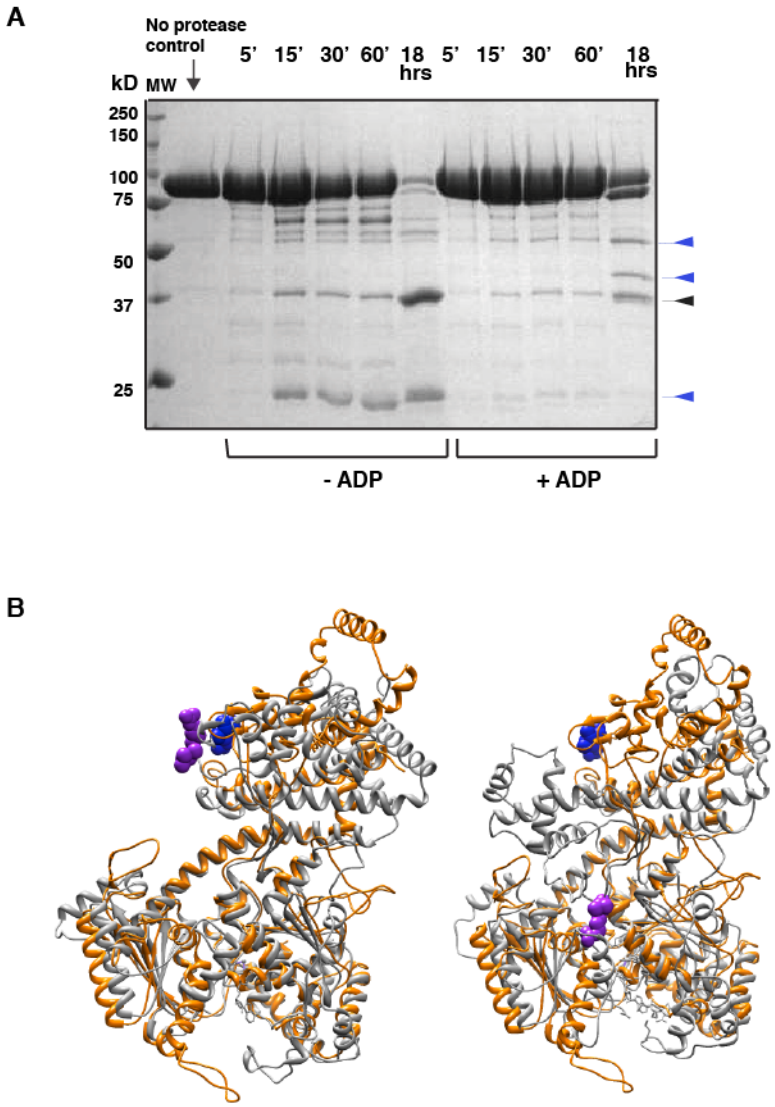

Figure 3-10: Limited proteolysis of SecA2.

(A) Cleavage of SecA2 by thrombin with time in the absence and presence of ADP. Cleavage products were separated on a 10% SDS gel. SecA2 shows increased protection to thrombin in the presence of ADP. The arrows show fragments that were subjected to N-terminal sequencing. Fragments shown with

blue arrows had the N-terminal sequence IAQL. (B) The predominant thrombin cleavage site with the N-terminal IAQL sequence is shown in blue ball representation on a model of *M. tuberculosis* SecA2 (orange) generated using the program 3D-JIGSAW (110). The SecA2 model has been overlaid with the structure of *T. maritima* SecA in the open form in gray on the left (PDB ID 3JUX (76)), and on the right, the closed form (PDB ID 3DIN (74)). Based on sequence alignment, the corresponding thrombin cleavage site on *T. maritima* SecA is shown in purple. The UCSF Chimera program (38) was used to generate the figures.

H. ADP binding closes the clamp of SecA2 but not of SecA1.

In order to test whether the mobility shift shown by SecA2 on an agarose gel in response to ADP binding could be due to movement of the PPXD to the 'closed clamp' state, the native cysteine residues in SecA1 and SecA2 were mutated to serines and two sets of double cysteine mutants were introduced in both SecA1 and SecA2 to restrain the PPXD by disulfide bond formation in a manner done by the Collinson group (111). Due to high sequence homology between *E. coli* SecA and *M. tuberculosis* SecA1 we were easily able to make the corresponding mutants in SecA1 representing the open clamp (D318C:E810C) and closed clamp (D318C:K463C). Position D318 is in the PPXD, while E810 is located in the helical scaffold domain, and K463 is in NBD2 (Figure 3-12). In SecA2, however, due to absence of sequence homology in these regions, as well as the lack of a crystal structure of any SecA2 protein, generation of cysteine pairs that would mimic the respective conformations proved challenging.

We used S332C:D713C to probe the open clamp conformation of SecA2, but had to generate several combinations of cysteine mutants for the closed clamp and tested for disulfide bond formation. Position S332 is modeled to be located in the PPXD of SecA2, while D713 is modeled in the helical scaffold domain. We initially generated S332C:K475C as the closed clamp of SecA2. Position K475 would be in NBD2. Disulfide bond formation could not be assessed by non-reducing SDS PAGE as a series of higher molecular weight bands were observed on the gel. This result cannot be explained as wild type

SecA2 as well as several mono cysteine mutants of SecA2 with cysteines in different locations also show these bands even in the presence of high salt conditions where SecA2 would be monomeric, ruling out the possibility of intra or inter-molecular disulfide bonds.

In order to probe for proximity of the cysteines in a manner that does not constrain the cysteine residues, we resorted to pyrene excimer fluorescence. Pyrene is a fluorescent probe that has emission peaks between 370 nm and 405 nm. When two pyrene molecules are within a distance of ~ 10 Å, pyrene rings adopt a stacked conformation giving rise to an excited state dimer or 'excimer' that has an emission peak of ~ 460 nm. The double cysteine mutants representing the open and closed clamp variants of SecA1 and SecA2 were labeled with N-(1-pyrene)iodoacetamide (Life technologies) via their cysteine residues. Under low salt conditions where SecA1 and SecA2 are predominantly dimeric, the proteins showed only a peak of pyrene monomer fluorescence and no excimer was seen. Since the cysteine residues would be close to the dimer interface, perhaps dimerization of the protein affected the stacking of the pyrene rings and prevented excimer formation. Under conditions of high salt however, where the proteins are mostly monomeric, pyrene excimer fluorescene peaks were seen in case of both SecA1 open and closed clamp variants showing that the cysteine residues were in close proximity (Figure 3-11). This was also the case for the SecA2 open clamp mutant but the closed clamp form of SecA2 S332C:K475C did not show an excimer peak under high or low salt conditions. This mutant of SecA2 also did not show a mobility shift on agaraose gel under

oxidizing conditions. This indicated that SC332C:K475C does not represent the closed clamp as the cysteine residues are not in close proximity and thus would not be able to form a disulfide bond. In order to confirm that the excimer was not an artifact caused by the presence of high salt, wild type SecA2 that possesses two cysteines was used as a control. The two cysteines are far apart and would not be able to form an intramolecular disulfide bond. When wild type SecA2 was labeled with N-(1-pyrene)iodoacetamide and then emission scans were performed, only typical pyrene monomer peaks were seen between 350 and 450 nm while no excimer peaks were observed even under high salt conditions. Finally we generated S332C:D580C as the closed clamp of SecA2 and D580 is in NBD2 (Figure 3-12).

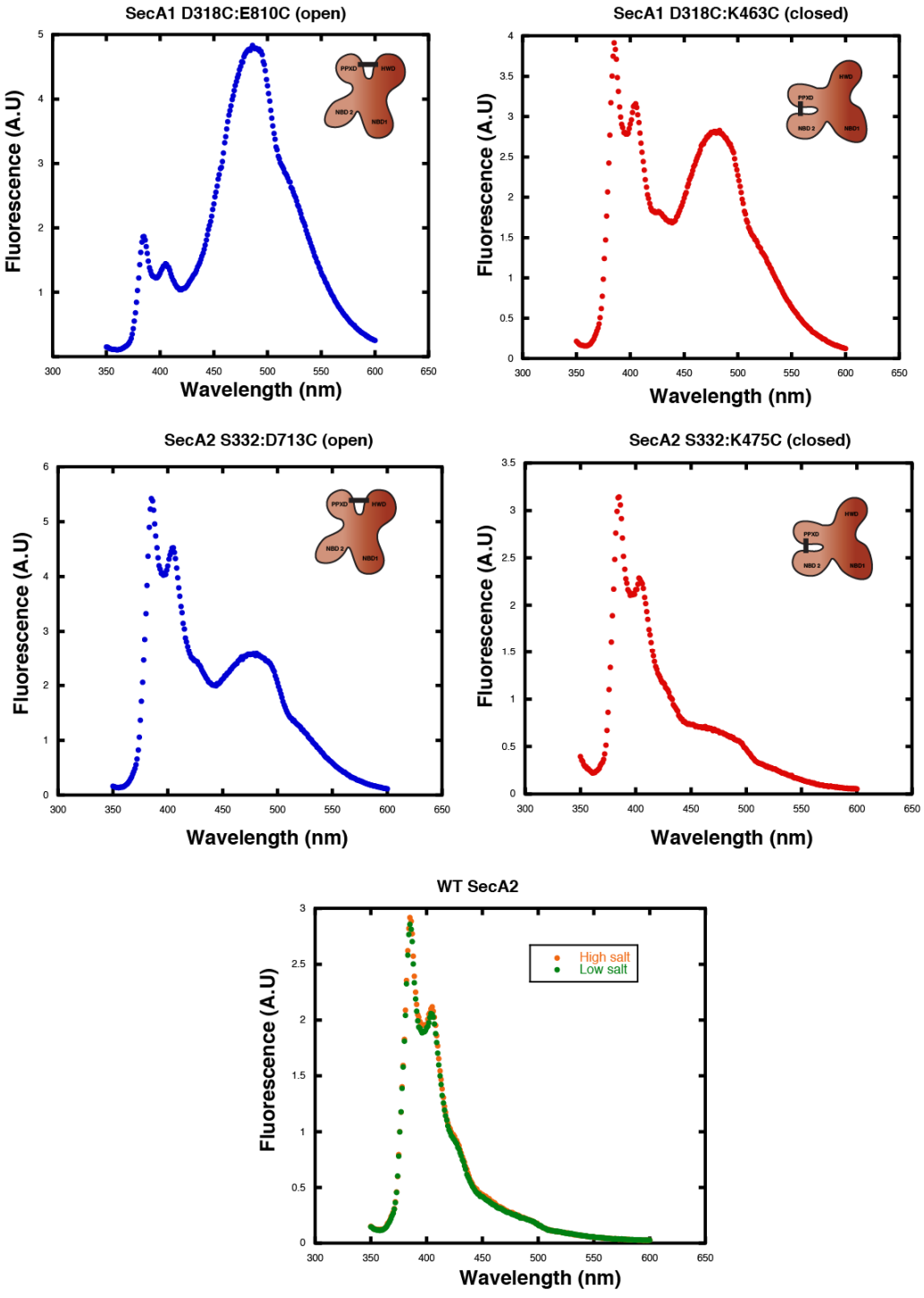

Figure 3-11: Probing the proximity of cysteines using pyrene excimer fluorescence.

Fluorescence scans of SecA1 and SecA2 open and closed clamp variants labeled with N-(1-pyrene)iodoacetamide. Scans were performed in buffer with high salt in order to probe the proximity of cysteine residues within SecA monomers. An excimer peak around 460 nm is indicative of the cysteine residues being in close proximity. WT SecA2 that has two native cysteines that are far apart and shows characteristic pyrene monomer peaks but does not show an excimer peak irrespective of the buffer used. (Inset) A cartoon of the SecA protein depicting positions of the cysteine residues and expected disulfide bond formation between them.

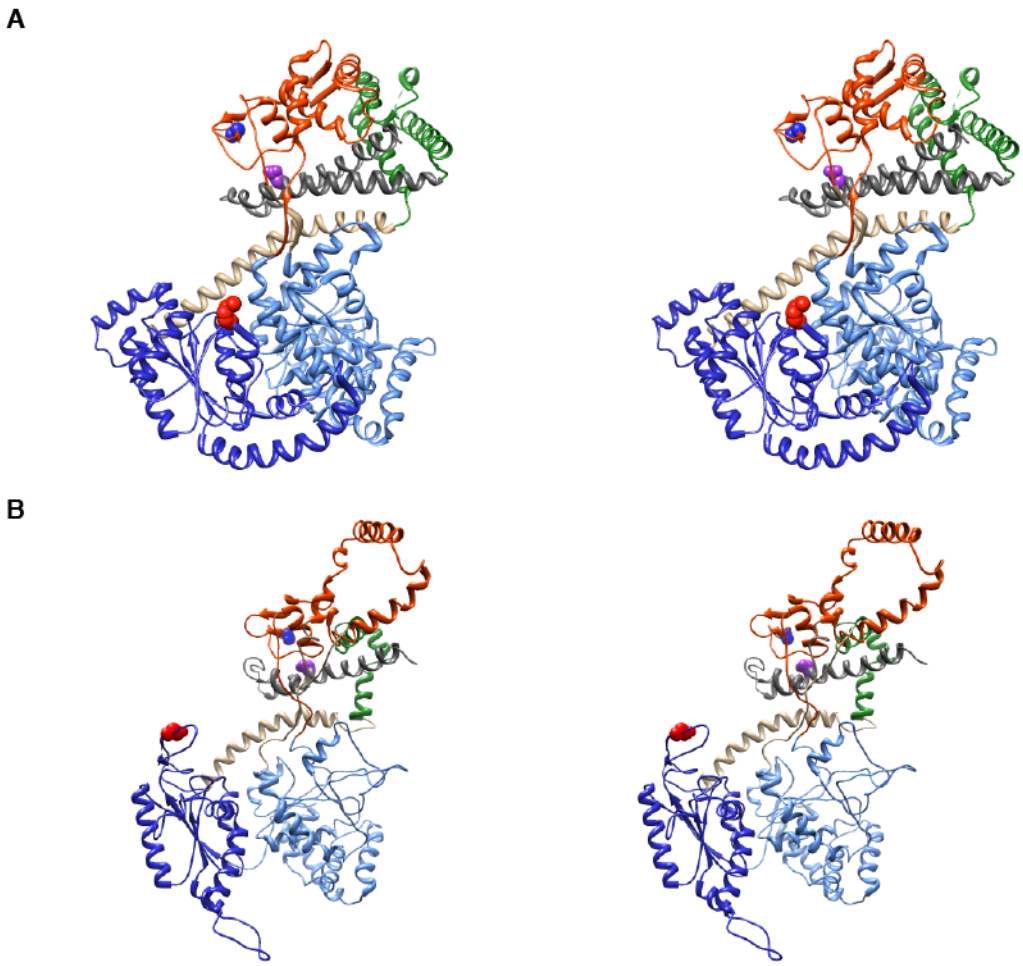

Figure 3-12: Probing clamp regulation in SecA2 using disulfide bond formation.

(A) The crystal structure of *M. tuberculosis* SecA1 (PDB ID 1NL3 (100)) is shown in stereo. NBD I and II are shown in light and dark blue respectively. The pre-protein crosslinking domain (PPXD) is shown in orange. The helical scaffold domain (HSD) is shown in tan and the two-helix finger that is part of the HSD is shown in dark gray. The helical wing domain (HWD) is shown in green. The cysteines introduced at positions 318 (PPXD), 810 (HWD) and 463 (NBD II) are

shown in ball representation in blue, purple and red respectively. (B) The model of SecA2 generated using 3D Jigsaw (110) is shown in stereo. Based on sequence homology to *M. tuberculosis* SecA1 and *E. coli* SecA, the domains are colored to match SecA1 shown in (A). The cysteines introduced at positions 332 (PPXD), 713 (HWD) and 580 (NBD II) in SecA2 are shown in ball representation in blue, purple and red respectively.

The PPXD in each mutant protein was restrained by disulfide bonds between the cysteines by air oxidation, or released using reducing agent. All variant proteins were able to bind nucleotide in a manner similar to wild type. Strikingly, when the open (D318C:E810C) and closed (D318C:K463C) clamp mutants of SecA1 were subjected to agarose gel electrophoresis in the oxidized state, a mobility shift was seen when the clamp was forced closed. This was similar to our observations with ADP-bound WT SecA2 (Figure 3-12). Consistent with our earlier results, ADP alone did not induce this mobility shift in WT SecA1. By comparison, in SecA2 the oxidized open clamp mutant did not show a mobility shift on the agarose gel. However, a fraction of the closed clamp mutant of SecA2 showed faster migration. This is consistent with the observation that ADP-bound WT SecA2 shifted almost entirely to the fast migrating form. When the oxidized SecA2 closed clamp mutant was reduced with TCEP, the faster migrating band is lost to the slower migrating band (Figure 3-12). These results show that the faster migrating form is only present when the closed clamp mutant was air oxidized but was absent when reduced. We expected the closed clamp mutant of SecA2 to shift entirely to the fast migrating form when oxidized; however, only a fraction shifted. This suggests that the open conformation of SecA2, in which the PPXD remains close to the helical wing domain, is favored until the protein is ADP bound. Alternatively, in SecA2 the sites chosen for the closed clamp cysteines might not be a perfect representation of the true closed clamp. Regardless, these results are consistent with the hypothesis that the

faster migrating species observed on the gel corresponds to SecA2 in its closed clamp form.

Furthermore in SecA2, but not in SecA1, movement of the PPXD is regulated by nucleotide binding.

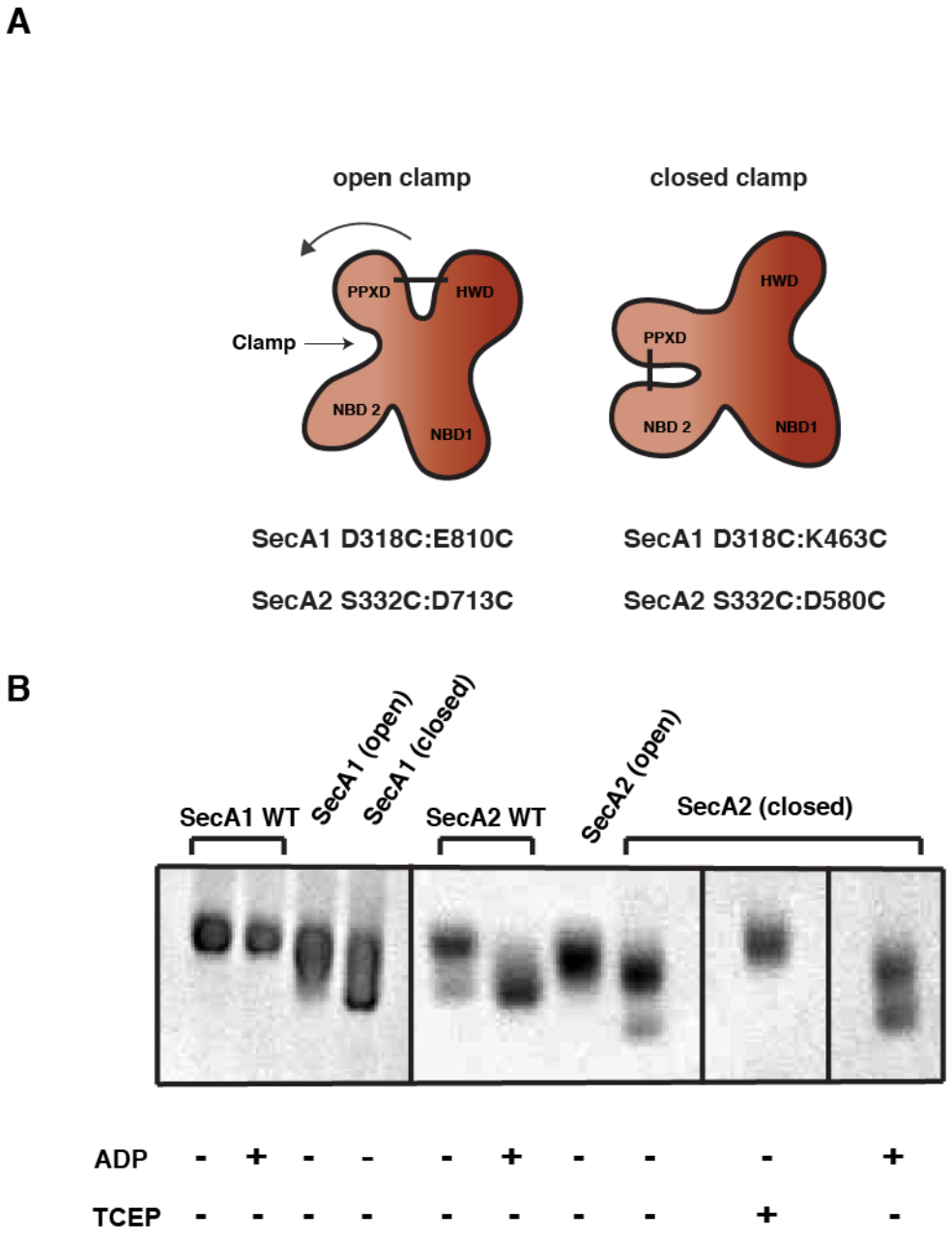

Figure 3-13: Binding of ADP induces movement of the PPXD to close the clamp of SecA2 but not in SecA1.

(A) Cartoon representation of *M. tuberculosis* SecA proteins in the open or closed clamp forms by disulfide bond formation between pairs of cysteines introduced by site-directed mutagenesis. (B) A 1% native agarose gel shows SecA1 only shifts mobility to a faster migrating form upon forced closure of the clamp by air oxidation of the cysteine residues. SecA2 shows a shift in mobility in the presence of ADP or if it's clamp is forced closed by oxidation of the introduced cysteines by air. The faster band that corresponds to the oxidized form in the closed clamp mutant of SecA2 shifts back to the slow migrating species in the presence of 20 µM TCEP.

Discussion

The identification of an additional SecA protein in several pathogenic bacteria has raised questions regarding the role of the accessory SecA in precursor translocation. In these systems, since SecA1 and SecA2 are functionally distinct (41,92), how are pre-proteins targeted to their respective SecA proteins given the redundancy in signal sequences? We set out to investigate some basic differences between the two SecA proteins of *M. tuberculosis* with the aim that our study might provide insight into the differences in regulation of the two SecA homologues. Our data show that SecA2 binds ADP with high affinity and that binding of ADP induces a large conformational change in SecA2. Interestingly, nucleotide binding does not induce this change in SecA1.

Conventional SecA proteins have been shown to undergo rapid ATP hydrolysis at the membrane ('translocation ATPase' activity) (25) in a reaction where ADP release is rate-limiting (67). Association of SecA with the SecYEG translocon (68,70) promotes ADP release, and this step is closely coupled to translocation of precursor proteins (112,113). From kinetic data using MANT-ADP, it is evident that SecA2 releases ADP much more slowly than SecA1; consequently the affinity of SecA2 for ADP is much higher than SecA1. *E. coli* SecA has been reported to bind MANT-ADP with a k_{on} of 7.8 x 10^4 $M^{-1}s^{-1}$ and k_{off} of 6.8 x 10^{-4} s^{-1} resulting in a K_d of 9 nM (70). Despite higher affinity of *E. coli* SecA for ADP compared to SecA2 (K_d ~ 50 nM), indicating that it would be ADP bound in our agarose gel experiments, *E. coli* SecA does not show a nucleotide-dependent shift like SecA2

The ADP-dependent shift we observe for SecA2 on an agarose gel is a unique feature of Mycobacterial SecA2. Crystal structures of *M. tuberculosis* SecA1 in the apo form and when bound to ADP-β-S do not show any significant differences, except for a few residues that are directly involved in nucleotide-binding, suggesting that there were no significant structural changes in SecA1 upon ADP binding including in the PPXD (100). This is consistent with our observation that SecA1 does not change mobility on the agarose gel with binding of nucleotide.

The most dramatic conformational change seen in conventional SecA proteins involves the ~ 80º movement of the PPXD with respect to the helical wing domain and NDB2 that leads to opening or closing of the 'clamp' (74,77,111) (Figure 3-1). The clamp is suggested to hold the pre-protein in a manner that facilitates interaction of the pre-protein with the tip of a helix known as the 'two-helix finger' that directs it into the channel during translocation (74,78). How movement of the clamp is regulated in conventional SecA proteins is not known.

Since there is no structure of any SecA2 protein to date, analysis of the conformational change in SecA2 by mutagenesis was challenging. Based on sequence homology between SecA1 and SecA2, the greatest variation between the two proteins lies in the C-terminal domain, while the nucleotide binding domains are highly conserved. This led us to believe that the overall domain architecture of SecA2 would be similar to SecA1. Consequently the possibility of a large unique conformational change in SecA2 completely different than seen in

conventional SecA proteins seems unlikely, although it cannot be entirely ruled out. Based on biochemical and biophysical studies on conventional SecA proteins and analysis of crystal structures it seems likely the mobility shift we observe in SecA2 on an agarose gel involves movement of the PPXD. Consistent with structural data, our biochemical data suggest that the clamp in *M. tuberculosis* SecA1 remains open in both the ADP-bound and apo- forms of the protein, as seen with *E. coli* and *T. maritima* SecA proteins. In contrast, in SecA2 binding to ADP appears to cause closure of the clamp.

Based on the high affinity of SecA2 for ADP, and the slow K_{off}, SecA2 in the Mycobacterial cytosol of would be primarily ADP bound even in the presence of the 1 mM cellular concentration of ATP (43). Since the clamp of SecA2 would be closed in this form, it could serve as a mechanism to prevent binding of SecA1 dependent pre-proteins to SecA2. In a study done by the Braunstein group to determine the subcellular localization of the SecA proteins in *Mycobacterium smegmatis*, SecA1 was found equally distributed between the membrane and the cytosol, while SecA2 was predominantly cytosolic (97). Under normal growth conditions, SecA1 functions like conventional SecA proteins in translocating the majority of pre-proteins across the Sec translocon. Since SecA2 is not required for general protein export, but is implicated in the export of virulence factors (39,96), we hypothesize that under certain conditions when SecA2 is required, binding to an unknown factor or pre-protein signal sequence could promote ADP release, thereby opening the clamp of SecA2 to enable it to accommodate the pre-protein and target it to the membrane for translocation.

Our results provide the first evidence of biochemical differences between the two SecA homologues, which suggests a mechanism for the cell to distinguish between the proteins during translocation.

Chapter 4

‘ IT TAKES TWO TO TANGO-OR DOES IT?’

Introduction

The Sec-dependent secretion system in *E. coli* has been studied extensively over the past three decades. In particular, the ATPase protein SecA has been well characterized. However; after decades of work on this protein, its oligomeric state remains a puzzle to date. *E. coli* SecA has been shown to fold via a dimeric intermediate (114) and exist in a monomer-dimer equilibrium in solution (85,86). This equilibrium is affected by protein concentration, ionic strength and temperature. High protein concentration and low ionic strength favors dimerization while high ionic strength favors monomerization (85,86). The dissociation constant (K_d) for the dimer has been shown to be less that 1 nM by single molecule methods (81). At a salt concentration of 200 mM, which is closer to physiological conditions, the K_d is increased to 0.28 µM (86). Nevertheless, at a cellular concentration of 8 µM (80), *E. coli* SecA is expected to be predominantly dimeric. Biochemical studies have also shown that dimeric SecA is required for protein translocation (115-117). Yet several studies show that *E. coli* SecA functions as a monomer during translocation (118) and that ligands such as phospholipids (83) and nucleotides (119) monomerize the protein. Further, signal peptides have been shown to cause oligomerization in SecA (83) in some studies while other studies show signal peptides favor monomerization of SecA (82,86).

The fact that dimerization of SecA is affected by ionic strength suggests that the contacts between the two protomers must be stabilized by electrostatic interactions. The SecA protein has been crystallized from several organisms, however the dimer interfaces are different in all the crystal structures (84). Most of these structures are those of dimeric SecA and show an antiparallel orientation of the protomers in which the C-terminal domains of each protomer face away from each other in opposite directions.

The structure of *Thermatoga maritima* SecA bound to the translocon has only one protomer of SecA however; crystallization conditions including detergent treatment could have led to the loss of one protomer.

Recently, the structure of the SecA1 dimer from *M. tuberculosis* (1NL3) (100) and SecA dimer from *B. subtilis* (1M6N) (120) were re-analyzed using a bioinformatics program called EPPIC which identifies physiologically relevant dimers (87). The authors found that by a 60º rotation about one protomer, one of the structures could be converted to the other indicating that dimerization in both SecA proteins are mediated by the same contacts. This observation would support the theory that extreme N-terminal residues of one protomer would contact C-terminal residues (IRA1 regions, scaffold and wing domain residues) of the next protomer supporting previous biochemical data. Several groups have shown that deletion of the first few N-terminal residues or IRA1 residues (Δ783-795) render *E. coli* SecA predominantly monomeric (66,115,118,121). Since this would imply a rather large interface. SecA proteins would exist in several dimeric states involving the main contacts. These states would be dynamic and

interconvertible and would explain why different interfaces are seen in different crystal structures (87). The authors identified two main structural elements involved in N-terminal contacts (87). These elements involve a short helix (referred to as α0) and a longer helix (referred to as α1). The contacts made by α0 in *E. coli* SecA were shown to involve mostly hydrophobic interactions while contacts made by α1 were shown to involve electrostatic interactions (mainly mediated by six charged residues). When α0 was deleted or the six charged residues in α1 were changed to alanines (1-6A), the protein still remained dimeric. However, the combination (Δα0,1-6A) resulted in *E. coli* SecA being monomeric even under low salt conditions.

Even though the contacts involved in dimerization were identified based on the structure of *M. tuberculosis* SecA1, the authors performed all experiments on *E. coli* SecA and conclude that dimerization in all SecA proteins, involve the same structural features. The *M. tuberculosis* SecA1 protein was crystallized as a dimer by the Sacchettini group however; 3D electron microscopy (EM) reconstructions of the protein revealed that it forms a tetramer. This gave rise to two possible dimer configurations referred to as the A-B or A-C dimer by the Sacchettini group (100). Based on the crystal structure, in the A-B dimer, the residues involved in dimerization would be mostly hydrophobic in nature while the dimer interface in the A-C dimer would be stabilized by electrostatic interactions. The A-C dimer was not considered physiologically relevant as 17 residues involved in dimerization would involve vector-derived residues. The dimer of *M. tuberculosis* SecA1 described by Gouridis et al. using EPPIC, would

resemble the A-C dimer in which α0 and α1 would be the main structural elements mediating dimerization.

In this study, I investigated the oligomeric state of the *M. tuberculosis* SecA1 and SecA2 proteins and attempted to identify the structural elements involved in dimerization of SecA1.

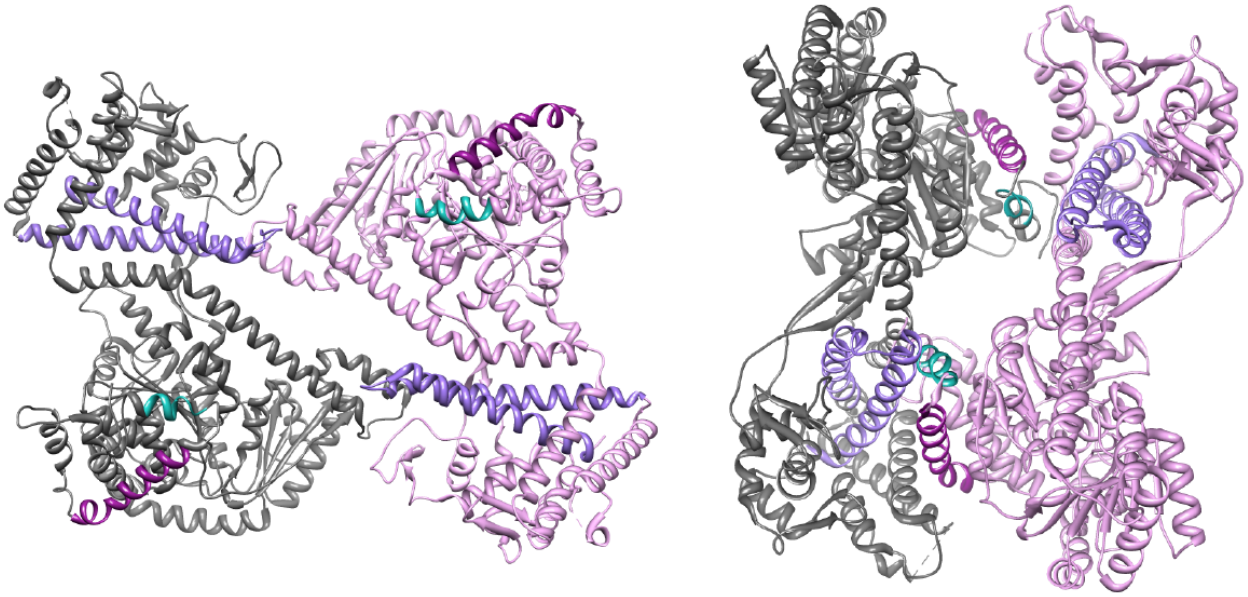

Figure 4-1: Dimer configurations of *M. tuberculosis* SecA1

The A-B dimer of *M. tuberculosis* SecA1 (1NL3) (100) is shown on the right while the A-C dimer configuration is shown on the left. One protomer of the dimer is shown in gray while the other protomer is shown in pink. The N-terminal elements that are believed to be involved in forming the dimer interface according to Gouridis et al. are colored in cyan (α0) and majenta (α1) while the C-terminal elements thought to form contacts with the corresponding protomer are shown in purple (IRA1).

Results and Discussion

A. Dimerization in *M. tuberculosis SecA1 and SecA2 is salt-dependent.*

An important step towards understanding the mechanism of translocation by the *M. tuberculosis* SecA motor and its interaction with the translocon is the determination of the oligomeric state of its SecA proteins. Since *M. tuberculosis* SecA1 and SecA2 share only around fifty percent sequence homology with *E. coli* SecA, we sought to investigate the oligomeric states of SecA1 and SecA2. Dimerization of *E. coli* SecA is salt sensitive (81,85,86), so we investigated the association states of SecA1 and SecA2 under low salt (25 mM KCl) and high salt (300 mM KCl) conditions by size exclusion chromatography. When purified SecA1 or SecA2 were subjected to size exclusion chromatography under conditions of low salt, both showed elution profiles consistent with the proteins being dimeric based on calibration standards. However, in the presence of 300 mM KCl, the elution volumes of both proteins increased significantly, consistent with monomeric forms of the proteins. This indicates that SecA1 and SecA2 dissociate into monomers in high salt conditions (Figure 4-2).

Since formation of oligomers is dependent on protein concentration, we assessed dimerization of both SecA proteins at varying protein concentrations in order to gain insight into the strength of the association. From analysis of the column profiles, we confirmed that both SecA1 and SecA2 are predominantly dimeric in low salt buffer, even at very low protein concentrations (~0.3 μM) indicating that under low salt conditions, the dissociation constant (K_d) for

dimerization must be lower than 0.3 μM. This is consistent with *E. coli* SecA which has a K_d < 1 nM in low salt but is monomeric in high salt. These data also show that the dimer interface in *M. tuberculosis* ScA1 and SecA2 must be stabilized by electrostatic interactions.

Since conditions of high salt mimic physiological conditions, the self-association reactions of SecA1 and SecA2 were further studied in high salt using sedimentation velocity analytical ultracentrifugation. The peak fractions from the size exclusion column were concentrated and subjected to analytical ultracentrifugation at multiple protein concentrations. In order to gain insight into the stoichiometry and heterogeneity of the samples, as well as get a rough estimate of the sedimentation coefficients, the time derivative method ('*dc/dt*') was used (122). Normalized sedimentation coefficient distributions g(s*) for SecA1 and SecA2 generated by this method show that for both SecA1 and SecA2, the sedimentation coefficients shift towards higher S values with increasing protein concentration, indicating that the two proteins undergo self-association; however, the proteins exist in a weak monomer-dimer equilibrium in high salt. The sedimentation coefficient of the monomer was determined to be 5.25 S for SecA1 (Figure 4-2C) and 5.01 S for SecA2 (Figure 4-2D). In order to determine the equilibrium constants (K_d) for the dissociation reactions, the sedimentation velocity data were analyzed with the program Sedanal (122). For SecA1, a monomer-dimer self-association model was used to fit the data and the dissociation constant (K_d) obtained from the fit was approximately 64 μM. Since preliminary analysis of the data for SecA2 indicated the presence of aggregates

(~ 7% by weight), the data were fit to a monomer-dimer self-association model including the presence of a fixed amount of aggregate. From the fit, the K_d for SecA2 self-association in high salt was approximately 240 µM. In case of both SecA1 and SecA2, the overall fits were good and had RMS errors of 0.002 and 0.0017 fringes respectively.

Interestingly, *E. coli* SecA has a K_d of ~ 3 µM under conditions of 300 mM KCl at 20 ºC (86). This is still below the concentration of E. coli SecA in the cell suggesting that under physiological conditions, *E. coli* SecA would be primarily dimeric in the cytosol. On the other hand, our data indicate that the K_d s for SecA1 and SecA2 oligomerization are much higher than the respective mycobacterial SecA concentrations in the cell suggesting that in the salt environment of the cytosol both proteins may be monomeric at least in the absence of interaction with pre-proteins, lipids or SecYEG.

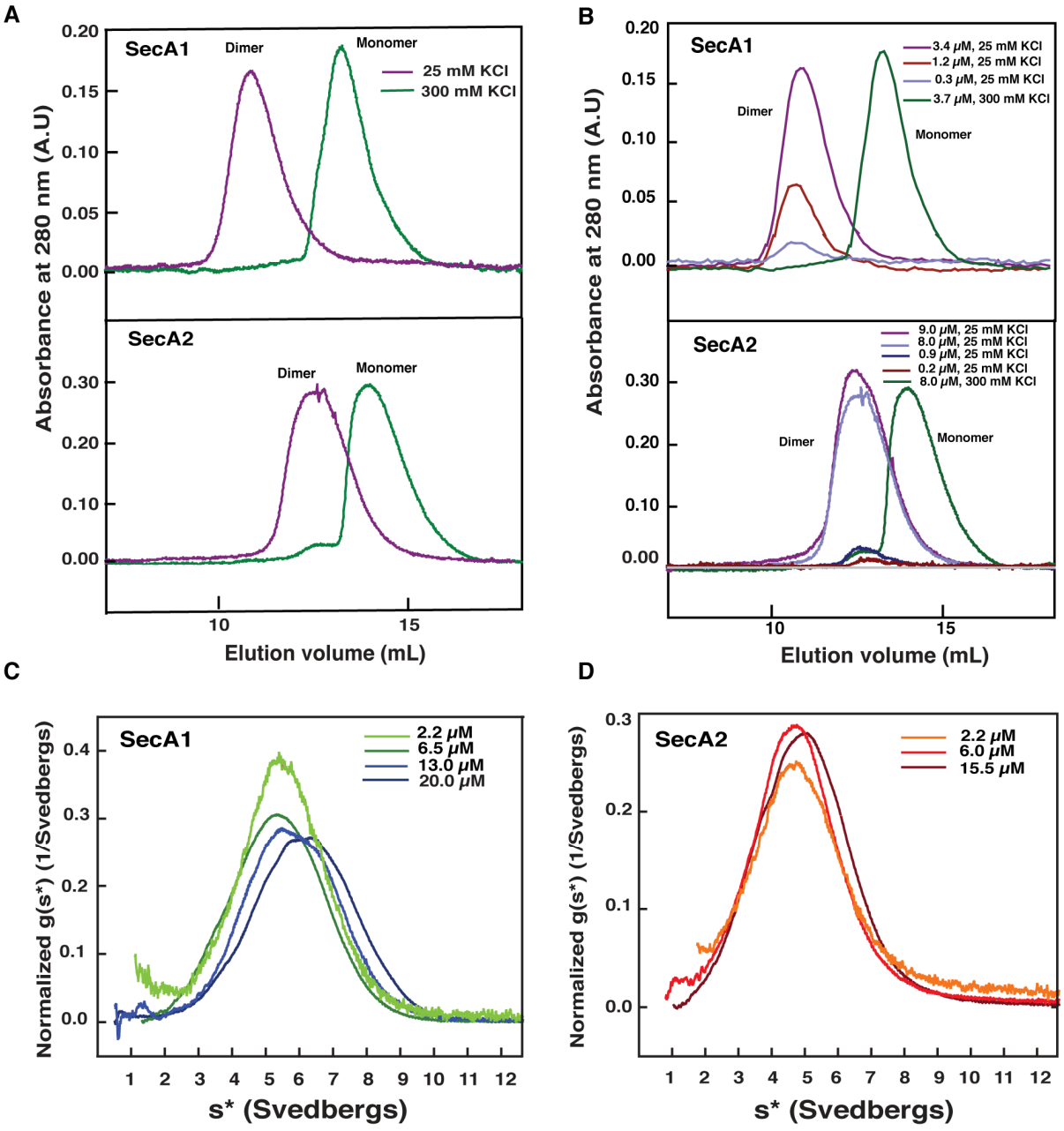

Figure 4-2: Oligomeric state of *M. tb* SecA1 and SecA2

(A) Size exclusion chromatography column profiles of SecA1 and SecA2 run on a Superdex 200 column in buffer with 25 mM KCl (low salt) or 300 mM KCl (high salt). (B) SecA1 and SecA2 were run on the column at varying protein concentrations in low salt buffer. The traces of SecA1 and SecA2 in high salt are shown again in green on this profile to denote the elution volume of the monomeric protein. Self-association of *M. tb.* SecA1 (C) and SecA2 (D) characterized by sedimentation velocity analytical ultracentrifugation. The plots show the normalized sedimentation coefficient distributions g(s*) for SecA1 and SecA2 at increasing concentrations, as analyzed by DCDT+.

B. SecA1 does not exist as a salt resistant dimer

In a study by Kusters et al. (81) to investigate the oligomeric state of SecA during various stages of translocation, they found that monomeric SecA binds to SecY in a salt-resistant manner, while association of the second protomer was salt sensitive. Recently, a study by Gouridis et al. suggested that SecA exists mainly in two dimeric forms; in one form the dimer interface is stabilized by electrostatic interactions mediated by the α1 region while the other conformer is mostly stabilized by hydrophobic interactions mediated by α0 (87). The former was referred to as the 'electrostatic dimer' (ED) while the latter was called the 'salt-resistant dimer' (SRD). Even though ~ 95 % of *E. coli* SecA dissociated into monomers under high salt conditions, around 5 % remained dimeric. This dimeric conformer was believed to be that of the SRD. In our experiments with *M. tb* SecA1 we do not observe a SRD form under high salt conditions however; in SecA2 around 5 % of the protein remains dimeric in 300 mM KCl and may represent the SRD form (Figure 4-2A). It was also shown by Gouridis et al. that by mutation of six charged residues in α1 to alanines (1-6A), the protein still remained dimeric in low salt. Under high salt conditions around 50% of the 6A protein did not monomerize but remained dimeric. This was attributed to the fact that upon mutation of the charged residues, dimerization could still be mediated by the hydrophobic α0 region favoring the SRD.

In order to test if this was true for *M. tb* SecA1 as suggested by the authors, the corresponding charged residues in SecA1 were changed to alanine residues and the SecA1_6A protein was subjected to size exclusion

chromatography under conditions of low and high salt. Our data show that under low salt conditions, the elution volume of the *M. tb* SecA1_6A mutant is significantly increased compared to WT SecA1 (Figure 4-3). This is unlike the case with *E. coli* SecA; where the 6A mutant does not show any shift in elution volume compared to WT, consistent with it being dimeric in low salt. On the other hand; under high salt conditions, the peak of *M. tb* SecA1_6A perfectly overlaps with that of the WT protein. This suggests complete monomerization of the protein in high salt like WT SecA1 without any evidence of a SRD peak, unlike the 6A mutant of *E. coli* SecA where ~ 50% of the protein remains dimeric (SRD) even in high salt. Since SecA1 does not show evidence of a SRD, we wanted to test the contribution of the probable α0 region so we made SecA1Δα0 as well as SecA1Δα0, 6A however deletion of the α0 region in SecA1 led to rapid proteolysis of the protein and analysis of the mutants could not be carried out as a consequence.

Nevertheless, our data suggest that dimerization may not be mediated by the same elements in all SecA proteins. In *M. tb* SecA1, the dimer seems to be stabilized mainly by electrostatic interactions. In order to identify the interface, cysteine residues could be introduced into the SecA1 protein in a cysteine free background, at probable dimer contact sites and disulfide or chemical cross linking reagents could be used to identify disulfide-linked dimers. Since the dissociation constants for dimerization of SecA1 and SecA2 under physiological salt concentrations are not as low as that of *E. coli* SecA suggesting that the proteins in the mycobacterial system may be monomeric, it would be interesting

to probe the oligomeric state of these proteins in the presence of other ligands like SecY or precursor proteins.

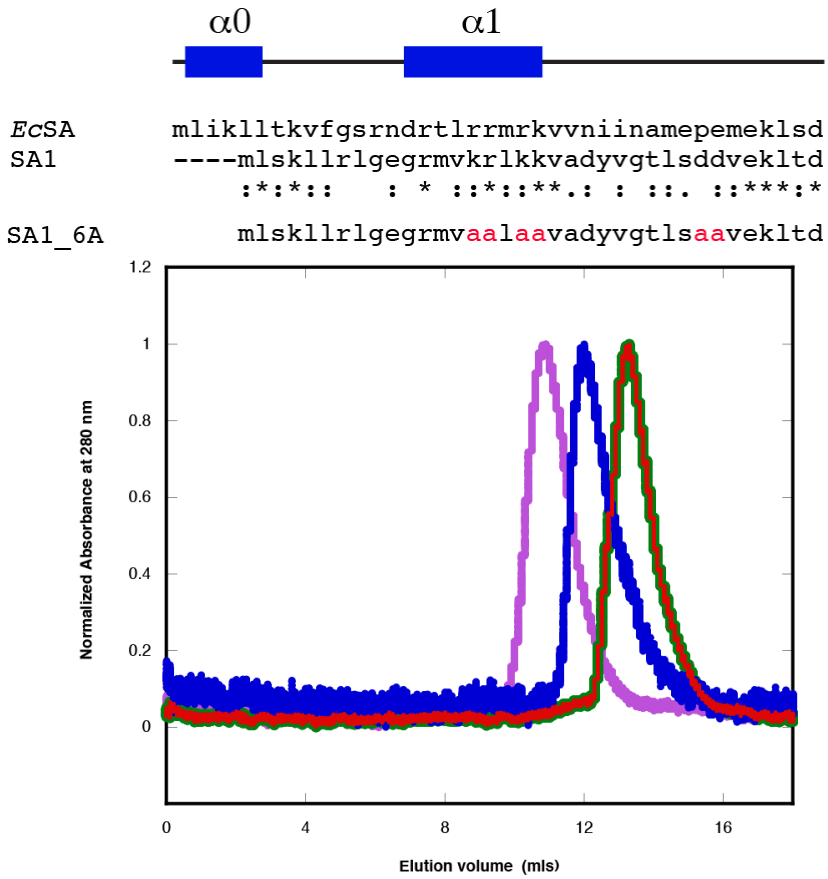

Figure 4-3: *M. tb* SecA1 does not form a salt-resistant dimer

(Top) An alignment of the first 40 residues of *E. coli* SecA (EcSA) and *M. tb* SecA1 (SA1) using Clustal is shown. Conservation is represented by the symbols below the alignment. Stars represent the same residue while bullets represent similar residues. Above the alignment, the regions of the N-termina helices representing α0 and α1 according to Gouridis et al.(87) are shown in blue. In the SecA1_6A mutant the alanines that substituted the charged residues are shown in red. (Bottom) Size exclusion column profiles of WT SecA1 in 25 mM KCl (pink trace) and 300 mM KCl (green trace) are shown. Absorbance traces for the SecA1_6A mutant in 25 mM KCl and 300 mM KCl are shown in blue and red respectively

Chapter 5

ASSOCIATION OF THE *M. tb* SECA PROTEINS WITH MEMBRANES

Introduction

The presence of an additional SecA protein in *M. tuberculosis* as well as several pathogenic bacteria raises several questions regarding the role of the 'accessory' SecA. In *M. tuberculosis*, SecA2 is functionally distinct from SecA1 as deletion of *secA2* attenuates bacterial virulence (92). Also, the ATPase activity of SecA2 has been shown to be important for the intracellular survival of the bacteria in macrophages (43). SecA2 has shown to localize to the cytosol unlike SecA1, but a Walker A box variant of SecA2 switches localization to the membrane in vivo (97). Similar results are seen with the corresponding Walker A box variant in *Clostridium difficile*, a bacterium that possesses a SecA2 protein without a SecY2 (45). These results suggest that the role of SecA2 is probably not just restricted to the cytosol instead, it gets recruited to the membrane under some condition that is yet to be identified. Since mycobacteria lack a *secY2* homolog, mycobacterial SecA2 is thought to work with the canonical SecYEG translocon. Further evidence for this comes for the fact that strains of *M. tuberculosis, M. smegmatis* as well as *C. difficile* containing a Walker A box variant of SecA2 exhibit a dominant negative phenotype (97). Extragenic suppressor mutations of the SecA2 K129R Walker A box variant in *M. smegmatis* could be mapped to the SecY promoter region that leads to overexpression of the canonical SecY protein (98) and can alleviate the *secA2 K129R* phenotype.

Since SecA2 is thought to function at the translocon at some stage, possibly during the export of virulence factors, the questions arise; how is SecA2 differentiated from SecA1 and recognized by SecY and precursor proteins? What is the oligomeric state of SecA2 during translocation?

Answers to these questions are not yet known due to several difficulties associated with studying mycobacterial components *in vivo*. *M. tuberculosis* grows extremely slowly and is a pathogen that requires biosafety level 3 (BSL3) practices. Genetic manipulation of mycobacteria is also not as trivial as it is in *E. coli*. Additionally, since *secA1* is essential, it is difficult to study the role of SecA2 independently *in vivo*. In order to study the dependence of pre-proteins on SecA2, oligomeric state of SecA2 during stages of translocation, association of SecA2 with membrane lipids and SecYEG, it is essential to have a system reconstituted from purified components in vitro. This would allow the study of the SecA proteins independently as well as with other ligands such as pre-proteins, lipids. One could also vary salt concentrations to favor monomers or dimers of the SecA proteins.

Several attempts were made to express *M. tuberculosis* SecYEG in *E. coli* using different expression vectors and varying expression conditions; however due to rapid proteolysis of SecY in all cases, this was not feasible. Finally, vesicles were made from a strain of *M. smegmatis* that contains hemagglutinin (HA) tagged SecY in addition to the endogenous SecY on the chromosome. *M. tuberculosis secA2* can complement a *M. smegmatis ΔsecA2* strain and *M. smegmatis secA2* can substitute for *M. tb* secA2 during growth of *M. tb* in

macrophages and restore the rough colony phenotype to a *M. tb ΔsecA2* strain (which shows a smooth colony phenotype) (92,97). Since these results demonstrate the functional conservation between the two systems we believe that the *M. tb* SecA1 and SecA2 proteins will be able to function along with membrane vesicles containing *M. smegmatis* translocon components.

Results and Discussion

A. Membrane vesicles containing HA-tagged *M. smegmatis* SecY are sealed and can establish a proton gradient.

Generation of sealed membrane vesicles with SecYEG incorporated would have several applications in the study of Mycobacterial protein export. These vesicles could be used to develop an *in vitro* translocation assay, similar to assays used to study export in *E. coli*. However; the presence of an unusually thick cell wall in Mycobacteria comprised of a layer of mycolic acids makes the generation of membrane vesicles challenging.

Following the protocol of Haagsma et al. (123,124) with a few modifications, membrane vesicles of *M. smegmatis* were obtained. In order to check if these vesicles were sealed, the establishment of a proton gradient using various substrates was tested by the 9-amino-6-chloro-2-methoxyacridine (ACMA) quenching method (123). ACMA is a lipophilic dye that is fluorescent when bound to membranes (125). The establishment of a proton gradient across membranes due to components of the electron transport chain (ETC) upon addition of electron donors, causes quenching of ACMA fluorescence.

Upon addition of the substrate (NADH, succinate or ATP) to the *M. smegmatis* vesicles, the ACMA fluorescence was quenched with time. Further, the addition of an uncoupler carbonyl cyanide *m*-chlorophenyl hydrazone **(**CCCP) caused the ACMA fluorescence to increase again, indicative of the collapse of the proton gradient by the uncoupler (Figure 5-1).

When NADH or succinate were used as electron donors, the proton gradient was successfully established and collapsed by the addition of CCCP as observed by Haagsma et al. (124) indicating that the *M. smegmatis* vesicles generated are functional. However; when Mg^{2+}- ATP was used as a substrate, no significant quenching of ACMA fluorescence was observed, consistent with results seen by Haagsma et al. and fluorescence did not increase upon the addition of uncoupler (124). Since the F1F0 ATP synthase in *M. smegmatis* cannot hydrolyze ATP to make a proton gradient like the case with some Mycobacteria, the absence of a proton gradient with ATP as a substrate serves as a negative control for this assay (Figure 5-1).

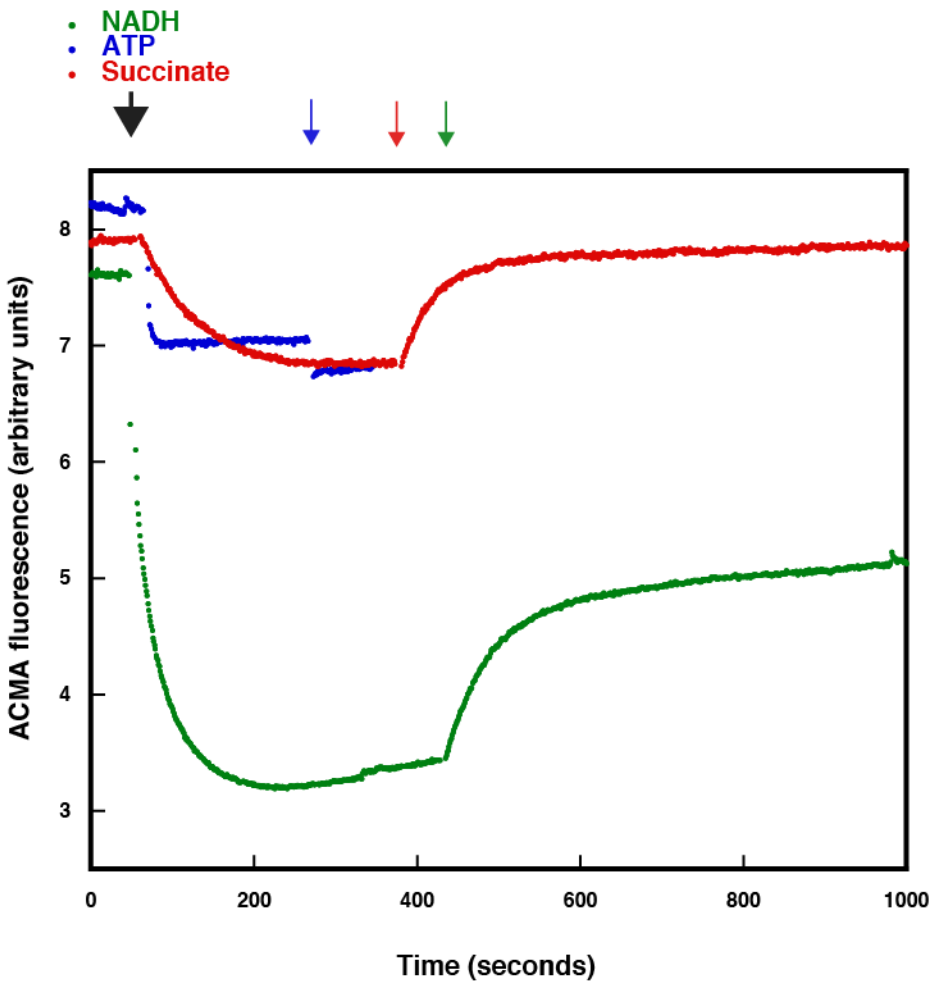

Figure 5-1: Establishment of a proton gradient across *M. smegmatis* vesicles assessed by ACMA fluorescence quenching.

M. smegmatis vesicles (MVs) were treated with the dye ACMA, followed by the addition of NADH, ATP or succinate as electron donors. Once the fluorescence was fully quenched, the uncoupler CCCP was added (indicated by the respective colored arrow) which caused a collapse in the proton gradient and consequent increase in ACMA fluorescence.

B. SecA1 interacts with the membrane while SecA2 does not.

In *E. coli*, the number of copies of SecA (13,000 copies) greatly exceeds that of SecYEG (500 copies) (63). The presence of an additional functionally distinct SecA protein in Mycobacteria that is expressed at similar levels to the canonical SecA (43) made us question how SecA1 might function at the translocon without competing with SecA2 for the limited number of translocon sites. On the other hand, since Mycobacteria do not possess a SecB homolog, there has been speculation about SecA2's ability to fulfill the role of a cytoplasmic chaperone (126). In order to gain insight into the subcellular localization of SecA1 and SecA2, association of these proteins with membranes and SecY was tested using *M. smegmatis* vesicles incorporating HA-SecY.

Membrane vesicles were checked for the establishment of a proton gradient using ACMA quenching by succinate as the electron donor (Figure 5-2A). Incorporation of HA-SecY into the vesicles was tested by separating the proteins from the membrane vesicles by SDS PAGE followed by Western blotting using antibodies to the HA tag (Figure 5-2B). The vesicles showed successful incorporation of HA-SecY and were sealed indicated by quenching of ACMA fluorescence by the addition of succinate and re-establishment of the proton gradient upon addition of CCCP (Figure 5-2).

Iodixanol (OptiPrep) density gradients were set up so that following centrifugation, membrane vesicles would float and would be located in the top fractions while proteins would remain in the bottom fractions upon fractionation of

the gradients. Our data clearly show that when membrane vesicles are present, SecA1 shows movement to the top fractions indicating associations with the membrane vesicles. SecA2 however, remains in the bottom fractions and does not associate with the vesicles (Figure 5-3). These data are consistent with western blotting data from the Braunstein lab that show that SecA1 is equally distributed between the membrane and the cytosol while SecA2 is mostly cytosolic in both *M. tuberculosis* and *M. smegmatis* (97). Further, our data show that SecA1 can associate with the membrane independently and does not require SecA2 or any other factor such as pre-proteins for recruitment to the membrane, while SecA2 may either function in the cytosol or require an additional factor for recruitment to the membrane.

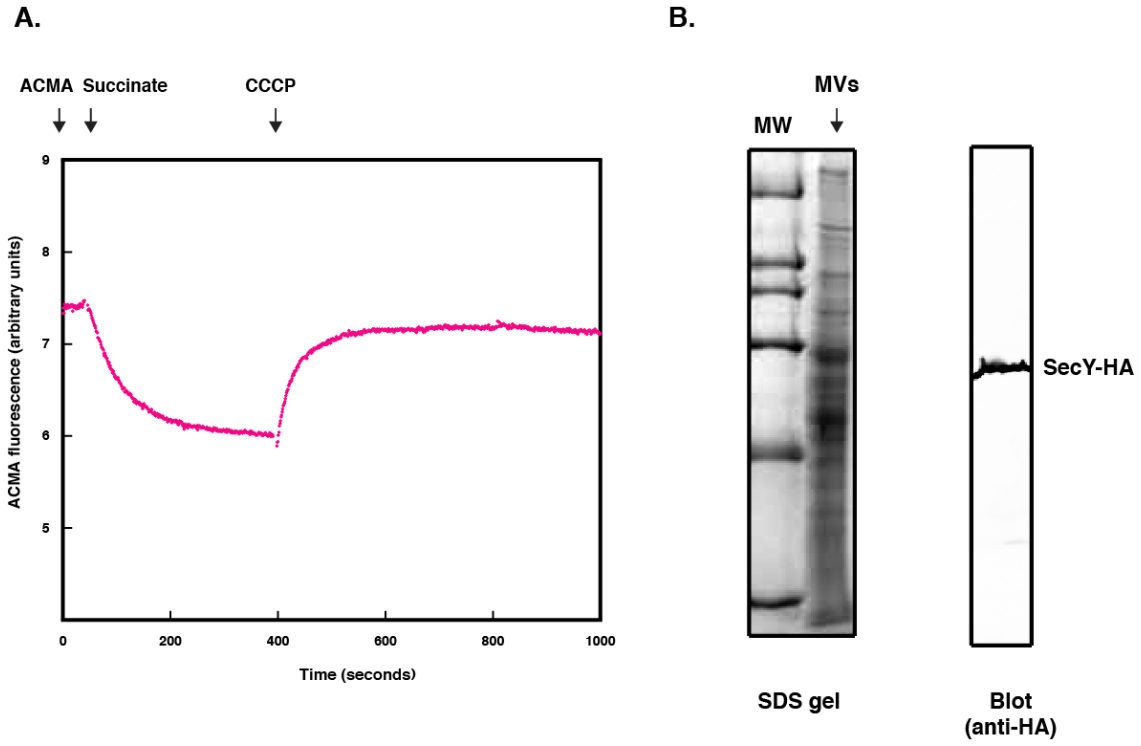

Figure 5-2: *M. smegmatis* vesicles containing HA-tagged SecY are sealed and can maintain a proton gradient.

A. The *M. smegmatis* vesicles (MVs) were tested for their ability to maintain a proton gradient by the ACMA assay as a method to check if the vesicles were sealed. B. Since the strain of *M. smegmatis* used to prepare the MVs has hemagglutinin tagged SecY in addition to endogenous SecY, the incorporation of HA-SecY into the vesicles was checked by separating the proteins in the vesicles by SDS PAGE followed by western blotting using anti-HA antibodies.

C. SecA2 K115R associates with membrane vesicles more than WT SecA2.

Studies have shown that the Walker box variant of SecA2 in *M. smegmatis* (SecA2 K129R) has a dominant negative phenotype and SecA2 K129R shifts localization to the membrane fraction compared to WT SecA2 which is cytosolic. When *M. tuberculosis* SecA2 K115R was tested for association with membrane vesicles, a small fraction of the protein was found in the membrane fraction. The membrane associated protein fraction was more than wild type SecA2 but significantly less than the fraction of SecA1 that shows association with membranes (Figure 5-3).

Since SecA1 is thought to function as the 'housekeeping' SecA in general protein export, we reasoned that perhaps SecA2 requires SecA1 for recruitment to the membrane. SecA1 and SecA2 or SecA2 K115R were incubated together before testing membrane association using the OptiPrep gradients, however SecA2 did not show recruitment to the membrane fraction even in the presence of SecA1, while SecA1 migrated to the membrane fraction. SecA2 K115R did not showed any enhancement of membrane binding with the addition of SecA1. These data show that SecA1 does recruit SecA2 to the membrane. SecA2 may either function in the cytosol or require an additional factor for recruitment to the membrane.

In order to test the possibility that SecA2 requires association with another protein or factor for recruitment to the membrane, the proteins SecA2 and SecA2 K115R were supplemented with *M. smegmatis* cytosol in addition to the

membrane vesicles prior to centrifugation and resolution of the gradients. However; neither did SecA2 show recruitment to the membrane nor SecA2 K115R show enhanced association with membranes even in the presence of cytosol (Figure 5-3). Membrane association was also tested in the presence of various other factors (data not shown) such as nucleotides (ATP, ADP, AMP-PNP), proton gradient, precursor proteins and other potential binding partners (protein 3311), however unlike SecA1, SecA2 did not show recruitment to the membrane under any of the conditions tested. It occurred to us that *M. smegmatis* vesicles would have endogenous SecA bound to it that may occlude binding of added SecA1 and SecA2 so membrane association was tested using urea treated vesicles however; we did not observe association of SecA2 with membranes even when binding sites of *M. smegmatis* SecY were available.

Since SecA2 appears to function in the export of virulence factors, it is necessary to detect association of a pre-protein with SecA2 *in vitro* and test membrane binding of the SecA2-precursor complex. Due to the fact that SecA2 Walker A box variants in *M. smegmatis, M. tuberculosis* and *C. difficile* shift localization to the membrane fraction *in vivo*, it would be interesting to probe the features of these mutants that recruit them to the membrane fraction. Perhaps recruitment is mediated by a downstream effector that is yet to be identified. Nevertheless, the presence of two SecA homologs, one that interacts with the translocon routinely and the other that may only interact transiently suggests that SecY in this system would have also evolved to facilitate such interactions that must be rather unique.

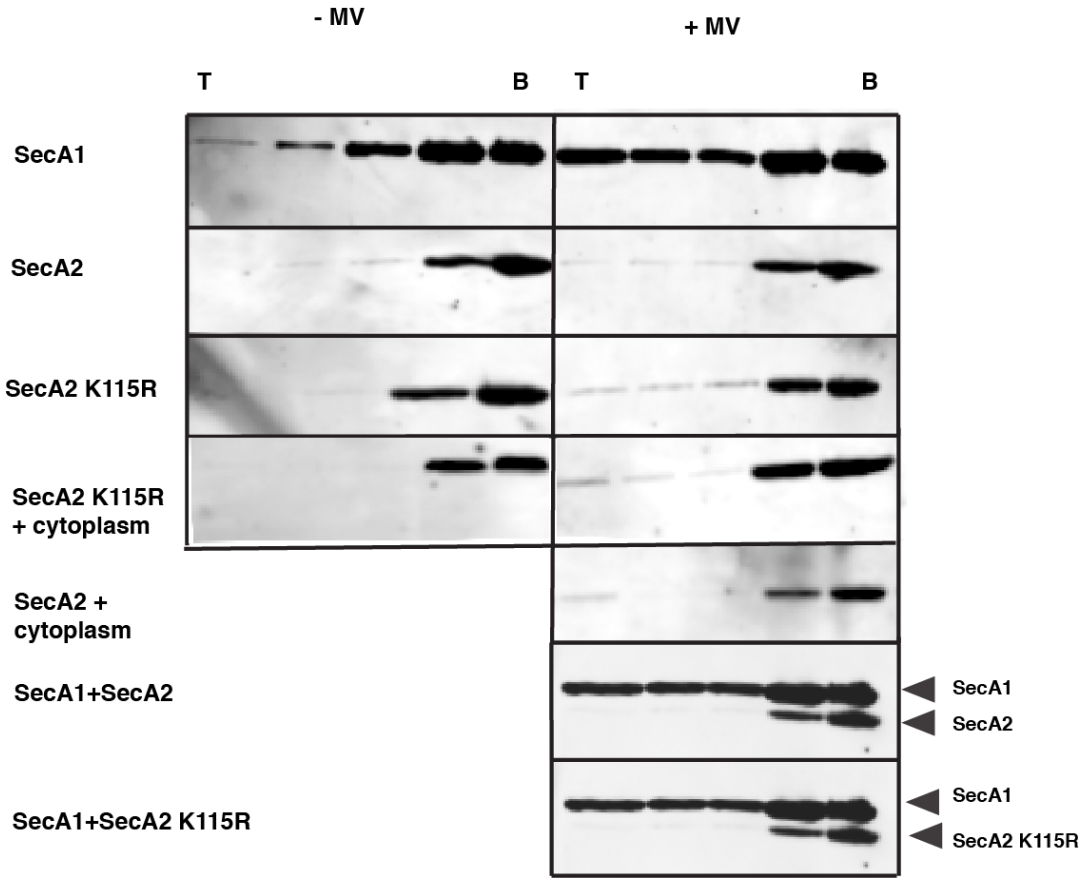

Figure 5-3: *M. tb* SecA1 associates with the membrane while SecA2 does not.

M. tuberculosis SecA1, SecA2 or SecA2 K115R was tested for association with *M. smegmatis* membrane vesicles (MVs) using Opti-Prep floatation gradients. MVs were found in the top fraction (T) while proteins were localized to the bottom fraction (B). Association of SecA1 with membranes caused a shift in migration to the top fractions. SecA2 K115R showed a slight association with MVs compared to WT SecA2. The addition of *M. smegmatis* cytoplasm or SecA1 did not recruit SecA2 to the membranes or enhance the migration of SecA2 K115R to the membrane fraction.

SIGNIFICANCE OF THIS STUDY

Every second, a new person in the world is infected with *Mycobacterium tuberculosis*, the causative agent of Tuberculosis (TB). In fact, around 2 billion people are believed to harbor latent TB (127) and around 1.8 million people succumb to the disease each year. Even though the causative agent of TB was identified by Robert Koch over a century ago in 1882, the disease continues to be a leading infectious disease killer and attempts to combat it have proved to be difficult due to the survival strategies employed by this bacterium. Recently, the emergence of multi drug resistant (MDR) and extensively drug resistant (XDR) strains of the bacterium has caused world-wide concern. TB is an airborne disease that is acquired through inhalation of the bacteria. The bacteria are engulfed by alveolar macrophages resulting in infection foci in the tissue of the alveolar wall. Most bacteria are destroyed after being engulfed by alveolar macrophages; however mycobacteria have evolved strategies to evade destruction by these host cells. *M. tuberculosis* arrests phagosome maturation and thereby prevents its destruction in the lysosome. Instead, these bacteria survive and replicate in the host macrophage (128). Growth of the foci due to bacterial replication leads to recruitment of macrophages and lymphocytes resulting in granuloma formation. Even though this prevents the spread of the bacteria, it also protects the bacteria from other host immune cells and contributes to the survival of the bacteria in a latent mode (128). Being 'walled off', the bacteria are also protected from drugs and other agents. Inhibiting *M. tuberculosis* growth is also difficult due to the fact that mycobacteria have an

unusually thick outer wall made of mycolic acids. They are also naturally resistant to antibiotics and chemicals due to production of beta-lactamases (129).

Currently, the only licensed vaccine against TB is the Bacille Calmette Guérin (BCG) vaccine. Although this live attenuated vaccine from *Mycobacterium bovis* is somewhat effective in preventing widespread TB infection especially in children, the benefits and negative aspects of the vaccine have been debated extensively. Being a live attenuated vaccine, it has the ability to cause disseminated infection in immuno-compromised hosts (130,131). Additionally, the vaccine is not very effective in preventing pulmonary tuberculosis. BCG also does not confer sufficient immunity as it does not stimulate the appropriate populations of T cells (130). Therefore, there is an urgent need for a better vaccine against TB.

Deletion of the *secA2* gene has been shown to render *M. tuberculosis* highly attenuated and proapoptotic (132). Recently, two promising vaccine strains of *M. tuberculosis* were developed that have a deletion of the *secA2* gene. The first strain has a lysine auxotrophy mutation (*ΔlysA*) combined with deletion of *secA2* (*ΔsecA2*) (95). The strain was attenuated in SCID mice and showed enhanced apoptosis of host macrophages. Also mice vaccinated with this strain showed enhanced $CD8^+$ T cell priming and immunity as they resisted infection by *M. tuberculosis* when challenged (95). Since TB infection is the leading cause of death in people with HIV (Human Immunodeficiency virus)-1 infection, this vaccine strain was further tested for immunogenicity in mice when engineered to express a HIV envelope antigen. The strain was able to generate $CD8^+$ T cell

responses against both HIV and *M. tuberculosis* in neonatal mice (133). Recently another vaccine strain of *M. tuberculosis* was developed that combines deletion of replication genes (*panCD* and *leuCD*) with deletion of *secA2*. A plasmid for expression of simian immunodeficiency virus (SIV) Gag protein was introduced into this strain. The strain was found to be safe as it did not cause disease and induced persistent antibody responses in infant macaques (134). These strains are promising candidates for the replacement of BCG as a safe and effective vaccine against TB. Since attenuation of virulence is mainly conferred by deletion of *secA2*, but the function of SecA2 and its role in bacterial virulence is still unknown, progress and development of these vaccines will be hindered by stringent pharmacological guidelines.

This study represents a biochemical analysis of the SecA2 protein in an attempt to decipher its function. SecA2 represents the 'accessory' SecA protein due to the fact that the *secA2* gene unlike *secA1* in *M. tuberculosis* is not essential for viability. In order to gain insight into the role of SecA2, the atypical features of this protein were probed. In an earlier study, we showed SecA2 can bind and hydrolyze ATP in vitro and the ATPase activity of SecA2 is critical for the survival of *M. tuberculosis* in macrophages (43). This study shows that both SecA1 and SecA2 bind nucleotides but SecA2 binds ADP with much higher affinity and releases the nucleotide much more slowly compared to SecA1. ADP also induces a dramatic conformational change in SecA2 involving closure of the precursor binding groove as a result of the rotation of the precursor binding domain (PPXD or PBD) towards the nucleotide binding domain 2 (NBD2). This

nucleotide-induced movement is unique to SecA2 and is not induced in SecA1 upon ADP binding.

This study also shows that SecA2 does not associate with membrane under normal conditions and cannot be recruited to the membrane by SecA1. On the other hand, SecA1 associates with the membrane by itself. These data consistent with results from SecA1 and SecA2 localization studies *in vivo* done by the Braunstein group. Based on results from my study, a model for Sec-dependent export of pre-proteins can be put forth (Figure 6-1). Under normal growth conditions in *M. tuberculosis*, SecA2 would be localized to the cytosol while SecA1 would associate with the membrane and function to export proteins across the SecY translocon. Due to high affinity of SecA2 for ADP (K_d ~ 50 nM) even under high salt conditions, cytosolic SecA2 would be ADP bound owing to the high ADP concentrations in the cytosol. Since the interaction of SecA with precursors is not sequence specific, but rather involves regions from both the signal sequence and mature regions (135), it is unknown how mycobacterial precursor proteins not only recognize SecA but distinguish between two SecA proteins. However; since cytosolic SecA2 would be ADP bound, the precursor-binding groove in SecA2 would be occluded preventing it from interacting with pre-proteins allowing SecA1 instead to associate with these precursors. Under certain conditions, perhaps during infection or for the export of a specific type of pre-protein when SecA2 is required, ADP release would be stimulated by a factor (yet to be identified). This could open the pre-protein binding groove by rotation of the PPXD away from NBD2, towards the HWD (helical wing domain).

Precursor-bound SecA2 would be targeted to the membrane where it would function in the export of the pre-protein across the SecY translocon either by itself or with the aid of SecA1.

This study paves the way for future studies on SecA2-precursor interaction. Identification of the features that distinguish SecA2-dependent pre-proteins from SecA1 precursors, as well as identification of the factor that would target SecA2 to the membrane, would further shed light on the role of SecA2 in export of virulence factors. *M. smegmatis* membrane vesicles (MVs) described in this study could be used to set up an *in vitro* translocation assay for investigation of SecA1 and SecA2-dependent export and association with SecY. Since SecA2 is thought to play an important role in export of virulence factors, identification of the role of SecA2 would not only shed light on mechanism of pathogenesis of *M. tuberculosis* but also pave the way for the development of drug targets and vaccines against TB.

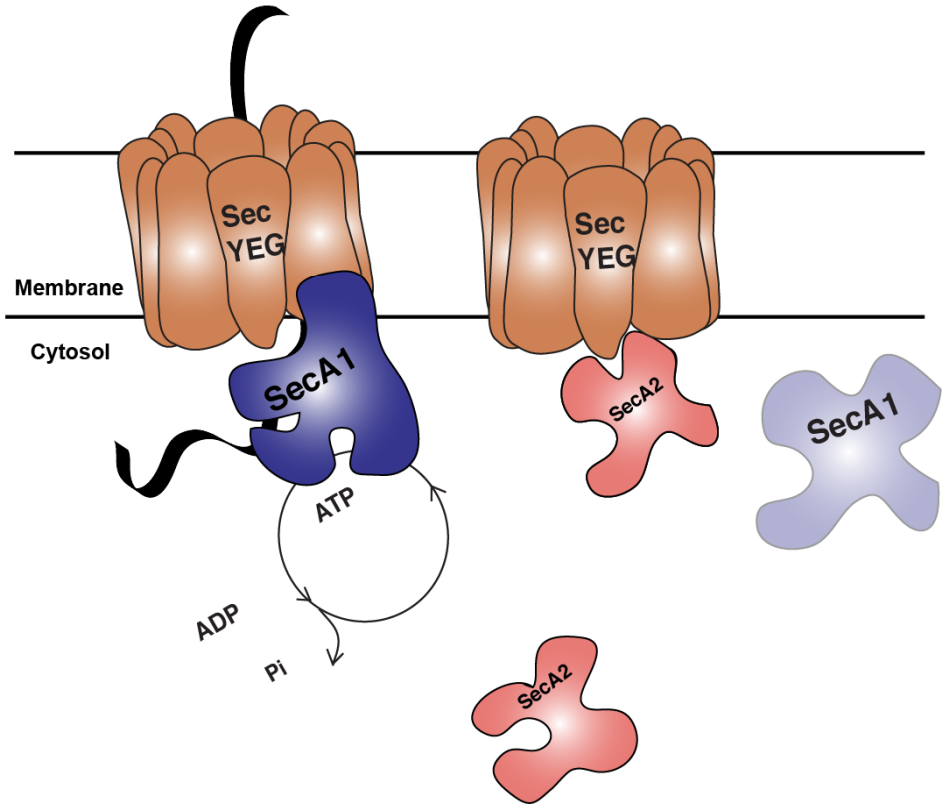

Figure 6-1: Model to explain Sec-dependent translocation in *M. tuberculosis*

Description can be found in the text.

REFERENCES

1. Effrosyni Papanikou, S. K., Anastassios Economou. (2007) Bacterial protein secretion through the translocase nanomachine. *Nature Reviews Microbiology* **5**, 839-851

2. Kawasaki, H., Matsuyama, S., Sasaki, S., Akita, M., and Mizushima, S. (1989) SecA protein is directly involved in protein secretion in Escherichia coli. *FEBS Lett* **242**, 431-434

3. Douville, K., Price, A., Eichler, J., Economou, A., and Wickner, W. (1995) SecYEG and SecA are the stoichiometric components of preprotein translocase. *The Journal of biological chemistry* **270**, 20106-20111

4. Chatzi, K. E., Sardis, M. F., Karamanou, S., and Economou, A. (2013) Breaking on through to the other side: protein export through the bacterial Sec system. *Biochem J* **449**, 25-37

5. Lingappa, V. R., and Blobel, G. (1980) Early events in the biosynthesis of secretory and membrane proteins: the signal hypothesis. *Recent Prog Horm Res* **36**, 451-475

6. Fekkes, P., and Driessen, A. J. (1999) Protein targeting to the bacterial cytoplasmic membrane. *Microbiol Mol Biol Rev* **63**, 161-173

7. Beck, K., Wu, L. F., Brunner, J., and Muller, M. (2000) Discrimination between SRP- and SecA/SecB-dependent substrates involves selective recognition of nascent chains by SRP and trigger factor. *Embo J* **19**, 134-143

8. von Loeffelholz, O. B., Matthieu; Schaffitzel, Christiane. (2011) Escherichia coli Cotranslational Targeting and Translocation. in *Encyclopedia of Life Sciences (ELS)*, John Wiley & Sons Ltd., Chichester

9. Poritz, M. A., Bernstein, H. D., Strub, K., Zopf, D., Wilhelm, H., and Walter, P. (1990) An E. coli ribonucleoprotein containing 4.5S RNA resembles mammalian signal recognition particle. *Science* **250**, 1111-1117

10. Romisch, K., Webb, J., Herz, J., Prehn, S., Frank, R., Vingron, M., and Dobberstein, B. (1989) Homology of 54K protein of signal-recognition particle, docking protein and two E. coli proteins with putative GTP-binding domains. *Nature* **340**, 478-482

11. Shan, S. O., and Walter, P. (2005) Co-translational protein targeting by the signal recognition particle. *FEBS Lett* **579**, 921-926

12. Zhang, X., Kung, S., and Shan, S. O. (2008) Demonstration of a multistep mechanism for assembly of the SRP x SRP receptor complex: implications for the catalytic role of SRP RNA. *Journal of molecular biology* **381**, 581-593

13. Zhang, X., Schaffitzel, C., Ban, N., and Shan, S. O. (2009) Multiple conformational switches in a GTPase complex control co-translational protein targeting. *Proceedings of the National Academy of Sciences of the United States of America* **106**, 1754-1759

14. Weiche, B., Burk, J., Angelini, S., Schiltz, E., Thumfart, J. O., and Koch, H. G. (2008) A cleavable N-terminal membrane anchor is involved in membrane binding of the Escherichia coli SRP receptor. *Journal of molecular biology* **377**, 761-773

15. Halic, M., Gartmann, M., Schlenker, O., Mielke, T., Pool, M. R., Sinning, I., and Beckmann, R. (2006) Signal recognition particle receptor exposes the ribosomal translocon binding site. *Science* **312**, 745-747

16. Connolly, T., and Gilmore, R. (1989) The signal recognition particle receptor mediates the GTP-dependent displacement of SRP from the signal sequence of the nascent polypeptide. *Cell* **57**, 599-610

17. Randall, L. L., and Hardy, S. J. (1986) Correlation of competence for export with lack of tertiary structure of the mature species: a study in vivo of maltose-binding protein in E. coli. *Cell* **46**, 921-928

18. Bechtluft, P., Nouwen, N., Tans, S. J., and Driessen, A. J. (2010) SecB--a chaperone dedicated to protein translocation. *Mol Biosyst* **6**, 620-627

19. Topping, T. B., Woodbury, R. L., Diamond, D. L., Hardy, S. J., and Randall, L. L. (2001) Direct demonstration that homotetrameric chaperone SecB undergoes a dynamic dimer-tetramer equilibrium. *The Journal of biological chemistry* **276**, 7437-7441

20. Hardy, S. J., and Randall, L. L. (1991) A kinetic partitioning model of selective binding of nonnative proteins by the bacterial chaperone SecB. *Science* **251**, 439-443

21. Diamond, D. L., and Randall, L. L. (1997) Kinetic partitioning. Poising SecB to favor association with a rapidly folding ligand. *The Journal of biological chemistry* **272**, 28994-28998

22. Breukink, E., Nouwen, N., van Raalte, A., Mizushima, S., Tommassen, J., and de Kruijff, B. (1995) The C terminus of SecA is involved in both lipid

binding and SecB binding. *The Journal of biological chemistry* **270**, 7902-7907

23. Fekkes, P., de Wit, J. G., Boorsma, A., Friesen, R. H., and Driessen, A. J. (1999) Zinc stabilizes the SecB binding site of SecA. *Biochemistry* **38**, 5111-5116

24. Gouridis, G., Karamanou, S., Gelis, I., Kalodimos, C. G., and Economou, A. (2009) Signal peptides are allosteric activators of the protein translocase. *Nature* **462**, 363-367

25. Lill, R., Dowhan, W., and Wickner, W. (1990) The ATPase activity of SecA is regulated by acidic phospholipids, SecY, and the leader and mature domains of precursor proteins. *Cell* **60**, 271-280

26. Robson, A., Booth, A. E., Gold, V. A., Clarke, A. R., and Collinson, I. (2007) A large conformational change couples the ATP binding site of SecA to the SecY protein channel. *J Mol Biol* **374**, 965-976

27. Lycklama, A. N. J. A., and Driessen, A. J. (2012) The bacterial Sec-translocase: structure and mechanism. *Philos Trans R Soc Lond B Biol Sci* **367**, 1016-1028

28. du Plessis, D. J., Berrelkamp, G., Nouwen, N., and Driessen, A. J. (2009) The lateral gate of SecYEG opens during protein translocation. *The Journal of biological chemistry* **284**, 15805-15814

29. Hanada, M., Nishiyama, K. I., Mizushima, S., and Tokuda, H. (1994) Reconstitution of an efficient protein translocation machinery comprising SecA and the three membrane proteins, SecY, SecE, and SecG (p12). *The Journal of biological chemistry* **269**, 23625-23631

30. Gumbart, J., and Schulten, K. (2008) The roles of pore ring and plug in the SecY protein-conducting channel. *J Gen Physiol* **132**, 709-719

31. Zhang, B., and Miller, T. F., 3rd. (2010) Hydrophobically stabilized open state for the lateral gate of the Sec translocon. *Proceedings of the National Academy of Sciences of the United States of America* **107**, 5399-5404

32. Duong, F., and Wickner, W. (1997) Distinct catalytic roles of the SecYE, SecG and SecDFyajC subunits of preprotein translocase holoenzyme. *EMBO J.* **16**, 2756-2768

33. Yi, L., and Dalbey, R. E. (2005) Oxa1/Alb3/YidC system for insertion of membrane proteins in mitochondria, chloroplasts and bacteria. *Mol. Membr. Biol.* **22**, 101-111

34. Auclair, S. M., Bhanu, M. K., and Kendall, D. A. (2012) Signal peptidase I: cleaving the way to mature proteins. *Protein Sci* **21**, 13-25

35. Hagan, C. L., Silhavy, T. J., and Kahne, D. (2011) beta-Barrel membrane protein assembly by the Bam complex. *Annual review of biochemistry* **80**, 189-210

36. Okuda, S., and Tokuda, H. (2011) Lipoprotein sorting in bacteria. *Annu Rev Microbiol* **65**, 239-259

37. Van den Berg, B., Clemons, W. M., Jr., Collinson, I., Modis, Y., Hartmann, E., Harrison, S. C., and Rapoport, T. A. (2004) X-ray structure of a protein-conducting channel. *Nature* **427**, 36-44

38. Pettersen, E. F., Goddard, T. D., Huang, C. C., Couch, G. S., Greenblatt, D. M., Meng, E. C., and Ferrin, T. E. (2004) UCSF Chimera--a visualization system for exploratory research and analysis. *J Comput Chem* **25**, 1605-1612

39. Braunstein, M., B. J. Espinosa, J. Chan, J. T. Belisle, and W. R. Jacobs, Jr (2003) SecA2 functions in the secretion of superoxide dismutaseA and in the virulence of Mycobacterium tuberculosis. *J. Bacteriol.* **48**, 453-464

40. Gibbons, H. S., Wolschendorf, F., Abshire, M., Niederweis, M., and Braunstein, M. (2007) Identification of two Mycobacterium smegmatis lipoproteins exported by a SecA2-dependent pathway. *J Bacteriol* **189**, 5090-5100

41. Bensing, B. A., and P. M. Sullam. (2002) An accessory sec locus of Streptococcus gordonii is required for export of the surface protein GspB and for normal levels of binding to human platelets. *Molecular Microbiology* **44**, 1081-1094

42. Lenz, L. L., and Portnoy, D. A. (2002) Identification of a second Listeria secA gene associated with protein secretion and the rough phenotype. *Mol Microbiol* **45**, 1043-1056

43. Hou, J.M., D'Lima,N.G, Rigel,N.W, Gibbons, H.S, McCann, J.R., Braunstein, M and Teschke, C.M. (2008) ATPase Activity of Mycobacterium tuberculosis SecA1 and SecA2 Proteins and Its Importance for SecA2 Function in Macrophages. *J. Bacteriol.* **190**, 4880-4887

44. Caspers, M., and Freudl, R. (2008) Corynebacterium glutamicum possesses two secA homologous genes that are essential for viability. *Arch Microbiol* **189**, 605-610

45. Fagan, R. P., and Fairweather, N. F. (2011) Clostridium difficile has two parallel and essential Sec secretion systems. *The Journal of biological chemistry* **286**, 27483-27493

46. Feltcher, M. E., and Braunstein, M. (2012) Emerging themes in SecA2-mediated protein export. *Nat Rev Microbiol* **10**, 779-789

47. Bensing, B. A., Gibson, B. W., and Sullam, P. M. (2004) The Streptococcus gordonii platelet binding protein GspB undergoes glycosylation independently of export. *J Bacteriol* **186**, 638-645

48. Bensing, B. A., Siboo, I. R., and Sullam, P. M. (2007) Glycine residues in the hydrophobic core of the GspB signal sequence route export toward the accessory Sec pathway. *Journal of bacteriology* **189**, 3846-3854

49. Bensing, B. A., and Sullam, P. M. (2010) Transport of preproteins by the accessory Sec system requires a specific domain adjacent to the signal peptide. *Journal of bacteriology* **192**, 4223-4232

50. Bensing, B. A., Seepersaud, R., Yen, Y. T., and Sullam, P. M. (2013) Selective transport by SecA2: An expanding family of customized motor proteins. *Biochim Biophys Acta*

51. Takamatsu, D., Bensing, B. A., and Sullam, P. M. (2005) Two additional components of the accessory sec system mediating export of the Streptococcus gordonii platelet-binding protein GspB. *Journal of bacteriology* **187**, 3878-3883

52. Seepersaud, R., Bensing, B. A., Yen, Y. T., and Sullam, P. M. (2010) Asp3 mediates multiple protein-protein interactions within the accessory Sec system of Streptococcus gordonii. *Molecular microbiology* **78**, 490-505

53. Yen, Y. T., Seepersaud, R., Bensing, B. A., and Sullam, P. M. (2011) Asp2 and Asp3 interact directly with GspB, the export substrate of the Streptococcus gordonii accessory Sec System. *Journal of bacteriology* **193**, 3165-3174

54. Bensing, B. A., and Sullam, P. M. (2009) Characterization of Streptococcus gordonii SecA2 as a paralogue of SecA. *Journal of bacteriology* **191**, 3482-3491

55. van der Woude, A. D., Stoop, E. J., Stiess, M., Wang, S., Ummels, R., van Stempvoort, G., Piersma, S. R., Cascioferro, A., Jimenez, C. R., Houben, E. N., Luirink, J., Pieters, J., van der Sar, A. M., and Bitter, W. (2013) Analysis of SecA2-dependent substrates in Mycobacterium marinum identifies protein kinase G (PknG) as a virulence effector. *Cellular microbiology*

56. Lenz, L. L., Mohammadi, S., Geissler, A., and Portnoy, D. A. (2003) SecA2-dependent secretion of autolytic enzymes promotes Listeria monocytogenes pathogenesis. *Proc Natl Acad Sci U S A* **100**, 12432-12437

57. Archambaud, C., Nahori, M. A., Pizarro-Cerda, J., Cossart, P., and Dussurget, O. (2006) Control of Listeria superoxide dismutase by phosphorylation. *The Journal of biological chemistry* **281**, 31812-31822

58. Burkholder, K. M., Kim, K. P., Mishra, K., Medina, S., Hahm, B. K., Kim, H., and Bhunia, A. K. (2009) Expression of LAP, an SecA2-dependent secretory protein, is induced under anaerobic environment. *Microbes Infect*

59. Nguyen-Mau, S. M., Oh, S. Y., Kern, V. J., Missiakas, D. M., and Schneewind, O. (2012) Secretion genes as determinants of Bacillus anthracis chain length. *Journal of bacteriology* **194**, 3841-3850

60. Chen, Q., H. Wu, and P. M. Fives-Taylor. (2004) Investigating the role of secA2 in secretion and glycosylation of a fimbrial adhesin in Streptococcus parasanguis FW213. *Mol. Microbiol.* **53**, 843-856

61. Mistou, M. Y., Dramsi, S., Brega, S., Poyart, C., and Trieu-Cuot, P. (2009) Molecular dissection of the secA2 locus of group B Streptococcus reveals that glycosylation of the Srr1 LPXTG protein is required for full virulence. *Journal of bacteriology* **191**, 4195-4206

62. Siboo, I. R., Chaffin, D. O., Rubens, C. E., and Sullam, P. M. (2008) Characterization of the accessory Sec system of Staphylococcus aureus. *Journal of bacteriology* **190**, 6188-6196

63. Kusters, I., and Driessen, A. J. (2011) SecA, a remarkable nanomachine. *Cellular and molecular life sciences : CMLS* **68**, 2053-2066

64. Musial-Siwek, M., Rusch, S. L., and Kendall, D. A. (2007) Selective photoaffinity labeling identifies the signal peptide binding domain on SecA. *J. Mol. Biol.* **365**, 637-648

65. Papanikou, E., Karamanou, S., Baud, C., Frank, M., Sianidis, G., Keramisanou, D., Kalodimos, C. G., Kuhn, A., and Economou, A. (2005) Identification of the preprotein binding domain of SecA. *The Journal of biological chemistry* **280**, 43209-43217

66. Randall, L. L., Crane, J. M., Lilly, A. A., Liu, G., Mao, C., Patel, C. N., and Hardy, S. J. (2005) Asymmetric binding between SecA and SecB two symmetric proteins: implications for function in export. *Journal of molecular biology* **348**, 479-489

67. Fak, J. J., Itkin, A., Ciobanu, D. D., Lin, E. C., Song, X. J., Chou, Y. T., Gierasch, L. M., and Hunt, J. F. (2004) Nucleotide exchange from the high-affinity ATP-binding site in SecA is the rate-limiting step in the ATPase cycle of the soluble enzyme and occurs through a specialized conformational state. *Biochemistry* **43**, 7307-7327

68. Robson, A., Gold, V. A., Hodson, S., Clarke, A. R., and Collinson, I. (2009) Energy transduction in protein transport and the ATP hydrolytic cycle of SecA. *Proc Natl Acad Sci U S A* **106**, 5111-5116

69. Gold, V. A., Robson, A., Clarke, A. R., and Collinson, I. (2007) Allosteric regulation of SecA: magnesium-mediated control of conformation and activity. *J Biol Chem* **282**, 17424-17432

70. Natale, P., Swaving, J., van der Does, C., de Keyzer, J., and Driessen, A. J. (2004) Binding of SecA to the SecYEG complex accelerates the rate of nucleotide exchange on SecA. *J Biol Chem* **279**, 13769-13777

71. Karamanou, S., Vrontou, E., Sianidis, G., Baud, C., Roos, T., Kuhn, A., Politou, A. S., and Economou, A. (1999) A molecular switch in SecA protein couples ATP hydrolysis to protein translocation. *Mol Microbiol* **34**, 1133-1145

72. Karamanou, S., Gouridis, G., Papanikou, E., Sianidis, G., Gelis, I., Keramisanou, D., Vrontou, E., Kalodimos, C. G., and Economou, A. (2007) Preprotein-controlled catalysis in the helicase motor of SecA. *Embo J* **26**, 2904-2914

73. Osborne, A. R., Clemons, W. M., and Rapoport, T. A. (2004) A large conformational change of the translocation ATPase SecA. *Proc. Natl Acad. Sci. USA* **101**, 10937-10942

74. Zimmer, J., Nam, Y., and Rapoport, T. A. (2008) Structure of a complex of the ATPase SecA and the protein-translocation channel. *Nature* **455**, 936-943

75. Hunt, J. F. (2002) Nucleotide control of interdomain interactions in the conformational reaction cycle of SecA. *Science* **297**, 2018-2026

76. Zimmer, J., and Rapoport, T. A. (2009) Conformational flexibility and peptide interaction of the translocation ATPase SecA. *Journal of molecular biology* **394**, 606-612

77. Gelis, I., Bonvin, A. M., Keramisanou, D., Koukaki, M., Gouridis, G., Karamanou, S., Economou, A., and Kalodimos, C. G. (2007) Structural basis for signal-sequence recognition by the translocase motor SecA as determined by NMR. *Cell* **131**, 756-769

78. Erlandson, K. J., Miller, S. B., Nam, Y., Osborne, A. R., Zimmer, J., and Rapoport, T. A. (2008) A role for the two-helix finger of the SecA ATPase in protein translocation. *Nature* **455**, 984-987

79. Whitehouse, S., Gold, V. A., Robson, A., Allen, W. J., Sessions, R. B., and Collinson, I. (2012) Mobility of the SecA 2-helix-finger is not essential for polypeptide translocation via the SecYEG complex. *J Cell Biol* **199**, 919-929

80. Akita, M., Shinkai, A., Matsuyama, S., and Mizushima, S. (1991) SecA, an essential component of the secretory machinery of Escherichia coli, exists as homodimer. *Biochem. Biophys. Res. Commun.* **174**, 211-216

81. Kusters, I., van den Bogaart, G., Kedrov, A., Krasnikov, V., Fulyani, F., Poolman, B., and Driessen, A. J. (2011) Quaternary structure of SecA in solution and bound to SecYEG probed at the single molecule level. *Structure* **19**, 430-439

82. Or, E., Navon, A., and Rapoport, T. (2002) Dissociation of the dimeric SecA ATPase during protein translocation across the bacterial membrane. *EMBO J.* **21**, 4470-4479

83. Benach, J. C. Y., Fak JJ, Itkin A, Nicolae DD, Smith PC, Wittrock G, Floyd DL, Golsaz CM, Gierasch LM, Hunt JF. (2003) Phospholipid-induced monomerization and signal-peptide-induced oligomerization of SecA. *J. Biol. Chem.* **278**, 3628-3638

84. Sardis, M. F., and Economou, A. (2010) SecA: a tale of two protomers. *Molecular microbiology* **76**, 1070-1081

85. Woodbury, R. L., Hardy, S. J., and Randall, L. L. (2002) Complex behavior in solution of homodimeric SecA. *Protein Sci.* **11**, 875-882

86. Wowor, A. J., Yu, D., Kendall, D. A., and Cole, J. L. (2011) Energetics of SecA dimerization. *Journal of molecular biology* **408**, 87-98

87. Gouridis, G., Karamanou, S., Sardis, M. F., Scharer, M. A., Capitani, G., and Economou, A. (2013) Quaternary Dynamics of the SecA Motor Drive Translocase Catalysis. *Mol Cell* **52**, 655-666

88. Papanikolau, Y., Papadovasilaki, M., Ravelli, R. B., McCarthy, A. A., Cusack, S., Economou, A., and Petratos, K. (2007) Structure of dimeric SecA, the Escherichia coli preprotein translocase motor. *Journal of molecular biology* **366**, 1545-1557

89. den Blaauwen, T., Terpetschnig, E., Lakowicz, J. R., and Driessen, A. J. (1997) Interaction of SecB with soluble SecA. *FEBS Lett* **416**, 35-38

90. Hartl, F. U., Lecker, S., Schiebel, E., Hendrick, J. P., and Wickner, W. (1990) The binding cascade of SecB to SecA to SecY/E mediates preprotein targeting to the E. coli plasma membrane. *Cell* **63**, 269-279

91. Fekkes, P., van der Does, C., and Driessen, A. J. (1997) The molecular chaperone SecB is released from the carboxy-terminus of SecA during initiation of precursor protein translocation. *EMBO J.* **16**, 6105-6113

92. Braunstein, M., B. J. Espinosa, J. Chan, J. T. Belisle, and W. R. Jacobs, Jr. (2001) Two nonredundant SecA homologues function in mycobacteria. *J. Bacteriol.* **183**, 6979-6990

93. Owens, M. U., Swords, W. E., Schmidt, M. G., King, C. H., and Quinn, F. D. (2002) Cloning, expression, and functional characterization of the Mycobacterium tuberculosis secA gene. *FEMS Microbiol Lett* **211**, 133-141

94. Hinchey, J., Lee, S., Jeon, B. Y., Basaraba, R. J., Venkataswamy, M. M., Chen, B., Chan, J., Braunstein, M., Orme, I. M., Derrick, S. C., Morris, S. L., Jacobs, W. R., Jr., and Porcelli, S. A. (2007) Enhanced priming of adaptive immunity by a proapoptotic mutant of Mycobacterium tuberculosis. *J Clin Invest* **117**, 2279-2288

95. Hinchey, J., Jeon, B. Y., Alley, H., Chen, B., Goldberg, M., Derrick, S., Morris, S., Jacobs, W. R., Jr., Porcelli, S. A., and Lee, S. Lysine auxotrophy combined with deletion of the SecA2 gene results in a safe and highly immunogenic candidate live attenuated vaccine for tuberculosis. *PLoS One* **6**, e15857

96. Sullivan, J. T., Young, E. F., McCann, J. R., and Braunstein, M. The Mycobacterium tuberculosis SecA2 System Subverts Phagosome

Maturation To Promote Growth in Macrophages. *Infect Immun* **80**, 996-1006

97. Rigel, N. W., Gibbons, H. S., McCann, J. R., McDonough, J. A., Kurtz, S., and Braunstein, M. (2009) The Accessory SecA2 System of Mycobacteria Requires ATP Binding and the Canonical SecA1. *J Biol Chem* **284**, 9927-9936

98. Ligon, L. S., Rigel, N. W., Romanchuk, A., Jones, C. D., and Braunstein, M. (2013) Suppressor analysis reveals a role for SecY in the SecA2-dependent protein export pathway of Mycobacteria. *Journal of bacteriology* **195**, 4456-4465

99. Feltcher, M. E., Gibbons, H. S., Ligon, L. S., and Braunstein, M. (2013) Protein export by the mycobacterial SecA2 system is determined by the preprotein mature domain. *Journal of bacteriology* **195**, 672-681

100. Sharma, V. V. S., Arulandu Arockiasam, Donald R. Ronning, Christos G. Savva Andreas Holzenburg, Miriam Braunstein□, William R. Jacobs, Jr. and James C. Sacchettini. (2003) Crystal structure of Mycobacterium tuberculosis SecA, a preprotein translocating ATPase. *Proc. Natl Acad. Sci. USA* **100**, 2243-2248

101. du Plessis, D. J., Nouwen, N., and Driessen, A. J. (2011) The Sec translocase. *Biochim Biophys Acta* **1808**, 851-865

102. Simossis, V. A., and Heringa, J. (2005) PRALINE: a multiple sequence alignment toolbox that integrates homology-extended and secondary structure information. *Nucleic Acids Res* **33**, W289-294

103. Zheng, L., Baumann, U., and Reymond, J. L. (2004) An efficient one-step site-directed and site-saturation mutagenesis protocol. *Nucleic Acids Res* **32**, e115

104. Pollard, T. D. (2010) A guide to simple and informative binding assays. *Mol Biol Cell* **21**, 4061-4067

105. Hulme, E. C., and Trevethick, M. A. (2010) Ligand binding assays at equilibrium: validation and interpretation. *Br J Pharmacol* **161**, 1219-1237

106. Philo, J. S. (2006) Improved methods for fitting sedimentation coefficient distributions derived by time-derivative techniques. *Anal Biochem* **354**, 238-246

107. Laue T.M., S. B. D., Ridgeway T.M., and Pelletier S.L. (1992) Computer-aided interpretation of analytical sedimentation data for proteins In

Analytical ultracentrifugation in biochemistry and polymer science, Royal Society of Chemistry, Cambridge. pp 90-125

108. Feltcher, M. E., Sullivan, J. T., and Braunstein, M. (2010) Protein export systems of Mycobacterium tuberculosis: novel targets for drug development? *Future Microbiol* **5**, 1581-1597

109. Scopes, R. K. (1993) *Protein Purification: Principles and Practice*, Third ed., Springer, New York

110. Bates, P. A., Kelley, L. A., MacCallum, R. M., and Sternberg, M. J. (2001) Enhancement of protein modeling by human intervention in applying the automatic programs 3D-JIGSAW and 3D-PSSM. *Proteins* **Suppl 5**, 39-46

111. Gold, V. A., Whitehouse, S., Robson, A., and Collinson, I. (2013) The dynamic action of SecA during the initiation of protein translocation. *Biochem J* **449**, 695-705

112. Tomkiewicz, D., Nouwen, N., van Leeuwen, R., Tans, S., and Driessen, A. J. (2006) SecA supports a constant rate of preprotein translocation. *J Biol Chem* **281**, 15709-15713

113. De Keyzer, J., Van Der Does, C., and Driessen, A. J. (2002) Kinetic analysis of the translocation of fluorescent precursor proteins into Escherichia coli membrane vesicles. *J. Biol. Chem.* **277**, 46059-46065

114. Doyle, S. M., Braswell, E. H., and Teschke, C. M. (2000) SecA Folds via a Dimeric Intermediate. *Biochemistry* **39**, 11667-11676

115. Jilaveanu, L. B., Zito, C. R., and Oliver, D. (2005) Dimeric SecA is essential for protein translocation. *Proceedings of the National Academy of Sciences of the United States of America* **102**, 7511-7516

116. de Keyzer, J., van der Sluis, E. O., Spelbrink, R. E., Nijstad, N., de Kruijff, B., Nouwen, N., van der Does, C., and Driessen, A. J. (2005) Covalently dimerized SecA is functional in protein translocation. *The Journal of biological chemistry* **280**, 35255-35260

117. Wang, H., Na, B., Yang, H., and Tai, P. C. (2008) Additional in vitro and in vivo evidence for SecA functioning as dimers in the membrane: dissociation into monomers is not essential for protein translocation in Escherichia coli. *Journal of bacteriology* **190**, 1413-1418

118. Or, E., Boyd, D., Gon, S., Beckwith, J., and Rapoport, T. (2005) The bacterial ATPase SecA functions as a monomer in protein translocation. *J. Biol. Chem.* **280**, 9097-9105

119. Bu, Z., Wang, L., and Kendall, D. A. (2003) Nucleotide binding induces changes in the oligomeric state and conformation of Sec A in a lipid environment: a small-angle neutron-scattering study. *J Mol Biol* **332**, 23-30

120. Hunt, J. F., Weinkauf, S., Henry, L., Fak, J. J., McNicholas, P., Oliver, D. B., and Deisenhofer, J. (2002) Nucleotide control of interdomain interactions in the conformational reaction cycle of SecA. *Science* **297**, 2018-2026

121. Karamanou, S., Sianidis, G., Gouridis, G., Pozidis, C., Papanikolau, Y., Papanikou, E., and Economou, A. (2005) Escherichia coli SecA truncated at its termini is functional and dimeric. *FEBS Lett* **579**, 1267-1271

122. Stafford, W. F., and Sherwood, P. J. (2004) Analysis of heterologous interacting systems by sedimentation velocity: curve fitting algorithms for estimation of sedimentation coefficients, equilibrium and kinetic constants. *Biophys Chem* **108**, 231-243

123. Haagsma, A. C., Podasca, I., Koul, A., Andries, K., Guillemont, J., Lill, H., and Bald, D. (2011) Probing the interaction of the diarylquinoline TMC207 with its target mycobacterial ATP synthase. *PloS one* **6**, e23575

124. Haagsma, A. C., Driessen, N. N., Hahn, M. M., Lill, H., and Bald, D. (2010) ATP synthase in slow- and fast-growing mycobacteria is active in ATP synthesis and blocked in ATP hydrolysis direction. *FEMS Microbiol Lett* **313**, 68-74

125. Han, J., and Burgess, K. (2010) Fluorescent indicators for intracellular pH. *Chem Rev* **110**, 2709-2728

126. Rigel, N. W., and Braunstein, M. (2008) A new twist on an old pathway--accessory Sec [corrected] systems. *Mol Microbiol* **69**, 291-302

127. Gomez, J. E., and McKinney, J. D. (2004) M. tuberculosis persistence, latency, and drug tolerance. *Tuberculosis (Edinb)* **84**, 29-44

128. Russell, D. G. (2000) Tuberculosis: Not just a bad cough. *Nature Medicine*

129. Jarlier, V., and Nikaido, H. (1994) Mycobacterial cell wall: structure and role in natural resistance to antibiotics. *FEMS Microbiol Lett* **123**, 11-18

130. Andersen, P. (2007) Tuberculosis vaccines - an update. *Nat Rev Microbiol* **5**, 484-487

131. Villarreal-Ramos, B. (2009) Towards improved understanding of protective mechanisms induced by the BCG vaccine. *Expert Rev Vaccines* **8**, 1531-1534

132. Kurtz, S., McKinnon, K. P., Runge, M. S., Ting, J. P., and Braunstein, M. (2006) The SecA2 secretion factor of Mycobacterium tuberculosis promotes growth in macrophages and inhibits the host immune response. *Infect Immun* **74**, 6855-6864

133. Ranganathan, U. D., Larsen, M. H., Kim, J., Porcelli, S. A., Jacobs, W. R., Jr., and Fennelly, G. J. (2009) Recombinant pro-apoptotic Mycobacterium tuberculosis generates CD8+ T cell responses against human immunodeficiency virus type 1 Env and M. tuberculosis in neonatal mice. *Vaccine* **28**, 152-161

134. Jensen, K., Ranganathan, U. D., Van Rompay, K. K., Canfield, D. R., Khan, I., Ravindran, R., Luciw, P. A., Jacobs, W. R., Jr., Fennelly, G., Larsen, M. H., and Abel, K. (2012) A recombinant attenuated Mycobacterium tuberculosis vaccine strain is safe in immunosuppressed simian immunodeficiency virus-infected infant macaques. *Clin Vaccine Immunol* **19**, 1170-1181

135. Chatzi, K. E., Sardis, M. F., Economou, A., and Karamanou, S. (2014) SecA-mediated targeting and translocation of secretory proteins. *Biochim Biophys Acta*